

M Ű E G Y E T E M 1 7 8 2

Budapest University of Technology and Economics

Enhanced Methods for IPTV Delivery over Wireless Networks

A Dissertation Submitted to
the Faculty of Electrical Engineering and Informatics
in Candidacy for the Degree of
Doctor of Philosophy

Department of Networked Systems and Services

by

Tamás Jursonovics

Darmstadt

May 2014



Tamás Jursonovics received the M.Sc. degree in Electrical Engineering from the Budapest University of Technology and Economics (BME) in 2003. After graduation, he joined the Deutsche Telekom Group, where he is currently employed by Products & Innovation. He is now working towards his Ph.D. and MBA at the Budapest University of Technology and Economics and at the Hochschule Darmstadt (h_da) – University of Applied Sciences. His research interests include the delivery, charging and architectural aspects of the IPTV and wireless multimedia distribution technologies.

©2014 by Tamás Jursonovics

All rights reserved. Published 2014.
Version 1.0

This document and citations were formatted according to
The Chicago Manual of Style.

This paper meets the requirements of
ANSI/NISO z39.48-1992 (Permanence of Paper).



tűzcsap :)



Contents

| | |
|---|------------|
| List of Illustrations | ii |
| List of Tables | v |
| Acknowledgements | vi |
| List of Abbreviations | vii |
| Introduction | 1 |
| 1 Materials and Methods | 4 |
| 1.1 Terminology | 4 |
| 1.2 Markov Models | 4 |
| 1.3 H.264/MPEG-4 AVC | 6 |
| 1.4 Streaming Protocols | 7 |
| 1.5 Image Quality Metrics | 8 |
| 1.6 Test Sequences, Video Encoding, and Error Concealment | 9 |
| 1.7 Tools and Testbed | 10 |
| 2 Retransmission in IPTV Solutions over Burst-Error Channels | 14 |
| 2.1 Literature Review | 16 |
| 2.1.1 Open IPTV Forum | 16 |
| 2.1.2 ITU-T, ETSI | 17 |
| 2.1.3 Proprietary Solutions | 18 |
| 2.1.4 DCCP | 18 |
| 2.1.5 State-of-the-Art Research | 19 |
| 2.2 Theory | 20 |
| 2.2.1 Bandwidth Allocation in IPTV Solutions | 20 |
| 2.2.2 The Three State Channel Model | 28 |
| 2.3 Results and Discussion | 35 |



| | | |
|----------|--|------------|
| 2.3.1 | Evaluation of the 3SCM | 35 |
| 2.3.2 | Forecasting Performance of the 3SCM | 44 |
| 2.3.3 | The Optimal Bandwidth Allocation | 47 |
| 2.3.4 | The Optimal Retransmission Algorithm | 51 |
| 2.4 | Conclusion | 55 |
| 3 | Quality Based Charging Solutions | 60 |
| 3.1 | Literature Review | 62 |
| 3.1.1 | 3GPP | 62 |
| 3.1.2 | IETF | 63 |
| 3.1.3 | UMTS Forum | 64 |
| 3.1.4 | State-of-the-Art Research | 67 |
| 3.2 | Theory | 70 |
| 3.2.1 | Charging Difference Between Internet and Mobile Networks | 70 |
| 3.2.2 | Billing Requirements in Mobile Networks | 71 |
| 3.2.3 | Offline and Online Charging Terminology | 72 |
| 3.3 | Results and Discussion | 73 |
| 3.3.1 | Charging Requirements | 73 |
| 3.3.2 | The Proposed Business Model and Architecture | 74 |
| 3.3.3 | The Assessment of the Quality | 78 |
| 3.3.4 | Measurement and Prediction of the Loss Distribution | 81 |
| 3.3.5 | The Quality Based Charging Solution | 83 |
| 3.4 | Conclusion | 98 |
| | Afterwords | 102 |
| | A Configuration of the Testbed Components | 104 |
| | B Configuration of the JM Reference Software | 106 |
| | C Analysis of Different Video Sequences | 112 |
| | D Formulas of the Charging Policy Functions | 123 |
| | Glossary | 134 |
| | Bibliography | 136 |
| | Selected Bibliography | 142 |



Illustrations

| | | |
|------|--|----|
| 1 | Analogue switch-off date in various countries | 2 |
| 1.1 | Different Markov chains | 5 |
| 1.2 | Sample frame structure in MPEG-4 AVC | 6 |
| 1.3 | Error propagation in MPEG-4 AVC | 6 |
| 1.4 | Correct sequence | 10 |
| 1.5 | Error concealment | 10 |
| 1.6 | Testbed for IPTV retransmission simulation | 11 |
| 1.7 | Testbed for quality based charging simulation | 12 |
| 2.1 | Bandwidth allocation in the access network | 21 |
| 2.2 | Leveraging optimal bandwidth allocation. | 22 |
| 2.3 | Out-of-band packet retransmission | 23 |
| 2.4 | Intra-burst retransmission | 24 |
| 2.5 | Intra-burst limitation | 25 |
| 2.6 | Inter-burst retransmission | 26 |
| 2.7 | Inter-burst limitation | 27 |
| 2.8 | The common effect of the intra- and inter-burst limitation | 28 |
| 2.9 | Channel model for IPTV analysis | 29 |
| 2.10 | The Three State Channel Model | 31 |
| 2.11 | Monte Carlo analysis of the poles | 36 |
| 2.12 | Steady state probabilities of packet loss | 43 |
| 2.13 | Probabilities of loss run-lengths | 44 |
| 2.14 | Steady state estimation | 46 |
| 2.15 | Loss burst runlengths estimation | 48 |
| 2.16 | Retransmission burst runlengths estimation | 49 |
| 2.17 | Bandwidth allocation for IPTV solutions | 52 |
| 2.18 | Proposed retransmission algorithm | 53 |
| 2.19 | Retransmission throughput | 56 |



| | | |
|------|--|-----|
| 2.20 | Overall packet loss rate | 56 |
| 2.21 | Mean and standard deviation for overall packet loss rate | 56 |
| 3.1 | Network operator centric business model | 65 |
| 3.2 | Content aggregator centric business model | 66 |
| 3.3 | Content provider centric business model | 67 |
| 3.4 | Charging methods | 73 |
| 3.5 | The proposed network operator centric model with network entities . | 76 |
| 3.6 | Proxy based charging architecture | 77 |
| 3.7 | Error propagation in H.264 decoding | 79 |
| 3.8 | Redefined RTCP receiver report | 82 |
| 3.9 | Redefined RTCP report | 83 |
| 3.10 | Different charging policies | 84 |
| 3.11 | Charging algorithm | 87 |
| 3.12 | PSNR (bigbuckbunny) | 89 |
| 3.13 | MSE (bigbuckbunny) | 89 |
| 3.14 | Histogram of $d[k]$ (bigbuckbunny) | 89 |
| 3.15 | Q-Q plot (bigbuckbunny) | 90 |
| 3.16 | Linear charging policy in MSE units | 91 |
| 3.17 | Quality prediction | 94 |
| 3.18 | Workflow for quality based charging | 95 |
| 3.19 | Comparison of different charging methods | 96 |
| 3.20 | Occurrence of l length of loss bursts | 97 |
| 3.21 | Mean distance and \pm standard deviation for consecutive loss bursts . | 98 |
| C.1 | Inter frame difference (startrek) | 113 |
| C.2 | Inter frame difference (thehobbit) | 113 |
| C.3 | Inter frame difference (bigbuckbunny) | 113 |
| C.4 | Inter frame difference (foreman) | 114 |
| C.5 | Inter frame difference (bridge close) | 114 |
| C.6 | Inter frame difference (highway) | 114 |
| C.7 | Distribution of inter frame difference (startrek) | 115 |
| C.8 | Distribution of inter frame difference (thehobbit) | 115 |
| C.9 | Distribution of inter frame difference (bigbuckbunny)2 | 115 |
| C.10 | Distribution of inter frame difference (foreman) | 116 |
| C.11 | Distribution of inter frame difference (bridge close) | 116 |
| C.12 | Distribution of inter frame difference (highway) | 116 |



| | |
|--|-----|
| C.13 Q-Q plot (startrek) | 118 |
| C.14 Q-Q plot (thehobbit) | 119 |
| C.15 Q-Q plot (bigbuckbunny) | 120 |

Tables

| | |
|--|-----|
| 1 Global IPTV forecasts | 3 |
| 1.1 Test sequences | 9 |
| 3.1 Maximum likelihood fit (bigbuckbunny) | 88 |
| 3.2 Pearson's Chi-Square test (bigbuckbunny) | 88 |
| 3.3 Model parameters | 93 |
| 3.4 Comparison of different charging methods | 97 |
| A.1 Access line parameters | 105 |
| C.1 Parameter estimation (startrek) | 117 |
| C.2 Parameter estimation (thehobbit) | 121 |
| C.3 Parameter estimation (bigbuckbunny) | 122 |
| C.4 MSE-PSNR conversion table | 122 |



Acknowledgements

Foremost, I would like to express my sincere gratitude to my advisor Professor Dr. Imre Sándor for the continuous support of my Ph.D study and research, for his patience, motivation, enthusiasm, and immense knowledge. His guidance helped me in all the time of research and writing of this thesis.

I am deeply thankful to my family for their love, support, and sacrifices. Without them, this thesis would never have been written.

Most importantly, I would like to thank my wife Ági. Her support, encouragement, quiet patience, and unwavering love were undeniably the bedrock upon which my life has been built.



Abbreviations

3GPP 3rd Generation Partnership Project.
3SCM three state channel model.
AAA authentication, authorization and accounting.
AV audio-video.
AVC advanced video coding.
CDF charging data function.
CDR charging data record.
CGF charging gateway function.
DCCP data congestion control protocol.
DRM digital rights management.
DSL digital subscriber lines.
DT Deutsche Telekom.
ENB evolved Node B.
EPS evolved packet system.
GGSN gateway GPRS support node.
GOP group of pictures.
GPRS general packet radio service.
IDR instantaneous decode refresh.
IETF Internet Engineering Task Force.
IMS IP multimedia subsystem.
IPTV internet protocol television.
LTE long term evolution.
MAC media access control.
ME mobile equipment.
MSE mean square error.
OCS online charging system.
OIPF The Open IPTV Forum.
OITF open IPTV terminal function.



OTT over-the-top.
PDP packet data protocol.
PSNR peak signal noise ratio.
QOS quality of service.
RET retransmission.
RNC radio network controller.
RNS radio network subsystem.
RTCP real-time control protocol.
RTCP-RR real-time control protocol - receiver report.
RTT round-trip time.
SGSN serving GPRS support node.
SGW serving gateway.
SSIM structural similarity.
STB set-top-box.
UMTS universal mobile telecommunications system.
WLAN wireless local area network.



Introduction

Television won't be able to hold onto any market it captures after the first six months. People will soon get tired of staring at a plywood box every night.

—Darryl F. Zanuck, president, 20th Century Fox, 1946

Since Swinton (1908) described its theory of “Distant electric vision” in *Nature*, television and—as a consequence—ourselves changed dramatically. Today, television plays an important role in the day-by-day life, the broadcast industry shapes our knowledge, desire, expectation, and vision of future.

Several countries made a commitment to the *digital switchover*, launching a digital terrestrial television platform, and switching off the former analogue terrestrial broadcast systems (see figure 1). The legacy services are not able to compete with the expectations of the digital generation and the efficient transport requirements of the increasing number of TV channels any more. The regulatory force speeds up the transition, and creates a demand for digital and interactive television (Adda and Ottaviani 2005; Iosifidis 2006). The age of the analogue broadcast comes to its end, and the digital services will emerge in the next years, which create a perfect opportunity for internet protocol television (IPTV).

The Internet era, as the second driving force in the last decade, triggered an evolution in the telecommunication industry. In spite of the increasing share of fixed broadband connections, the revenue of the fixed line retail services continues to decline, reported the Commerce Commission (2011). To preserve business profitability, the legacy telecommunication industry extended its portfolio with various value adding services, like rich communication, mobile payment, and triple-play services to attract customers. This successful strategy resulted a higher revenue, but the growing market of the new generation over-the-top (OTT) services challenged the competitiveness of these triple-play services.



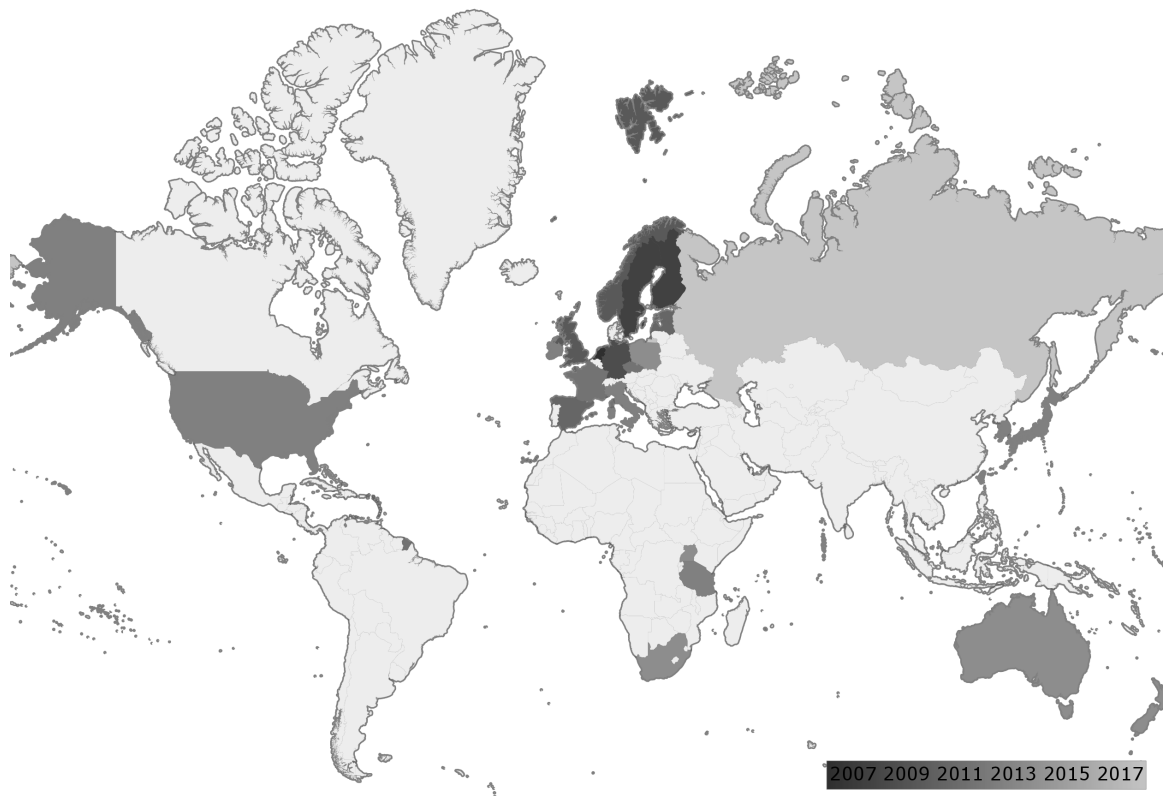


Figure 1. Analogue switch-off date in various countries. Data from DigiTAG 2013

Google recently introduced its interactive TV platform (Guardian US 2012; Choudhary 2010), which combines the television and web user experiences. Microsoft positioned the XBox One console as an equivalent gaming and home entertainment device (Microsoft 2013, 2006). Apple announced that HBO Go and WatchESPN come to AppleTV (Apple 2012a, 2013) and extended the features of its successful iTunes service (Apple 2012b). Amazon released an iPad application to access its on-demand video portal, and entered into contracts with several content owners to enlarge the content base of its video services (Amazon.com, Inc. 2013a, 2013b, 2012). It can be clearly seen that there is a big race for the customers and the telekom sector has to assess these threats and opportunities from OTT players with enhanced television and video services.

The Global IPTV Forecasts report estimates that the number of subscribers, paying for IPTV service in 97 countries, will double in the next 5 years (see table 1). This means a 15% yearly growth rate between 2013 and 2018, which will be resulted by the new IPTV deployments mainly in Asia (Broadband TV News 2013) and by the increasing penetration of IPTV again the traditional broadcast technologies. From financial point of view, the revenue will shoot up to \$21 billion from \$12.0 billion in



Table 1. Global IPTV forecasts

| | 2012 | 2013 | 2018 |
|----------------------------------|-----------|-----------|-----------|
| TV households (thousands) | 1,438,918 | 1,461,553 | 1,580,224 |
| Pay IPTV subscribers (thousands) | 69,369 | 88,294 | 167,247 |
| IPTV penetration (%) | 4.8 | 6.0 | 10.6 |
| Revenues (\$ millions) | 12,041 | 14,224 | 21,321 |

Note: Data from Murray 2013

2018.

Recognizing this importance and business potential, I decided to choose the *enhanced methods of IPTV delivery* for the topic of my research. In this dissertation, I investigate and develop new solutions for service quality improvements and competitive pricing methods for IPTV systems. In chapter 2, I propose an optimal bandwidth allocation method and a new retransmission algorithm for IPTV delivery to enable IPTV operators to extend their services with wireless local area network (WLAN) technologies, overcome the negative effect of the wireless transport, and increase service quality. In chapter 3, I present a novel approach for IPTV charging, based on service quality, with the aim of implementing a fair pricing model and increase customer's satisfaction.

In my opinion, these methods will help IPTV service providers to remain competitive on the market and attract new customers with the state-of-the-art technology.



Chapter 1

Materials and Methods

Let me begin my dissertation by describing the tools and methods, used during my research, with the aim of providing a solid basis for the readers to validate and reproduce my results. This chapter provides only a brief overview of these instruments, for further details, please refer to the given sources.

1.1 Terminology

I chose the terminology of Open IPTV Forum specification release 2 (Open IPTV Forum 2011) to describe the IPTV features in my dissertation, because I experienced a wide diversity of terms in several articles, which may confuse the reader. I believe, that the The Open IPTV Forum (OIPF) terms are straightforward, and they can be easily interpreted on any IPTV solutions, though my work is independent from the standard itself.

Some of the terms may sound unfamiliar, therefore I provide a small excerpt in the glossary to help the reader's accommodation to these expressions.

1.2 Markov Models

Several studies discussed that the loss attributes of the Internet and the wireless network traffic follow a random pattern, which can be effectively described by stochastic processes. One of the most widely used model is the discrete time Markov chain, which is able to capture the true nature of these connections, and predict the steady state packet loss rate and the probability of burst error losses, which parameters are essential for video transport evaluations.

To introduce the Markov chain, consider the series of an independent, identically distributed X_1, X_2, \dots, X_n random variables with the state space S , ($X_i \in S$) as the



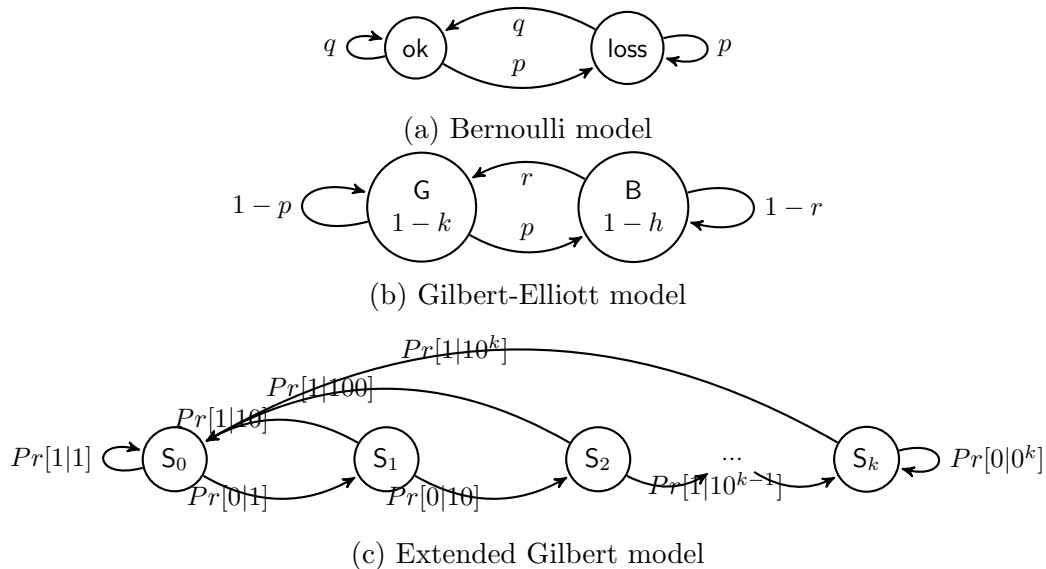


Figure 1.1. Different Markov chains

model of IP packet transmission. If the loss events can be considered independent, then X_n possess the Markov property (1.1), and can be described with a Markov chain:

$$P(X_{n+1} = x | X_1 = x_1, X_2 = x_2, \dots, X_n = x_n) = P(X_{n+1} = x | X_n = x_n). \quad (1.1)$$

The Bernoulli model is one of the simplest model of packet loss characterization for IP audio and multicast systems. It consist of only two states, describing successful and failed packet transmission (figure 1.1a). The p transition probability represents the probability of the current packet being transmitted, given the last packet was lost. The q transition probability represents the probability that the current packet was lost given the previous packet was transmitted. The predicted loss probabilities follows a geometric distribution.

The Gilbert-Elliott model (figure 1.1b) is widely used for analyzing the efficiency of coding for error detection and correction. Each state may generate errors as independent events at a state dependent error rate of $1 - k$ in the good and $1 - h$ in the bad state, respectively.

There are several other, complex models, like the Extended Gilbert Model (figure 1.1c), which is able to more accurately predict a more advanced loss situation.



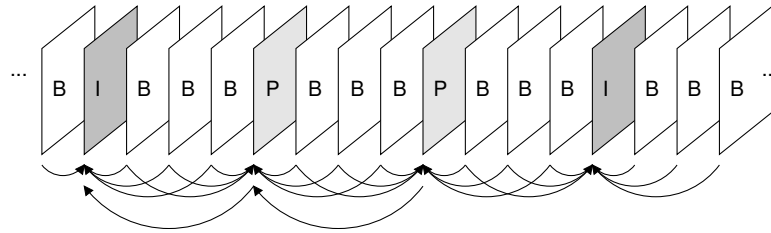


Figure 1.2. Sample frame structure in MPEG-4 AVC. The decoding dependences in an IBBBBP group of pictures are marked by the arrows.

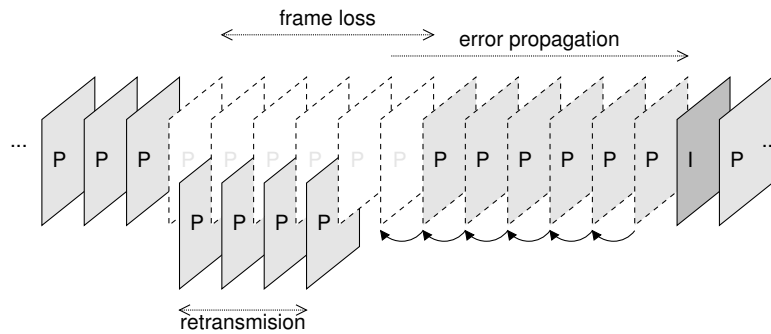


Figure 1.3. Error propagation in MPEG-4 AVC. In case of consecutive loss of frames, the IPTV solution may request the retransmission of the lost frames, but if a retransmitted frame does not arrive (or arrives too late), the decoder is not able to use it as a reference for further decoding, therefore the error propagates through the sequence.

1.3 H.264/MPEG-4 AVC

The MPEG-4 standard describes three main types of encoded frames (see figure 1.2): *I frames* are intra coded images (reference frames), coded independently of other frames. *P frames* are coded predicatively from the closest previous reference frame, and they serve as reference frames as well. *B frames* are coded bi-directionally from the preceding and succeeding reference frames.

The decoding of a multimedia stream depends on the successful receipt of the reference frames. If there is a packet loss with a reference frame, then the decoding of all dependent frames fails, the error propagates through the video sequence till the next I frame (figure 1.3). This causes skewing and degrades the quality. On the other hand, if there is a packet loss with a non reference frame, it causes only a small, mostly imperceptible pixelisation on a small part of the display. If the loss distribution is bursty, then the longer the loss burst, the higher the probability of loss of an I frame, therefore the quality of the streaming is determined by the loss distribution, and not by the average loss rate. I also note, that it is essential to avoid error propagation, which can be achieved by packet retransmission, forward error correction algorithms, or error concealment feature.



1.4 Streaming Protocols

Streaming is a network technology to real-time transmit scheduled content service or content on demand multimedia from one centralized streaming server to many clients on a wide network, used also in IPTV solutions. The technology usually implemented by unicast or multicast IP transport and it represents three, separate planes, based on the same IP network layer: management, transport and quality control plane (Kim and Park, 2005).

The management plane allows the users to control the streaming, such as: connection opening and closing, getting information about the media, preparing the server for the broadcast, and starting, pausing, and stopping the delivery. The transport plane provides the real time data delivery; it reserves the greatest part of available bandwidth. It must adjust oneself to the variable network parameters, so it cooperates with the quality control plane to avoid jitter and traffic congestion. The quality control plane measures the transport actual quality, and generates quality of service (QoS) reports for both sides.

Bandwidth

The available bandwidth between two points in a packed switched network is generally unknown and time varying. If the sender transmits faster than the available bandwidth then congestion occurs, packets are lost at the IP routers, which may cause deterioration in video quality. If the sender transmits slower than the available bandwidth, then the receiver produces sub-optimal video quality.

Delay and jitter

The end-to-end delay of an IP packet transmission may fluctuate. This variation in end-to-end delay is referred to as the jitter. Jitter could jeopardize the streaming quality, because the receiver must decode and display frames according to a predetermined timing, but high jitter could delay frames, which has to be excluded from the decoding process, if they arrive too late. This problem is typically addressed by implementing a playout buffer at the client, while it also introduces an additional, but constant delay.



1.5 Image Quality Metrics

The evaluation of the quality of a video codec or a quality degradation, caused by a frame loss, requires mathematical methods, which are able to provide an objective basis for comparison. To achieve this goal, several reference based image quality metrics have been developed, the peak signal noise ratio (PSNR) is one of the well known ones (Q. Huynh-Thu and M. Ghanbari 2008):

$$PSNR = 10 \log \left(\frac{MAX^2}{MSE} \right), \quad (1.2)$$

where MSE is the mean square error of the frame pixels.

Quan Huynh-Thu and Mohammed Ghanbari; Girod (2008; 1993) argue that a quality comparison of two images with PSNR provides valid results only, if the content of the two sequences are the same (only the encoding parameters are changed), but inaccurate and inappropriate comparing two different sources, because the calculated quality value highly depends on the content itself. To overcome this problem, Z. Wang et al. (2004) propose a new metric: the structural similarity (SSIM).

$$SSIM(f, g) = l(f, g) \cdot c(f, g) \cdot s(f, g), \text{ where} \quad (1.3)$$

$$l(f, g) = \frac{2\mu_f\mu_g + C_1}{\mu_f^2 + \mu_g^2 + C_1},$$

$$c(f, g) = \frac{2\sigma_f\sigma_g + C_2}{\sigma_f^2 + \sigma_g^2 + C_2},$$

$$s(f, g) = \frac{2\sigma_{fg} + C_3}{\sigma_f\sigma_g + C_3}.$$

The first term in (1.3) is the luminance comparison function, which measures the closeness of the two images' mean luminance (μ_f and μ_g). This factor is maximal and equal to 1 only if $\mu_f = \mu_g$. The second term is the contrast comparison function, which measures the closeness of the contrast of the two images. Here, the contrast is measured by the standard deviation σ_f and σ_g . This term is maximal and equal to 1 only if $\sigma_f = \sigma_g$. The third term is the structure comparison function, which measures the correlation coefficient between the two images f and g . Note, that σ_{fg} is the covariance between f and g . The positive values of the SSIM index are in $[0,1]$. A value of 0 means no correlation between images, and 1 means that $f = g$. The positive constants C_1 , C_2 , and C_3 are used to avoid a null denominator. Hore and Ziou (2010) analyzes the relation between PSNR and SSIM more deeply.



Kim and Park; Jain and Bhateja; Punchihewa, Bailey, and Hodgson; Bhat, Richardson, and Kannangara (2009; 2011; 2005; 2010) introduce other various image quality metrics as well.

1.6 Test Sequences, Video Encoding, and Error Concealment

The empirical evaluation of my work requires sample video sequences, encoding and decoding functionalities. I decided, that I will consecutively use the video sources introduced by Seeling and Reisslein (2012), because they are well known and widely used in several research article. This approach enables the easy validation of my own findings, though I extended this collection with two other sources to provide a broader basis for evaluation (see table 1.1).

Table 1.1. Test sequences

| Name | Length (minute) | Frames | Size | fps | Source |
|----------------|--------------------|--------|------|-----|----------------------------|
| bigbuckbunny | 10 | 14,315 | CIF | 24 | Seeling and Reisslein 2012 |
| startrek | 10 | 14,400 | CIF | 24 | BDRip |
| thehobbit | 10 | 14,400 | CIF | 24 | BDRip |
| foreman | 0.16 | 300 | CIF | 30 | Seeling and Reisslein 2012 |
| bridge (close) | 1 | 2,001 | CIF | 30 | Seeling and Reisslein 2012 |
| highway | 1 | 2,000 | CIF | 30 | Seeling and Reisslein 2012 |

To evaluate the video quality deterioration, caused by frame losses, I use the JM Reference Software (Tourapis et al. n.d.). The 18.4 decoder version has correctly implemented the error-concealment feature, which I highlight in figure 1.4 and 1.5. I encoded the foreman video sequence with the reference encoder, and then I proceed with the following two cases: first, the unmodified H.264 sequence was decoded to provide a basis for comparison showed by figure 1.4. Second, a frame loss was modeled by manually overwriting the network abstraction layer unit of the 99th frame with zeros, and the decoding function was also applied with error-concealment turned on. Figure 1.5 shows that the decoder recognized the loss event, and to mitigate the effect of the loss, it repeated the previous successfully decoded frame, however the propagation of the error can be observed on later frames as expected. (The detailed settings of the encoder and decoder software are enclosed in appendix B.)



Figure 1.4. Correct sequence



Figure 1.5. Error concealment. The 99th frame was lost during transmission, therefore the error concealment feature repeated the 98th frame to mitigate decoding error propagation. Due to the inappropriate precedent frame, a small blockiness (marked with an arrow) can be observed in the upcoming frames compared to correct decoding.

1.7 Tools and Testbed

This section introduces the environments, created for the evaluation of my models and methods. I carefully considered the realization of an NS2 simulation (Mccanne, Floyd, and Fall n.d.), but I found that the required efforts to implement such a complex element like a retransmission function would be too great compared to the easy setup of a testbed. My arguments are:

- NS2 supports only a bidirectional implementation of a custom protocol agent (one sink–receiver pair), but the retransmission (RET) function requires more complex interfaces.
- The implementation of the wireless multicast IP communication is complex in NS2.
- The next generation simulation environment (NS3) provides a better support, but it contains only a fraction of wireless simulation modules.
- A testbed can be realized in very short time, and all the measurements and tests can be conducted.

I did not conclude any disadvantages of implementing a testbed environment, therefore I followed the OIPF System Architecture (Open IPTV Forum 2011), and implemented the following OIPF functions showed by figure 1.6, with the aim of evaluating my model and methods in chapter 2.

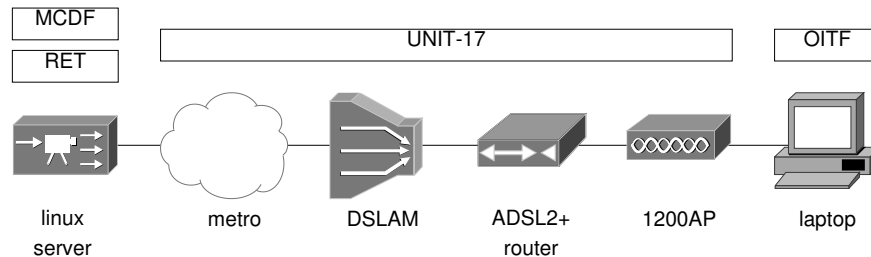


Figure 1.6. Testbed for IPTV retransmission simulation

Multicast content delivery function (MCDF). My c++ application (ser.cpp), a simple H.264 packetizer, generates UDP/RTP multicast traffic based on the RFC 6184 (Y.-K. Wang et al. 2011), and implements a simple control protocol. Hosted by an x86 Linux server connected to the core network of Deutsche Telekom (DT).

Retransmission server (RET). My own c++ application (ret.cpp), captures the multicast traffic in a circular buffer, and implements a simple retransmission request protocol. Hosted by the same x86 Linux server.

Unit-17 interface, part a. Core metro network of DT.

Unit-17 interface, part b. Digital subscriber line access multiplexer (DSLAM).

Unit-17 interface, part c. Realized by the ADSL2+ access network of DT, provided by a Speedport 720w ADSL2+ modem. (The configuration and statistics of the modem is enclosed in appendix A.)

Unit-17 interface, part d. Realized by a 802.11b WLAN network, provided by a Cisco 1200 series wireless access point, connected to the asymmetric DSL modem. (The configuration of the device is enclosed in appendix A.)

Open IPTV terminal function (OITF). My own c++ application (cli.cpp), implements a simple multicast receiver and control functions of the multicast content delivery function and RET Server. Hosted on a x86 Linux laptop, connected to the Cisco access point.

I built a second testbed based on the 3GPP charging architecture principles to conduct the measurements required by chapter 3, showed in figure 1.7.

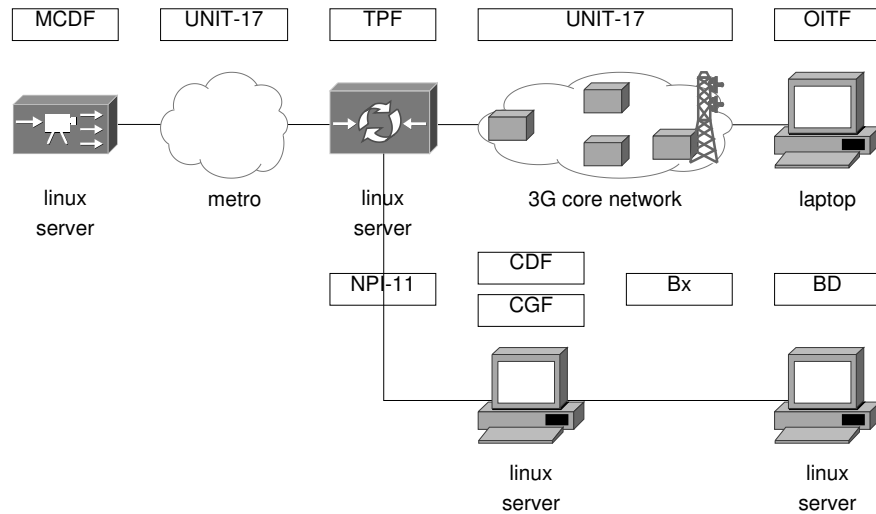


Figure 1.7. Testbed for quality based charging simulation

Multicast content delivery function (MCDF). c++ application, developed by myself (ser2.cpp), a simple H.264 packetizer, generates UDP/RTP multicast traffic based on the RFC 6184 (Y.-K. Wang et al. 2011), and implements a simple control protocol. Hosted by an x86 Linux server, connected to the core network of DT.

Unit-17 interface, part a. Core metro network of DT.

Transport processing function (TPF). My c++ application, a simple transparent streaming proxy based on the PCAP library. This functional entity includes the functions needed to support real-time multicast and unicast streams, optimizing network usage in the physical network, and enforcing related traffic policies coming from resource and admission control.

Unit-17 interface, part b. 3G mobile network of DT.

OITF. My c++ application (cli2.cpp), a simple UDP/RTP receiver, which implements the basic client functionality, streaming server control protocol, and an internal jitter buffer. The application issues commands for the streaming server, receives the RTP/UDP stream. It continuously analyzes the streaming flow and periodically reports the loss pattern according to the proposed RTSP-RR format to the steaming server. Hosted on a x86 Linux laptop with 4G data card.

NPI-11. Reference point for sending events and charging information. This is the Rf reference point defined by 3GPP (3rd Generation Partnership Project 2010b).

Charging data function (CDF). The CDF receives charging events from the CDF via the Rf reference point. It uses the information contained in the charging events to construct a charging data record (CDR).

Charging gateway function (CGF). My own script collection (ana.cpp, mse.cpp, hist.cpp, createtrace.sh, decompress.sh). The CDRs produced by the CDF are transferred immediately to the charging gateway function (CGF) via the Ga reference point. The CGF acts as a gateway between the 3GPP network and the billing domain. It uses the Bx reference point for the transfer of CDR files to the BD. It implements a basic charging gateway functionality. It correlates the receiver report files, and based on the metadata description, it estimates the quality of the streaming session (total distortion: $D[\kappa]$), and creates the appropriate charging data records, incorporating the quality estimate.

Bx. The Bx reference point supports interaction between a charging gateway function and the billing domain. The information crossing this reference point is comprised of CDR files. Implemented by a common, standard file transfer protocol, e.g. FTAM (file transfer, access and management) or FTP.

Billing domain (BD). My own c++ application (chg.cpp), implements the quality based charging functions inclusive the quality based policy decision, and creates the bill and discount for the streaming session.

The source codes of the implemented functions are available for download on <http://www.mcl.hu/~jursonovics>.

Chapter 2

Retransmission in IPTV Solutions over Burst-Error Channels

In the last decade, we have observed the rapid evolution of the IPTV services. The high-definition broadcast got popular since its introduction in 2004, and the accessibility of 3D content is growing year by year. The consumer electronic devices become integrated part of our life, customers access digital content from set-top boxes (STBs) to game consoles and mobile devices. In spite of the advanced methods, the main technology of providing Internet access remained the same, 20–30 years old twisted copper pairs, which barely able to fulfill the transport requirements of these new services (Canadian Radio-television and Telecommunications Commission 2012).

The IPTV service providers are interested by the maximization of their customer reach, but in many cases, long digital subscriber lines (DSLs) offer inadequate bandwidth for high definition services (Open IPTV Forum 2011). The network providers need to find a solution that enables them to utilize their current infrastructure. The answers may include the implementation of a more advanced encoding algorithm (H.264, H.265), which results in having the same quality on smaller throughput (Abramowski 2011); the introduction of a hybrid service, which replaces the most bandwidth consuming scheduled content service transport with digital video broadcasting (DVB-X) technology (Benoit 2008); the usage of progressive download; or—as I point out in my work—the implementation of a more effective bandwidth allocation in the access network, which will ensure a more efficient transport.

Besides optimizing delivery, IPTV service providers must face the new problem of mobile entertainment devices. Customers access content not only on STBs, but also from various hand-held devices. Today, the prime wireless technology within the consumer domain is the wireless local area network (WLAN), therefore operators have to adapt their IPTV solutions to support the specific requirements of this



communication channel. In addition to that, the rapid evolution of the WLAN technology enables set-top-box (STB) manufacturers to build a wireless interface into the devices (Sanchez et al. 2010), which creates value for customers by saving the effort of in-house cabling or the purchase of expensive powerline adapters.

Today, the core transport technology of the IPTV service is not sufficient for wireless delivery, it is not able to effectively handle the special requirements and attributes of the mixed, DSL and WLAN environment (Jursonovics and Imre 2013). As conclusion, I formulate my research question on the following way:

How can the quality of the traditional xDSL delivery of IPTV services, extended over WLAN networks, be enhanced to ensure excellent service delivery?

If IPTV service providers could improve the key factors and processes, which influences the IPTV delivery in a environment of mixed access technologies (xDSL and WLAN), they could increase the service quality, and—therefore—the customer satisfaction. Consecutively, they could also achieve progress in several other areas:

- **Cost saving:** telecommunication enterprises are challenged to achieve better efficiency and optimize their internal processes to operate with lower costs. Today, by a major US Internet provider, the installation time of a triple-play service takes about four hours (Multimedia Research Group 2008), but the introduction of a wireless STB could reduces the time of on site installation to three hours, and provides a real differentiator from cable providers by making the cabling unnecessary and improving the customer's satisfaction.
- **Service portability:** WLAN technology allows users to access the entertainment services more conveniently within the household on a tablet, or on the go on mobile devices.
- **Operational complexity:** maintaining one single, multipurpose IPTV platform instead of many, dedicated to legacy and OTT services, significantly reduces the operational costs and efforts on long term.

In this chapter, I address my research question and develop new methods for the optimization of IPTV delivery. First, I claim that the traditional IPTV solutions does not address both the limited resource environment of the xDSL technology and the specific requirements of the wireless channels at the same time. Second, quality



is determined by the bandwidth allocation, which is limited by the three aspects of packet retransmission: *general*, *intra-burst*, and *inter-burst*. Third, the packet loss and packet retransmission can be described by stochastic processes, which I unite in one, single model of *three state channel model (3SCM)*. Fourth, I define the optimal bandwidth allocation, which will ensure the maximal quality of service. Finally, I describe a new retransmission algorithm, which improves the quality of the IPTV delivery in wireless networks.

2.1 Literature Review

The technology of packet retransmission is already widely discussed by research papers and described in several standards. In this section, I am going to highlight those most important works and specifications, which are closely related to my research, and which are required to understand my effort and results.

2.1.1 Open IPTV Forum

The The Open IPTV Forum (OIPF) was founded in 2007, with the aim of creating an open, end to end IPTV specification that will serve as a future, interoperable guideline for industry partners, as STB manufacturers, middleware providers, head-end developers, and so on. Today, OIPF unites 47 members from all around the globe. Several partners (for instance, Huawei Technologies, Ericsson) already adapted the guideline, and developed their solutions accordingly.

The release 2 specifications divide the IPTV landscape in three main parts: managed, non-managed, and residential networks; and clearly differentiate the following four roles in the content flow: content provider, IPTV provider, service platform provider, and access provider. Several business models were developed among this segregation, which are individually considered by the flexible system design. The architecture is modular, and the interfaces among the individual domains are clearly defined.

One of the most important achievement of OPIF is the specification of the *Declarative Application Environment* (Open IPTV Forum 2011), which unites all the user interfaces in a CE-HTML based rich application development kit. This allows the easily integration of the identical user experience on a broad device basis from tablets, mobile phones, smart TVs till legacy STBs, and ensures the cheap development and interoperability of applications.



Concerning the multimedia delivery, OIPF relies on the well known network technologies (RTSP and multicast RTP), and extends them by the required components for managed networks: FCC/RET server and transport processing function are defined, which are responsible for reliable transport and network QoS enforcement, respectively. In my research, I adopt the system architecture and network technologies described by the OIPF standard to provide a general solution for my research goals.

The concept of modularity ensures two main advantages for telecom operators. The standard can be partially applied, and the system components can be easily exchanged, which allows the deeper implementation of a cost effective, dual vendor strategy. Any system component can be exchanged in any time, and the existing—typically charging and user management—system can be integrated with low effort.

I believe, that using this common framework for interpreting my results will provide substantial benefits, however, only a few commercial IPTV solution complies with the OIPF standard. The reason lies in the long system life cycle, which is resulted by the high initial investment, and the problematic of system upgrade. OIPF is a young organization, most of the telecom operators have already deployed their IPTV systems before. For a possible migration, all the STBs have to be upgraded remotely on the field, which is an extreme challenge for the monolithic, old systems.

2.1.2 ITU-T, ETSI

ITU Telecommunication Standardization Sector (ITU-T) is a global standardization institute with its headquarter in Geneva. ITU-T unites the experts from various fields, and creates industry wide recommendations for different areas of telecommunication. The ITU-T IPTV Global Standards Initiative was founded in 2007 with the aim of taking over the former work from the IPTV Focus Group and unite the several streams of IPTV standardization. ETSI, the European Telecommunications Standards Institute, produces globally-applicable standards for information and communications technologies, including fixed, mobile, radio, converged, broadcast, and internet technologies.

The approach of ITU-T, ETSI TISPAN unites the diverse access infrastructures of mobile, ISDN, IP, cable television systems in the next generation network, defines a multi service IP backbone, and a common, service & network control layer. This ensures a single, simple, and cost effective infrastructure for existing and new services, including IPTV. The recommendation considers the integration of the IP multimedia subsystem (IMS), which provides a seamless, integrated services opportunity.



This direction allows the implementation of higher, standardized open protocols, the separation of multimedia control and content delivery, TISPAN based QoS management, and shared service enablers to support more complex applications.

The driving forces behind this direction includes the opportunity to provide a convergent platform to deliver IPTV services and the possibility for applications to benefit from the initial investment of the IMS platform. In my opinion, the limited number of IMS capable true multimedia devices and the increasing penetration of over the top services already jeopardized the relevance of this approach, and IMS lost its original goal to be main service delivery platform in telecommunication.

2.1.3 Proprietary Solutions

It is important to address the topic of proprietary IPTV solutions, because they are widely used by several big telecommunication companies. They represent a quasi de-facto standard among industry players, but there are only marginal public information available on the technology, therefore I do not incorporate them in my dissertation. I think, that my results and conclusions can be interpreted with slight modifications here as well.

One example is the MediaroomTM platform (Ericsson 2013). This solution uses a monolithic system architecture, and implements different approach for application development by introducing the so called presentation framework application development kit. Microsoft already implemented a special version of retransmission service (called “R-UDP”) to overcome the negative effect of packet losses, which is very similar to the retransmission solution described in my dissertation.

2.1.4 DCCP

The delivery of an IPTV service requires reliable and low latency stream of datagrams to ensure high service quality. The standard transport layer protocols (TCP/UDP) only provide one of these two criteria: TCP achieves loss-free, in-sequence connection, however the individual value of the transmission delay can diverge from each other. UDP results low jitter, but the multimedia service could suffer from packet losses. The data congestion control protocol (DCCP) provides a compromise for multimedia systems: it implements bidirectional, unicast connections of congestion-controlled, unreliable datagrams (Kohler, Handley, and Floyd 2006). Compared to the application layer retransmission, proposed by my dissertation, DCCP assigns the



retransmission feature to a lower layer protocol, therefore media player can be implemented transparently to this feature, and no additional retransmission elements are required, but at the same time, all streaming components have to support this protocol. Unfortunately, DCCP is not part of the standard operating systems, it is used only in systems for academic purposes, therefore this protocol is out of consideration for my research.

2.1.5 State-of-the-Art Research

Several research addresses the quality improvement of the multimedia transmission on the radio bearer level. Lombardo, Panarello, and Schembra (2013) present a Markovian approach to optimize the energy consumption of the radio interface during rate adaptive multimedia transport. A new algorithm is developed and a cross layer approach is applied introducing a source rate controller. The automatic repeat-request (ARQ) protocol is modified, which successfully exploits of the correlation of the wireless channel behavior for power optimization.

Shih, Ke, and Xu (2013) investigate the effect of the ARQ mechanism in wireless network on the DCCP transport-layer protocol. The paper states that the partial payload protection mechanism can be inefficient owing to media access control (MAC) layer retransmissions, while varying packet size has an adverse effect on the TCP-friendliness of DCCP flows. The authors propose two solutions, namely (i) a DCCP protocol enhancement to benefit the partial payload protection mechanism by utilizing the ARQ retransmissions and then (ii) an in-packet segmentation scheme to improve the data throughput while preserving the TCP-friendliness of the DCCP flows. Both solutions promise great improvements, but in relation to my research, they are strongly related to the low layer wireless protocols, which prevents to offer an end to end, technology independent solution, which is my primary goal in my dissertation.

Becke et al. (2013) emphasizes that the popularity of mobile devices, smart phones, and tablet computers; the number of end-systems with more than one network access, like universal mobile telecommunications system (UMTS), long term evolution (LTE) and WLAN, are strongly increasing. This so-called multi-homing also leads to the desire of utilizing multiple network paths simultaneously, in order to improve application payload throughput. The research introduces two new send strategies to map payload data to different wireless paths by using measurements, and shows that a significant performance improvement for delay and loss-sensitive applications can be achieved in comparison to the existing approaches.



These approaches are effective for a specific wireless technology or environment, but in many cases, the IPTV Provider has no control on the various Internet access devices, deployed by the customers in the households. As I highlighted in the introduction, a more general approach is required, which can address the quality improvement on the application level.

Huszák and Imre (2008; 2006) present an application layer solution for multimedia streaming. The study points out that the retransmission algorithm can be optimized by differentiating the importance of the different packets. These efforts do solve the problem of user owned devices, but they do not address the limited environment of the access network for IPTV delivery. These two effects, the wireless transport and the limited resource environment of the DSL access lines have to be addressed in a universal, common model to ensure optimal service delivery.

Huszák and Imre (2009) also introduces a second approach for content-aware interface selection method for multi-path video streaming in best-effort networks, which chooses a set of paths maximizing the overall quality at the client. While the available paths have different bandwidth, delay and loss probability constraints, the packet distributor must take the video packet importance and the dependence between packets into account. Transmitting the reference video frames on the most reliable links will decrease the loss probability of important data packets and increase the measured video quality. The results show that the proposed solution provides higher video quality than common scheduling algorithms. This approach may extend my own conclusions, in which I do not consider the different frame types (see 2.4), but it could further improve the quality of the transmission.

2.2 Theory

This section provides an overview on the most important theoretical principles to allow the reader to understand the background of my research question and the following discussion in 2.3.

2.2.1 Bandwidth Allocation in IPTV Solutions

Let me continue by the introduction of a typical triple-play bandwidth allocation scheme in figure 2.1. Access network providers usually dedicate a reserved bandwidth in the access network for voice communication, and share the remaining throughput between IPTV and Internet services with a priority for the former one.

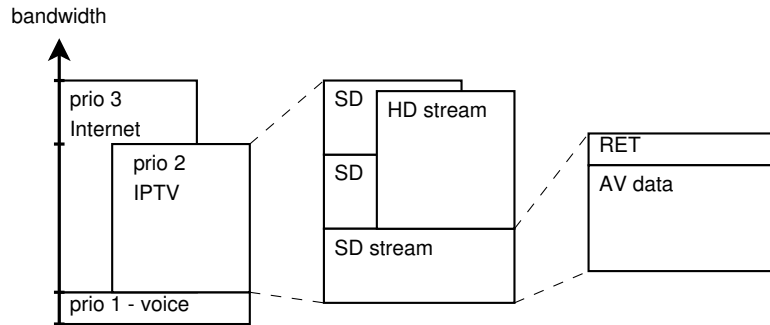


Figure 2.1. Bandwidth allocation in the access network

The actual throughput of IPTV service depends on the user's service profile. In most of the cases, a token-based stream management (or an overall throughput calculation based algorithm) allows the customers to simultaneously receive multiple streams for scheduled content service and personal video recorder (1SD+1HD or 3SD+0HD). One token allocates bandwidth for the audio-video (AV) data transport and reserves a dedicated bandwidth for the packet retransmission (RET) service, which may correct a packet loss by a retransmission feature.

The balance, between the assigned bandwidth for AV data and RET service, is crucial for providing maximal quality in IPTV solutions. The AV throughput is constant in time due to the widely applied constant bitrate video encoding. On one hand, the more throughput is assigned for the AV data, the better stream quality can be achieved by the increase of the encoding bitrate, but the less opportunity is given for error correction. A smooth, sharp stream may be disturbed by blocking or full frame outages due to the insufficient RET throughput. On the other hand, reserving high bandwidth for error correction degrades the overall stream quality due to the low encoding bitrate. Based on different network installations, the ratio of RET bandwidth to AV data is usually tuned between 10% and 25%, however a suboptimal value may significantly reduce the throughput and—consequently—the quality of the IPTV service.

PROBLEM 2.1. *The optimal selection of the reserved bandwidth for retransmission services is crucial to achieve the maximal IPTV service quality. A suboptimal value may jeopardizes the IPTV user experience.*

The main concept and benefit of my research is showed by figure 2.2. The solid line represents the theoretical throughput of the AV data stream at various packet loss probabilities in case of static bandwidth allocation. The function is constant till $P_{overload}$ loss probability, where the loss rate is so high that the retransmission



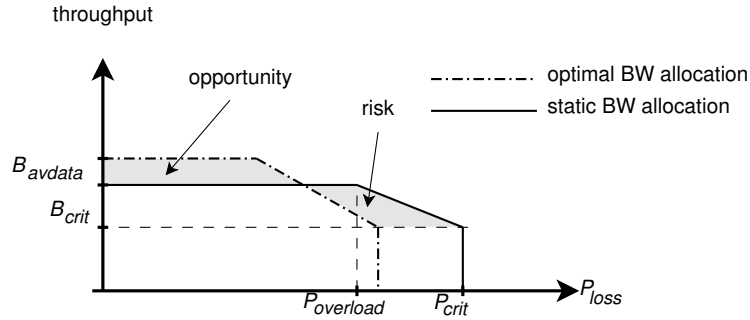


Figure 2.2. Leveraging optimal bandwidth allocation. By increasing the share of the audio-video transport in the bandwidth allocation scheme, an increased video quality can be achieved (opportunity), but the transport will be less tolerant for packet losses (risk).

traffic fully occupies its reserved bandwidth. Above this rate, the retransmission does not have enough bandwidth to recover all the packet losses therefore the actual throughput of AV data stream is decreasing (due to the not transmitted packets), customers experience quality deterioration. Below the B_{crit} critical bandwidth value, the IPTV service is not feasible due to the massive losses. If the service provider is able to more precisely allocate the bandwidth for AV transmission then it can achieve a better quality (opportunity), however the distribution will be less tolerant for transmission errors (marked with risk).

To find the answer for my research question, I investigate three aspects of the limitation of packet retransmission and formulate my solution to problem 2.1. I state my first thesis on the quality of the IPTV service followed by its discussion:

THESIS I.1 (Jursonovics and Imre 2013). *I claim that the optimal bandwidth allocation prevents frame losses due late packet arrival compared to its playout time. Considering the general, intra- and inter-burst limitations, there is an inverse relationship between the optimal bandwidth allocation and the playout buffer, and a direct relation with the round trip time and average packet size according to (2.13). I determined this optimal allocation by a minimization problem described in (2.6).*

2.2.1.1 Limitation of retransmission: general aspect

The bandwidth allocation of an IPTV solution reserves a dedicated bandwidth for retransmission requests to overcome the effect of packet losses. Figure 2.3 shows a typical scenario in case of a long burst of losses, where the retransmission server produces an out of band peak retransmission traffic, which may cause congestion (and therefore loss) for parallel streams. I show in the upcoming sections that certain loss



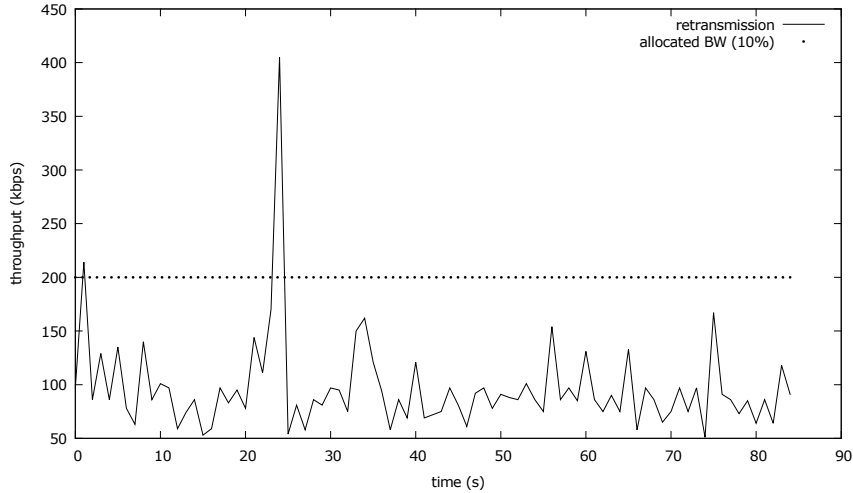


Figure 2.3. Out-of-band packet retransmission. A massive packet loss in the IPTV delivery caused a short burst of packet retransmission, which resulted to higher throughput than the allocated bandwidth. (A sample IPTV trace, capture by the author on the Entertain IPTV product of Deutsche Telekom.)

effects can jeopardize the efforts of error correction, and could cause a much worse congestion scenario, which has to be avoided.

First of all, the retransmission algorithm shall follow the obvious rule that the average retransmission throughput cannot exceed the allocated retransmission bandwidth. I assume that quasi equal size of packets are generated¹, therefore from n consecutive packets, the maximal number of retransmitted packets $k \in \mathbb{N}$ is

$$k_{R,general,max}(n) = n \frac{B_{RET}}{B_{AV}}. \quad (2.1)$$

PROBLEM 2.2. *The throughput of retransmission traffic should not exceed the allocated bandwidth to avoid the negative effects of congestion.*

2.2.1.2 Limitation of retransmission: intra-bursts

The events of the packet loss usually show a burstiness in wireless communication (Jursonovics and Butyka 2003; Jursonovics, Butyka, and Imre 2004; Nafaa, Taleb, and Murphy 2008) therefore, at first, I investigate an *intra-burst* scenario. Figure 2.4 describes three planes of the IPTV packet transmission: the *transmitter* plane represents the provider's network, *receiver* plane represents the OITF and *playout* plane the content presentation within the OITF. After the first $k \in \mathbb{N}$ consecutive packet losses

1. Please refer to the conclusion for the possible effect of this assumption on my results.



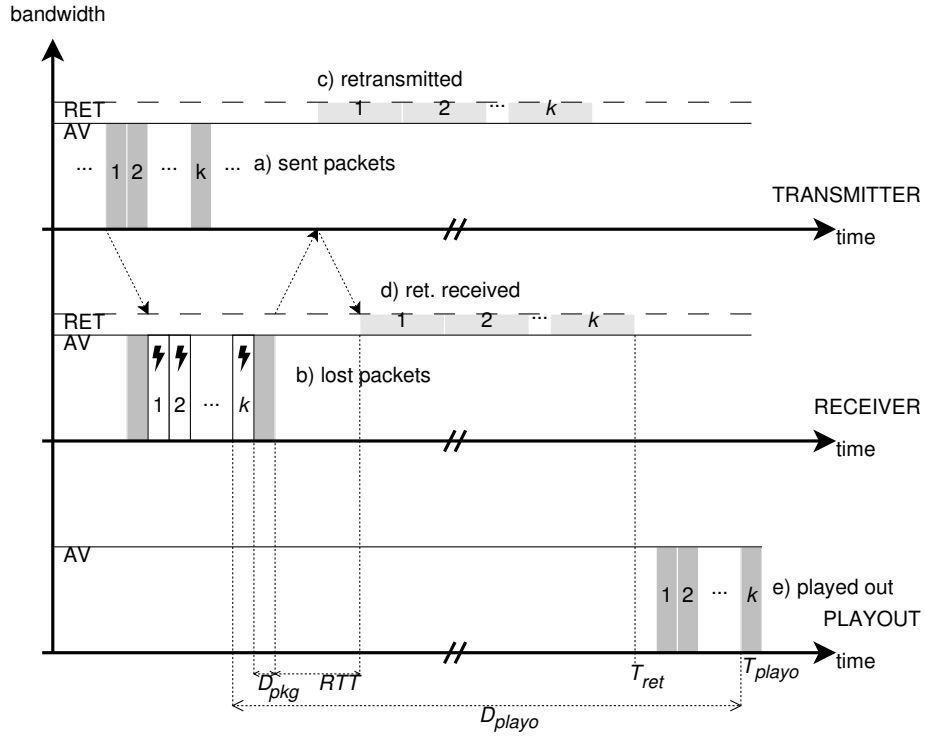


Figure 2.4. Intra-burst retransmission

(b) the receiver requests them for retransmission (c), which packets should be delivered within the allocated bandwidth for packet transmission (d) to the presentation device (e) according to problem 2.2. For a successful retransmission, all retransmitted packet should arrive earlier than their presentation time ($T_{ret} \leq T_{playo}$).

Expressing this condition with the time durations,

$$2D_{pkg} + RTT + k \frac{B_{AV}}{B_{RET}} D_{pkg} < D_{playo}, \quad (2.2)$$

where D_{pkg} is the average transmission time for a packet, RTT is the round-trip time, B_{AV} and B_{RET} are the allocated bandwidth on the communication channel, and D_{playo} is the packet playout buffer in the OITF. The formula of the maximal number of consecutive packets, which can be successfully retransmitted, is defined as

$$k_{RET,intra,max} \left(\frac{B_{RET}}{B_{AV}} \right) = \frac{D_{playo} - 2D_{pkg} - RTT}{D_{pkg}} \cdot \frac{B_{RET}}{B_{AV}}. \quad (2.3)$$

The actual throughput of the AV stream may vary by installations, therefore I expressed this value as a ratio of B_{RET} and B_{AV} . Figure 2.5 illustrates this relation at different values of D_{playo} . It can be easily observed that by 20% AV and RET ratio only 36 consecutive packet losses (approximately 1.5 s) can be retransmitted, assuming standard parameters for the IPTV transmission.



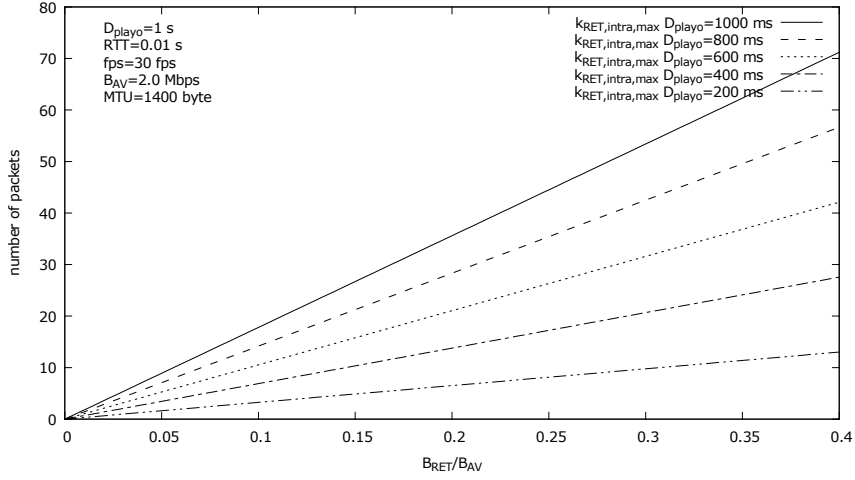


Figure 2.5. Intra-burst limitation

PROBLEM 2.3. Above a certain length of consecutive packet losses (intra-burst criterion) the retransmission will not be able to repair the packet losses therefore the retransmission of these packets are unnecessary.

2.2.1.3 Limitation of retransmission: inter-bursts

Third, I highlight the inter-burst behavior in figure 2.6. After a loss of long burst, the retransmission bandwidth is occupied by the traffic of the retransmitted packets, even if there is no other packet loss at the time in the video stream. This means that a loss event *blocks* the retransmission channel for a certain time. I am interested in the following question: assuming a $k \in \mathbb{N}, k < k_{RET,intra,max}$ long burst of loss, after how many packets ($n \in \mathbb{N}$) can a new loss burst occur, which would be also successfully retransmitted (e.g. what is the minimal distance ($n - k$) between two loss bursts, if the first burst lasts for k packets). Now $T_{ret,k} \stackrel{def}{<} T_{playo,k}$ and $T_{ret,n} \leq T_{playo,n}$, therefore

$$D_{pkg} + RTT + (k + 1) \frac{B_{AV}}{B_{RET}} D_{pkg} < (n - k - 1) D_{pkg} + D_{playo}, \quad (2.4)$$

where $n > k$. Expressing n , I obtain

$$n_{RET,inter,min} \left(k, \frac{B_{RET}}{B_{AV}} \right) = (k + 1) \frac{1}{\frac{B_{RET}}{B_{AV}}} + \frac{RTT - D_{playo}}{D_{pkg}} + k + 2. \quad (2.5)$$

Figure 2.7 shows that 6 packet loss blocks the retransmission channel for the upcoming 24 packets, assuming standard parameters for the IPTV transmission.



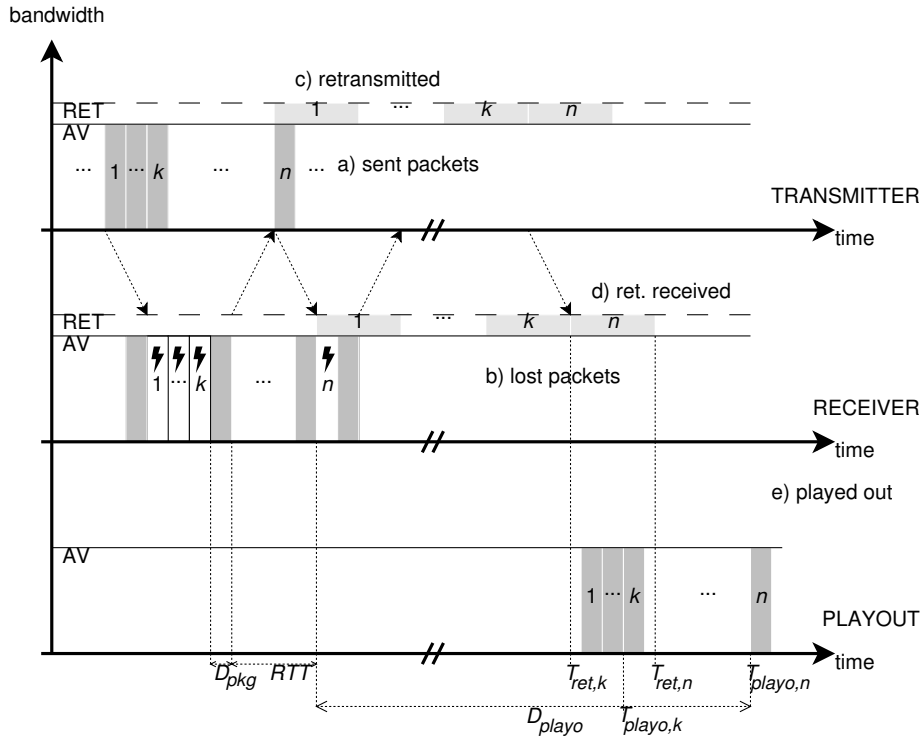


Figure 2.6. Inter-burst retransmission

PROBLEM 2.4. *The retransmission of a packet loss burst will block the allocated retransmission bandwidth therefore a second loss of packets may cause an overload on the retransmission channel.*

To support thesis I.1, I show the combined effect of the intra- and inter-burst limitation in figure 2.8. This graph tells us that at relatively small retransmission bandwidth ($\frac{B_{RET}}{B_{AV}} \approx .05$) only short burst of losses (≈ 10) can be retransmitted, and the allocated retransmission bandwidth will be blocked for a long number of packets (≈ 30). This negative effect annihilates on a slowing rate with the increase of the AV and RET ratio, but above 20% it becomes relative static compared to the intra-burst limitation; the two curves are going to fit each other. According to this effect, there is no extra gain from increasing $\frac{B_{RET}}{B_{AV}}$ above approximately 20-25%, which corresponds to the chosen value of AV and RET bandwidth in commercial IPTV implementations.

To achieve the optimal bandwidth allocation for the retransmission service, the negative effect of the channel blocking has to be minimized. This leads to the following minimization problem:



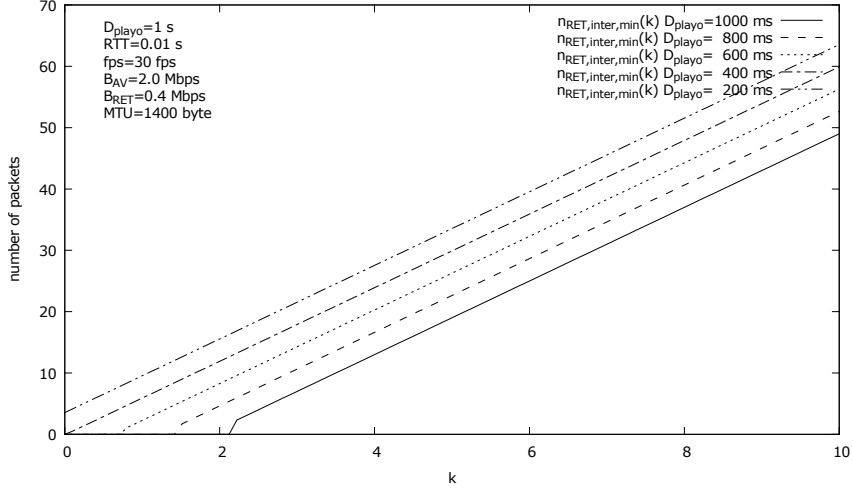


Figure 2.7. Inter-burst limitation

$$\min_{\frac{B_{RET}}{B_{AV}} \in \mathbb{R}^+} \left(n_{RET,inter,min} \left(k_{RET,intra,max}, \frac{B_{RET}}{B_{AV}} \right) \right), \text{ where} \quad (2.6)$$

$$k_{RET,intra,max} \left(\frac{B_{RET}}{B_{AV}} \right) = \frac{D_{playo} - 2D_{pkg} - RTT}{D_{pkg}} \frac{B_{RET}}{B_{AV}}. \quad (2.7)$$

In other words, the lowest points on each n_{RET} curves (showed by figure 2.8) have to be identified, which will represent the optimal bandwidth values. I solve this problem with the first derivative test, substituting $\frac{B_{RET}}{B_{AV}}$ with x for easier understanding:

$$\frac{d}{dx} \left(\frac{D_{playo} - 2D_{pkg} - RTT}{D_{pkg}} x + 1 \right) \frac{1}{x} + \frac{RTT - D_{playo}}{D_{pkg}} + \frac{D_{playo} - 2D_{pkg} - RTT}{D_{pkg}} x + 2 = 0, \text{ which yields} \quad (2.8)$$

$$\frac{d}{dx} \frac{1}{x} + \frac{D_{playo} - 2D_{pkg} - RTT}{D_{pkg}} x + C = 0, \quad (2.9)$$

$$-\frac{1}{x^2} + \frac{D_{playo} - 2D_{pkg} - RTT}{D_{pkg}} = 0, \quad (2.10)$$

$$\underbrace{\frac{D_{playo} - 2D_{pkg} - RTT}{D_{pkg}}}_a x^2 \underbrace{-1}_c = 0. \quad (2.11)$$

Solving the quadratic equation above yields to

$$x = \frac{B_{RET}}{B_{AV}} \Big|_{optimum} = \pm \sqrt{\frac{D_{pkg}}{D_{playo} - 2D_{pkg} - RTT}}, \quad (2.12)$$



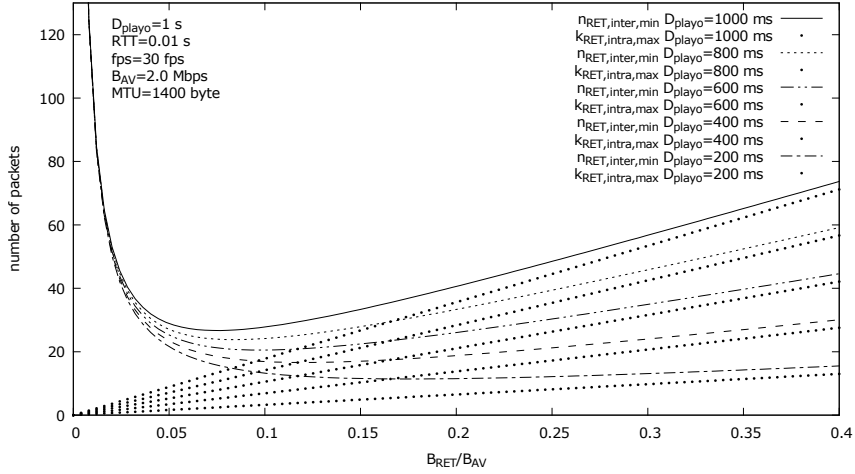


Figure 2.8. The common effect of the intra- and inter-burst limitation. The $n_{RET,inter,min}$ curves show the number of packets, during which the retransmission bandwidth is blocked (occupied) with retransmission traffic, therefore a new packet loss cannot be corrected. To minimize this negative effect, the optimal values of B_{RET}/B_{AV} should be chosen according to the minimum of the curves.

where the negative solution can be obviously ignored.

This equation shows, that there is an inverse relationship between the optimal choice for retransmission bandwidth and the size of the playout buffer. Due to its delay compensation role, a longer playout buffer can tolerate the same number of packet losses if smaller bandwidth is available for retransmission services. An increase in the round trip time will also require a higher retransmission bandwidth, because an additional delay in the retransmission handshake will shorten the time window, in which packets can be retransmitted. Convincingly, higher average packet size demands faster retransmission, which concludes thesis I.1.

This result can be used for retransmission bandwidth sizing in IPTV solutions:

$$B_{RET}|_{optimum} = B_{AV} \cdot \sqrt{\frac{1}{\frac{D_{playo}-RTT}{D_{pkg}} - 2}} \quad (2.13)$$

2.2.2 The Three State Channel Model

The previous section considered only the effect of the xDSL environment, now I look at my research question from a different viewpoint. To find the answer, I propose a new model for packet transmission and retransmission for IPTV solutions (Jursonovics and Imre 2011, 2013). This model does address the special features of the wireless channel, and does provide the necessary mathematical instruments for analysis, evaluation, and forecast of traffic parameters.



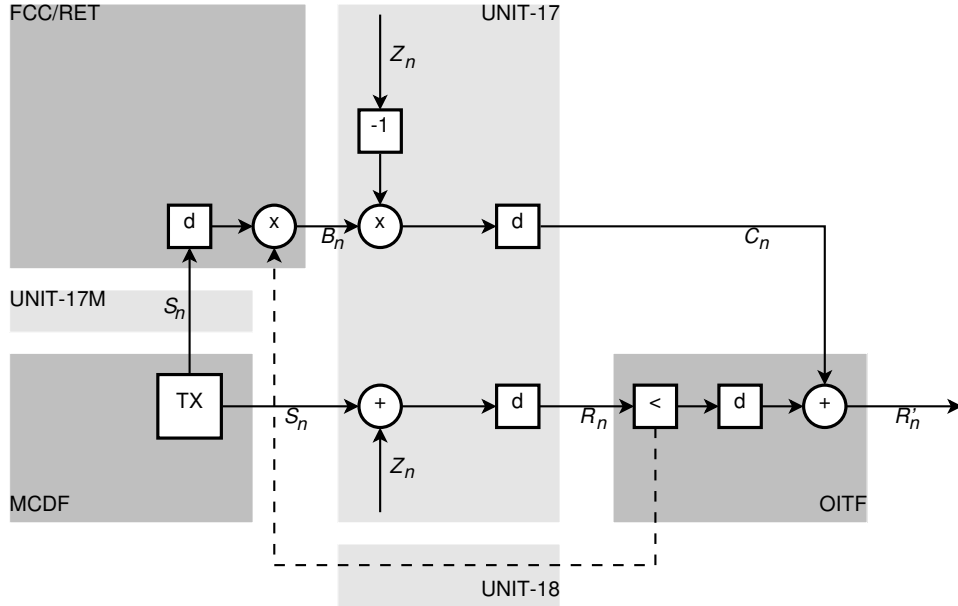


Figure 2.9. Channel model for IPTV analysis

THESIS I.2 (Jursonovics and Imre 2011, 2013). *I constructed a new mathematical model, the three state channel model (3SCM) for the description of the retransmission effect on bursty packet losses in wireless network for IPTV solution. My model unites the description of packet loss and retransmission, and I proposed the method of forecasting loss and retransmission probabilities.*

Let $S_n = \{0, \forall n\}$ represent the number of sent packets at the time n in figure 2.9, MCDF the Multicast Content Delivery Function, $Z_n = \{0; 1, \forall n\}$ an additive noise in the Unit-17 interface, d the transmission delay, and OITF the open IPTV terminal function. The received packets can be expressed with $R_n = \{0, \text{for successful packet transmission}; 1, \text{for packet loss}\}$:

$$R_n = S_{n-d} + Z_{n-d}. \quad (2.14)$$

I assume that the receiver (represented by $<$) detects a packet loss by checking the sequence numbers of packets, and requests the retransmission through the Unit-18 interface: $B_n = \{1, \text{for packet retransmission}; 0 \text{ otherwise}\}$ of every lost packets only once from the FCC/RET Server. I also assume that this communication is protected by an error-free protocol, like TCP, and the transmission delay on Unit-18 is negligible less than on Unit-17 due to the small size of the retransmission requests. By this definition, I obtain



$$B_n = R_n \cdot S_{n-d} = (S_{n-d} + Z_{n-d}) \cdot S_{n-d} = Z_{n-d}. \quad (2.15)$$

The B_n signal travels through the same wireless channel, therefore it is also affected by the same Z_n channel noise, and it may be also lost. It is really important to highlight that C_n does carry information only in that case, if a retransmission request happened and successfully arrived, otherwise C_n has an indefinite value in any other time. To model this condition, I express the received correction signal $C_n = \{0, 1\}$ with three operators, an inverter (-1), a multiplier (\times) and a channel transmission delay (d). These operators enable me to assign the value of 1 for C_n only in that case, when the retransmission signal does occurred and it is not affected by the channel noise (not lost), and the value of 0 otherwise.

The final, received, and corrected signal $R'_n = \{0, \text{for successful packet transmission, } 1 \text{ for packet loss (unsuccessful retransmission) and } 2 \text{ for successful packet retransmission}\}$ is

$$\begin{aligned} R'_n &= R_{n-d} + C_n = S_{n-2d} + Z_{n-2d} + B_{n-d} \cdot Z_{n-d}^{-1} \\ &= S_{n-2d} + Z_{n-2d} + Z_{n-2d} \cdot Z_{n-d}^{-1}. \end{aligned} \quad (2.16)$$

Let us observe that the first term of the addition equals to 0 by definition and the last term equals to the sampling of the Z_n white noise with its own delayed signal. The auto correlation function of the white noise is zero for all non-zero time shifts (Papoulis 1965), therefore R'_n can be described as a sequence of an independent random variable, which satisfies the Markov property. $X_n \stackrel{def}{=} R'_n$ is a discrete-time Markov chain.

Let $X_n = 0$, if the n -th packet is received correctly; $X_n = 1$, if the n -th packet is lost and has not been retransmitted; and $X_n = 2$, if the n -th packet is successfully retransmitted after loss. Construct a Markov chain (see figure 2.10) with the $p_{ij}[n]$ state transition probabilities from the state i to j at the time n :

$$p_{ij}[n] = P(X_{n+1} = j | X_n = i), \text{ where } i, j \in \{0, 1, 2\}. \quad (2.17)$$

I also assume, that the main characteristic of the communication channel will slowly change during one media session, therefore the transition probabilities are not depend on time and the Markov chain is time-homogeneous:

$$p_{ij}[n] = p_{ij}. \quad (2.18)$$



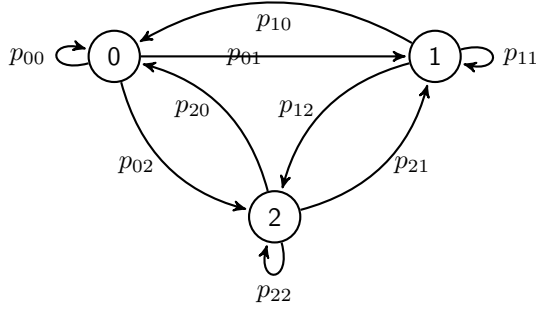


Figure 2.10. The Three State Channel Model

To state the second part of thesis I.2, I begin with an analysis, and I describe the system equations of the Markov chain:

$$y_0[n + 1] = (1 - p_{01} - p_{02})y_0[n] + p_{10}y_1[n] + p_{20}y_2[n], \quad (2.19)$$

$$y_1[n + 1] = (1 - p_{10} - p_{12})y_1[n] + p_{21}y_2[n] + p_{01}y_0[n], \quad (2.20)$$

$$y_2[n + 1] = (1 - p_{20} - p_{21})y_2[n] + p_{02}y_0[n] + p_{12}y_1[n], \quad (2.21)$$

$$p_{00} + p_{01} + p_{02} = 1, \quad (2.22)$$

$$p_{11} + p_{10} + p_{12} = 1, \quad (2.23)$$

$$p_{22} + p_{20} + p_{21} = 1, \quad (2.24)$$

where $y_0[n]$ is the probability at the time n of successfully packet transmission, $y_1[n]$ of loss and $y_2[n]$ of retransmission for $n \geq 0$. Taking the z transform from both sides of the system equations above, I move to the complex frequency domain, where $Y_0(z)$, $Y_1(z)$, $Y_2(z)$ are the z transforms of $y_0[n]$, $y_1[n]$ and $y_2[n]$ respectively:

$$z(Y_0(z) - y_0[0]) = (1 - p_{01} - p_{02})Y_0(z) + p_{10}Y_1(z) + p_{20}Y_2(z), \quad (2.25)$$

$$z(Y_1(z) - y_1[0]) = (1 - p_{10} - p_{12})Y_1(z) + p_{21}Y_2(z) + p_{01}Y_0(z), \quad (2.26)$$

$$z(Y_2(z) - y_2[0]) = (1 - p_{20} - p_{21})Y_2(z) + p_{02}Y_0(z) + p_{12}Y_1(z). \quad (2.27)$$

I express $Y_0(z)$, $Y_1(z)$ and $Y_2(z)$ by solving the equations:



$$\begin{aligned}
Y_0(z) &= z(y_0[0]z^2 + (y_1[0]p_{10} + y_0[0]p_{10} + p_{20}y_2[0] - 2y_0[0] + p_{12}y_0[0] + y_0[0]p_{20} + y_0[0]p_{21})z \\
&+ p_{21}p_{10}y_2[0] + p_{20}y_2[0]p_{10} + y_0[0]p_{20}p_{10} + y_0[0]p_{21}p_{10} + y_0[0] + y_1[0]p_{10}p_{20} - y_0[0]p_{21} \\
&- p_{20}y_2[0] - y_0[0]p_{12} - y_0[0]p_{20} + y_1[0]p_{20}p_{12} + y_1[0]p_{10}p_{21} + p_{20}y_0[0]p_{12} + p_{20}p_{12}y_2[0] \\
&\quad] - y_1[0]p_{10} - y_0[0]p_{10}) \\
&\quad / (z^3 + (p_{01} + p_{02} + p_{10} + p_{12} + p_{20} + p_{21} - 3)z^2 \\
&+ (p_{01}p_{21} + 3 + p_{01}p_{20} + p_{20}p_{12} + p_{20}p_{10} + p_{21}p_{10} + p_{12}p_{02} - 2p_{21} - 2p_{02} + p_{02}p_{21} + p_{02}p_{10} - 2p_{12} \\
&- 2p_{01} + p_{12}p_{01} - 2p_{20} - 2p_{10})z + p_{01} - p_{12}p_{01} - p_{12}p_{02} + p_{10} - p_{20}p_{10} - p_{20}p_{12} - 1 + p_{20} + p_{12} + p_{21} \\
&\quad + p_{02} - p_{10}p_{02} - p_{01}p_{20} - p_{01}p_{21} - p_{02}p_{21} - p_{21}p_{10}), \quad (2.28)
\end{aligned}$$

$$\begin{aligned}
Y_1(z) &= z(y_1[0]z^2 + (p_{02}y_1[0] + p_{01}y_0[0] + y_1[0]p_{21} - 2y_1[0] + y_2[0]p_{21} + p_{01}y_1[0] + y_1[0]p_{20})z \\
&+ y_1[0] - y_1[0]p_{20} + y_2[0]p_{02}p_{21} + p_{01}p_{20}y_2[0] - y_1[0]p_{21} + p_{01}y_1[0]p_{20} + p_{01}y_1[0]p_{21} - p_{21}y_2[0] \\
&+ p_{01}y_0[0]p_{20} + p_{01}y_0[0]p_{21} + p_{02}y_0[0]p_{21} + p_{02}y_1[0]p_{21} - y_1[0]p_{02} + y_2[0]p_{01}p_{21} - y_1[0]p_{01} \\
&\quad - p_{01}y_0[0]) \\
&\quad / (z^3 + (p_{01} + p_{02} + p_{10} + p_{12} + p_{20} + p_{21} - 3)z^2 \\
&+ (p_{01}p_{21} + 3 + p_{01}p_{20} + p_{20}p_{12} + p_{20}p_{10} + p_{21}p_{10} + p_{12}p_{02} - 2p_{21} - 2p_{02} + p_{02}p_{21} + p_{02}p_{10} - 2p_{12} \\
&- 2p_{01} + p_{12}p_{01} - 2p_{20} - 2p_{10})z + p_{01} - p_{12}p_{01} - p_{12}p_{02} + p_{10} - p_{20}p_{10} - p_{20}p_{12} - 1 + p_{20} + p_{12} + p_{21} \\
&\quad + p_{02} - p_{10}p_{02} - p_{01}p_{20} - p_{01}p_{21} - p_{02}p_{21} - p_{21}p_{10}), \quad (2.29)
\end{aligned}$$

$$\begin{aligned}
Y_2(z) &= z(y_2[0]z^2 + (y_2[0]p_{10} + p_{12}y_2[0] + y_2[0]p_{01} + y_2[0]p_{02} - 2y_2[0] + y_1[0]p_{12} + y_0[0]p_{02})z \\
&(y_2[0]p_{10} - p_{12}y_2[0] + p_{12}p_{01}y_2[0] - y_0[0]p_{02} + y_2[0]p_{10}p_{02} + y_2[0] - y_2[0]p_{01} - y_2[0]p_{02} \\
&+ y_1[0]p_{10}p_{02} + y_1[0]p_{12}p_{01} + y_1[0]p_{12}p_{02} - y_1[0]p_{12} + p_{10}p_{02}y_0[0] + p_{12}p_{01}y_0[0] + p_{12}p_{02}y_0[0] \\
&\quad + p_{12}p_{02}y_2[0])) \\
&\quad / (z^3 + (p_{01} + p_{02} + p_{10} + p_{12} + p_{20} + p_{21} - 3)z^2 \\
&+ (p_{01}p_{21} + 3 + p_{01}p_{20} + p_{20}p_{12} + p_{20}p_{10} + p_{21}p_{10} + p_{12}p_{02} - 2p_{21} - 2p_{02} + p_{02}p_{21} + p_{02}p_{10} - 2p_{12} \\
&- 2p_{01} + p_{12}p_{01} - 2p_{20} - 2p_{10})z + p_{01} - p_{12}p_{01} - p_{12}p_{02} + p_{10} - p_{20}p_{10} - p_{20}p_{12} - 1 + p_{20} + p_{12} + p_{21} \\
&\quad + p_{02} - p_{10}p_{02} - p_{01}p_{20} - p_{01}p_{21} - p_{02}p_{21} - p_{21}p_{10}). \quad (2.30)
\end{aligned}$$

Due to the structural similarities of these three equations, I continue my analysis with the description of the loss state (2.29), and after, I will use the same process to



express the other two steady states probabilities as well. Let observe, that $Y_1(z)$ can be written as a fraction of two polynomials in the following form:

$$Y_1(z) = \frac{B(z)}{A(z)} = \frac{\sum_{i=0}^M b_i z^{-i}}{\sum_{i=0}^N a_i z^{-i}}, \text{ where } M = 3, N = 2. \quad (2.31)$$

In the case above, the degree of the denominator polynomial is greater than the degree of the numerator polynomial ($M > N$), therefore $\frac{B(z)}{A(z)}$ is strictly proper. Applying partial fraction expansion:

$$Y_1(z) = \sum_{r=0}^{M-N} B_r z^{-r} + \sum_{i=1; i \neq n}^N \frac{A_i}{1 - d_i z^{-1}} + \sum_{j=1}^s \frac{C_j}{(1 - d_n z^{-1})^j}, \quad (2.32)$$

$$A_i = (1 - d_i z^{-1}) Y_1(z)|_{z=d_i},$$

$$C_j = \frac{1}{(s-j)! (-d_i)^{s-j}} \left(\frac{d^{s-j}}{dw^{s-j}} \left((1 - d_i w)^s X(w^{-1}) \right) \right)_{w=d_i^{-1}},$$

where B_r can be calculated with a long division, and d_i are the poles of $A(z)$, which can be calculated from (2.30) and (2.31):

$$d_1 = 1, \quad (2.33)$$

$$d_2 = 1 - \frac{1}{2}(p_{01} + p_{02} + p_{10} + p_{12} + p_{20} + p_{21})$$

$$+ \frac{1}{2}(-2p_{10}p_{02} - 2p_{12}p_{01} - 2p_{12}p_{02} - 2p_{21}p_{10} - 2p_{20}p_{10} - 2p_{20}p_{12} - 2p_{01}p_{20}$$

$$- 2p_{01}p_{21} - 2p_{02}p_{21} + p_{21}^2 + 2p_{21}p_{12} + 2p_{21}p_{20} + 2p_{20}p_{02} + p_{20}^2 + 2p_{12}p_{10}$$

$$+ p_{12}^2 + p_{02}^2 + 2p_{02}p_{01} + p_{01}^2 + 2p_{01}p_{10} + p_{10}^2)^{\frac{1}{2}}, \quad (2.34)$$

$$d_3 = 1 - \frac{1}{2}(p_{01} + p_{02} + p_{10} + p_{12} + p_{20} + p_{21})$$

$$- \frac{1}{2}(-2p_{10}p_{02} - 2p_{12}p_{01} - 2p_{12}p_{02} - 2p_{21}p_{10} - 2p_{20}p_{10} - 2p_{20}p_{12} - 2p_{01}p_{20}$$

$$- 2p_{01}p_{21} - 2p_{02}p_{21} + p_{21}^2 + 2p_{21}p_{12} + 2p_{21}p_{20} + 2p_{20}p_{02} + p_{20}^2 + 2p_{12}p_{10}$$

$$+ p_{12}^2 + p_{02}^2 + 2p_{02}p_{01} + p_{01}^2 + 2p_{01}p_{10} + p_{10}^2)^{\frac{1}{2}}. \quad (2.35)$$

In my model, all the roots of $A(z)$ are first order poles, therefore the third term of (2.32) does not exist, $Y_1(z)$ can be reduced to the form of

$$Y_1(z) = \sum_{r=0}^{M-N} B_r z^{-r} + \sum_{i=1}^3 \frac{A_i}{1 - d_i z^{-1}}, \text{ where} \quad (2.36)$$

$$A_i = (1 - d_i z^{-1}) Y_1(z)|_{z=d_i}.$$



Each term of $Y_1(z)$ can be inverse transformed by inspection, where $u[k]$ is the unit step and $\delta[k]$ is the Dirac delta function:

$$y_1[k] = B_r\delta[k] + \sum_{i=1}^3 u[k]A_i d_i^k = B_r\delta[k] + u[k]A_1 d_1^k + u[k]A_2 d_2^k + u[k]A_3 d_3^k. \quad (2.37)$$

The good state ($y_0[k]$) and the retransmission state ($y_2[k]$) can be also expressed using the same steps above:

$$y_0[k] = B_{0,r}\delta[k] + \sum_{i=1}^3 u[k]A_{0,i} d_{0,i}^k, \quad (2.38)$$

$$y_2[k] = B_{2,r}\delta[k] + \sum_{i=1}^3 u[k]A_{2,i} d_{2,i}^k, \quad (2.39)$$

where $A_{0,i}$, $A_{2,i}$ are the residues and $d_{0,i}$, $d_{2,i}$ are the poles of the denominator polynomials of $Y_0(z)$ and $Y_2(z)$ respectively.

The key attributes for the characterization of the IPTV transmission are the steady state probabilities ($P_{L,steady}$, $P_{R,steady}$ and $P_{G,steady}$), which determine the probability of loss, successful retransmission, and good transmission states; the run-length probabilities ($P_{L,burst}(l)$ and $P_{R,burst}(l)$), which determine the probabilities of an l long consecutive loss and a consecutively retransmission events respectively. These formulas can be calculated from the state functions (2.37), (2.38), (2.39) and the state transition probabilities (2.18).

$$P_{L,steady} = \lim_{k \rightarrow \infty} y_1[k] = \lim_{k \rightarrow \infty} (B_r\delta[k] + u[k]A_1 d_1^k + u[k]A_2 d_2^k + u[k]A_3 d_3^k), \quad (2.40)$$

$$P_{G,steady} = \lim_{k \rightarrow \infty} y_0[k] = \lim_{k \rightarrow \infty} (B_{0,r}\delta[k] + u[k]A_{0,1} d_{0,1}^k + u[k]A_{0,2} d_{0,2}^k + u[k]A_{0,3} d_{0,3}^k), \quad (2.41)$$

$$P_{R,steady} = \lim_{k \rightarrow \infty} y_2[k] = \lim_{k \rightarrow \infty} (B_{2,r}\delta[k] + u[k]A_{2,1} d_{2,1}^k + u[k]A_{2,2} d_{2,2}^k + u[k]A_{2,3} d_{2,3}^k), \quad (2.42)$$



$$\begin{aligned}
P_{L,burst}(l) &= (1 - (1 - p_{10} - p_{12}))(1 - p_{10} - p_{12})^{l-1} \\
&= (p_{10} + p_{12})(1 - p_{10} - p_{12})^{l-1},
\end{aligned} \tag{2.43}$$

$$P_{R,burst}(l) = (p_{20} + p_{21})(1 - p_{20} - p_{21})^{l-1}, \tag{2.44}$$

$$P_{G,burst}(l) = (p_{01} + p_{02})(1 - p_{01} - p_{02})^{l-1}. \tag{2.45}$$

These equations complete thesis I.2, but my work relies on the prediction capabilities of the 3SCM for the above described probabilities, therefore it is really important to prove that they are converging to a finite value.

PROBLEM 2.5. *The convergence of the steady state probabilities and run-length probabilities shall be determined and the limit shall to be expressed in closed-form to perform further qualitative analysis with the 3SCM.*

2.3 Results and Discussion

This section presents my results and discussion including the description of the conditions, under which I obtained them. I explain the meanings of my results, and I show how they fit into the existing body of knowledge.

2.3.1 Evaluation of the 3SCM

First, I introduce three theorems to proof the existence of the steady state convergence and closed-form expression of the run-length probabilities defined by thesis I.2 . Then, I show that the 3SCM can be reduced to the well known Gilber model.

2.3.1.1 Steady state analysis

The steady-state probabilities of the 3SCM are important parameters for statistical analysis and long term forecasts. I am going to use them in 2.3.4 to estimate the packet loss rate of an IPTV connection, and based on this information, make a decision on allowing or denying a packet retransmission. Unfortunately, these probabilities are not deduced in a closed form expression in (2.40), (2.41), and (2.42), and their current form does not allow fast and accurate prediction. In this section, I prove, that all of them can be expressed in a closed form².

2. The steady state probabilities can be also determined by the stationary distribution ($\pi \mathbf{P} = \pi$), which would require to solve a similar system of linear equations. In my opinion, the presented Z-transformation and convergence analysis explain these expressions more straightforward, and highlights their origin.



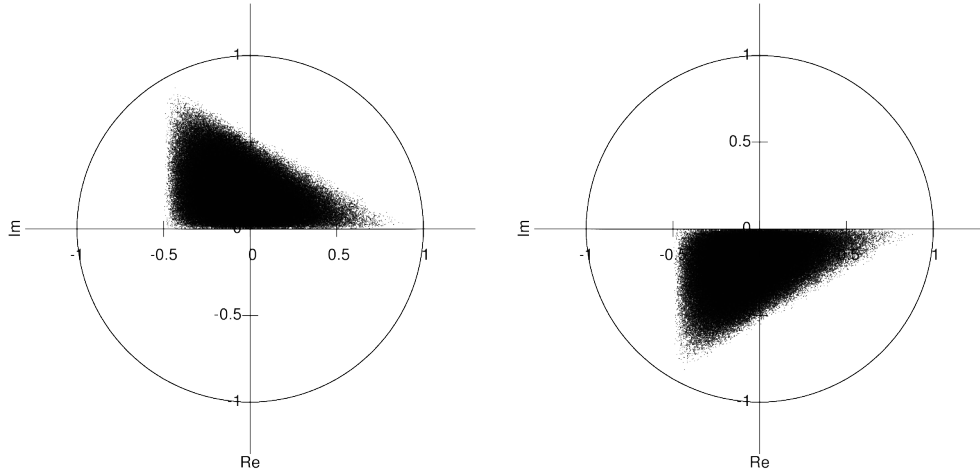


Figure 2.11. Monte Carlo analysis of the poles. These two graphs show that every simulation point of the d_2 , d_3 poles, represented by black dots, lie within the unit circle, therefore the model is concluded to be stable.

First, let have a look on the steady-state packet loss rate of $y_1[k]$:

$$P_{L,steady} = \lim_{k \rightarrow \infty} y_1[k] = \lim_{k \rightarrow \infty} (B_r \delta[k] + u[k]A_1 d_1^k + u[k]A_2 d_2^k + u[k]A_3 d_3^k), \quad (2.46)$$

where A_1 , A_2 , and A_3 are the the residues, and d_1 , d_2 , and d_3 are the poles of the denominator polynomial of $Y_1(z)$. Due to my model's simplicity, I conjectured the existence of the convergence above, which requires that all the d_i poles are less or equal than 1, therefore I examined the values of the d_i poles with a Monte Carlo analysis performed on one million random samples, according to the following conditions from (2.22) and (2.24):

$$0 \leq p_{ij} \leq 1, \text{ where } i, j \in (0, 1, 2) \quad (2.47)$$

$$0 \leq p_{01} + p_{02} \leq 1 \quad (2.48)$$

$$0 \leq p_{10} + p_{12} \leq 1 \quad (2.49)$$

$$0 \leq p_{20} + p_{21} \leq 1 \quad (2.50)$$

I found, that $d_1 \stackrel{def}{=} 1$ and the complex values of d_2 and d_3 are within the unit circle (figure 2.11) in all my test cases, therefore I state the following three theorems:



THEOREM 2.1 (Jursonovics and Imre 2011). *The convergence of the d_2 pole exists: $|d_2| \leq 1$.*

Proof.

$$\begin{aligned}
d_2 = & 1 - \frac{1}{2}(p_{01} + p_{02} + p_{10} + p_{12} + p_{20} + p_{21}) \\
& + \frac{1}{2}(-2p_{10}p_{02} - 2p_{12}p_{01} - 2p_{12}p_{02} - 2p_{21}p_{10} - 2p_{20}p_{10} - 2p_{20}p_{12} - 2p_{01}p_{20} \\
& - 2p_{01}p_{21} - 2p_{02}p_{21} + p_{21}^2 + 2p_{21}p_{12} + 2p_{21}p_{20} + 2p_{20}p_{02} + p_{20}^2 + 2p_{12}p_{10} \\
& + p_{12}^2 + p_{02}^2 + 2p_{02}p_{01} + p_{01}^2 + 2p_{01}p_{10} + p_{10}^2)^{\frac{1}{2}},
\end{aligned} \tag{2.51}$$

where

$$0 \leq p_{ij} < 1 \forall i, j \in \{0, 1, 2\}, \text{ and} \tag{2.52}$$

$$0 \leq p_{01} + p_{02} \leq 1, \tag{2.53}$$

$$0 \leq p_{10} + p_{12} \leq 1, \tag{2.54}$$

$$0 \leq p_{20} + p_{21} \leq 1. \tag{2.55}$$

Let express d_2 in the following form:

$$d_2 = 1 - \frac{1}{2}E + \frac{1}{2}(E^2 - F)^{1/2}, \tag{2.56}$$

where

$$E \stackrel{def}{=} (p_{01} + p_{02}) + (p_{10} + p_{12}) + (p_{20} + p_{21}), \tag{2.57}$$

$$F \stackrel{def}{=} 4(p_{10}p_{02} + p_{12}p_{01} + p_{12}p_{02} + p_{21}p_{10} + p_{20}p_{10} + p_{20}p_{12} \tag{2.58}$$

$$+ p_{01}p_{20} + p_{01}p_{21} + p_{02}p_{21}). \tag{2.59}$$

From (2.53) and (2.55)

$$0 \leq E \leq 3, \tag{2.60}$$

$$0 \leq F. \tag{2.61}$$

$$\tag{2.62}$$



The value of d_2 can be real or complex depending on the square root of $(E^2 - F)$. First, I analyze the former case, where the absolute value can be expressed

$$\Re(d_2) = 1 - \frac{1}{2}E + \frac{1}{2}(E^2 - F)^{1/2}, \quad (2.63)$$

$$\Im(d_2) = 0, \quad (2.64)$$

$$|d_2| = \left| 1 - \frac{1}{2}E + \frac{1}{2}(E^2 - F)^{1/2} \right|, \quad (2.65)$$

$$0 \leq (E^2 - F). \quad (2.66)$$

From (2.66)

$$0 \leq (E^2 - F)^{1/2} \leq E, \quad (2.67)$$

$$0 \leq E - (E^2 - F)^{1/2} \leq E, \quad (2.68)$$

$$0 \leq \frac{1}{2}(E - (E^2 - F)^{1/2}) \leq \frac{E}{2}, \quad (2.69)$$

$$1 - \frac{E}{2} \leq 1 - \frac{1}{2}(E - (E^2 - F)^{1/2}) \leq 1, \quad (2.70)$$

$$1 - \frac{E}{2} \leq d_2 \leq 1. \quad (2.71)$$

$$(2.72)$$

Applying (2.60)

$$-0.5 \leq 1 - \frac{E}{2}, \quad (2.73)$$

therefore

$$-0.5 \leq d_2 \leq 1 \text{ and} \quad (2.74)$$

$$|d_2| \leq 1, \text{ if } (E^2 - F) \geq 0. \quad (2.75)$$

Second, if d_2 possess a complex value, $|d_2|$ can be written on the following form

$$\Re(d_2) = 1 - \frac{1}{2}E, \quad (2.76)$$

$$\Im(d_2) = \frac{1}{2}(F - E^2)^{1/2}, \quad (2.77)$$

$$|d_2| = 1 - E + \frac{1}{4}F, \quad (2.78)$$

$$0 > (E^2 - F). \quad (2.79)$$



I am going to prove that d_2 is within (or on) the unit circle:

$$1 - E + \frac{1}{4}F \leq 1, \quad (2.80)$$

$$0 \leq E - \frac{1}{4}F. \quad (2.81)$$

Substituting (2.57) and (2.59) yields to

$$0 \leq p_{21} - p_{01}p_{21} + p_{20} - p_{20}p_{10} + p_{12} - p_{12}p_{01} + p_{01} - p_{01}p_{20} + p_{02} - p_{02}p_{21} + p_{10} - p_{10}p_{02} - p_{12}p_{02} - p_{21}p_{10} - p_{20}p_{12}, \quad (2.82)$$

$$0 \leq p_{21}(1 - p_{01}) + p_{20}(1 - p_{10}) - p_{20}p_{12} + p_{12}(1 - p_{01}) - p_{12}p_{02} + p_{01}(1 - p_{20}) + p_{02}(1 - p_{21}) + p_{10}(1 - p_{02}) - p_{21}p_{10}, \quad (2.83)$$

$$0 \leq p_{21}(1 - p_{01}) + p_{20}(1 - p_{10} - p_{12}) + p_{12}(1 - p_{01} - p_{02}) + p_{01}(1 - p_{20}) + p_{02}(1 - p_{21}) + p_{10}(1 - p_{02}) - p_{21}p_{10}, \quad (2.84)$$

$$0 \leq p_{20}(1 - p_{10} - p_{12}) + p_{12}(1 - p_{01} - p_{02}) + p_{21}(1 - p_{01} - p_{02}) + p_{01}(1 - p_{20}) + p_{02}(1 - p_{10}) + p_{10}(1 - p_{21}), \quad (2.85)$$

$$0 \leq p_{20}p_{11} + p_{12}p_{00} + p_{21}p_{00} + p_{01}(1 - p_{20}) + p_{02}(1 - p_{10}) + p_{10}(1 - p_{21}). \quad (2.86)$$

It can be observed, that all tags of the addition above are greater than 0, therefore

$$|d_2| \leq 1, \text{ if } (E^2 - F) < 0. \quad (2.87)$$

I also state, that d_2 is on the unit circle ($|d_2| = 1$) if and only if all $p_{ij} = 0 \forall i, j \in \{0, 1, 2\}$. This is a very special and rare case, which does not occur in a real-life environment, therefore I omit this case from my model. \square

THEOREM 2.2 (Jursonovics and Imre 2011). *The convergence of the d_3 pole exists: $|d_3| \leq 1$.*

Proof.

$$\begin{aligned} d_3 = & 1 - \frac{1}{2}(p_{01} + p_{02} + p_{10} + p_{12} + p_{20} + p_{21}) \\ & - \frac{1}{2}(-2p_{10}p_{02} - 2p_{12}p_{01} - 2p_{12}p_{02} - 2p_{21}p_{10} - 2p_{20}p_{10} - 2p_{20}p_{12} - 2p_{01}p_{20} \\ & - 2p_{01}p_{21} - 2p_{02}p_{21} + p_{21}^2 + 2p_{21}p_{12} + 2p_{21}p_{20} + 2p_{20}p_{02} + p_{20}^2 + 2p_{12}p_{10} \\ & + p_{12}^2 + p_{02}^2 + 2p_{02}p_{01} + p_{01}^2 + 2p_{01}p_{10} + p_{10}^2)^{\frac{1}{2}}, \end{aligned}$$



where

$$0 \leq p_{ij} < 1 \forall i, j \in \{0, 1, 2\}, \quad (2.88)$$

$$0 \leq p_{01} + p_{02} \leq 1, \quad (2.89)$$

$$0 \leq p_{10} + p_{12} \leq 1, \quad (2.90)$$

$$0 \leq p_{20} + p_{21} \leq 1. \quad (2.91)$$

Express d_3 in the following form (the only difference is the minus sign before the second term compared to (2.51):

$$d_3 = 1 - \frac{1}{2}E - \frac{1}{2}(E^2 - F)^{1/2}. \quad (2.92)$$

The value of d_3 can be also real or complex depending on the square root of $(E^2 - F)$. First I analyze the former case. I express the absolute value of d_3 :

$$\Re(d_3) = 1 - \frac{1}{2}E - \frac{1}{2}(E^2 - F)^{1/2}, \quad (2.93)$$

$$\Im(d_3) = 0, \quad (2.94)$$

$$|d_3| = \left| 1 - \frac{1}{2}E - \frac{1}{2}(E^2 - F)^{1/2} \right|, \quad (2.95)$$

$$0 \leq (E^2 - F). \quad (2.96)$$

I am going to prove that d_3 is within the unit circle, which requires

$$-1 \leq 1 - \frac{1}{2}E - \frac{1}{2}(E^2 - F)^{1/2} \leq 1 \quad (2.97)$$

$$-2 \leq -\frac{1}{2}E - \frac{1}{2}(E^2 - F)^{1/2} \leq 0, \quad (2.98)$$

$$0 \leq E + (E^2 - F)^{1/2} \leq 4. \quad (2.99)$$

$$(2.100)$$

From (2.60) and (2.96) I deduce that the the above described term is greater than 0.



$$E + (E^2 - F)^{1/2} \leq 4, \quad (2.101)$$

$$(E^2 - F)^{1/2} \leq 4 - E, \quad (2.102)$$

$$E^2 - F \leq 16 - 8E + E^2, \quad (2.103)$$

$$0 \leq 4 - 2E + \frac{F}{4}. \quad (2.104)$$

$$(2.105)$$

Substituting (2.57) and (2.59):

$$4 - p_{01} - p_{01} - p_{02} - p_{02} - p_{10} - p_{10} - p_{12} - p_{12} - p_{20} - p_{20} - p_{21} - p_{21} + p_{10}p_{02} \\ + p_{12}p_{01} + p_{12}p_{02} + p_{21}p_{10} + p_{20}p_{10} + p_{20}p_{12} + p_{01}p_{20} + p_{01}p_{21} + p_{02}p_{21}, \quad (2.106)$$

$$4 - p_{01} - p_{02} - p_{01} - p_{02} - p_{10} - p_{12} - p_{10} - p_{12} - p_{20} - p_{21} - p_{20} - p_{21} \\ + p_{12}(p_{01} + p_{02}) + p_{10}p_{02} + p_{21}p_{10} + p_{20}(p_{10} + p_{12}) + p_{01}(p_{20} + p_{21}) + p_{02}p_{21}, \quad (2.107)$$

$$4 - p_{01} - p_{02} - p_{10} - p_{12} - p_{20} - p_{21} + p_{02}p_{21} + p_{21}p_{10} + p_{10}p_{02} \\ + (p_{12} - 1)(p_{01} + p_{02}) + (p_{20} - 1)(p_{10} + p_{12}) + (p_{01} - 1)(p_{20} + p_{21}), \quad (2.108)$$

$$1 - p_{01} - p_{02} - p_{21} + p_{02}p_{21} + p_{21}p_{10} + p_{10}p_{02} + 1 - p_{12} + (p_{12} - 1)(p_{01} + p_{02}) \\ + 1 - p_{20} + (p_{20} - 1)(p_{10} + p_{12}) + 1 - p_{10} + (p_{01} - 1)(p_{20} + p_{21}), \quad (2.109)$$

$$1 - p_{02} - p_{10} - p_{21} + p_{02}p_{21} + p_{21}p_{10} + p_{10}p_{02} + (p_{12} - 1)(p_{01} + p_{02} - 1) + \\ (p_{20} - 1)(p_{10} + p_{12} - 1) + (p_{01} - 1)(p_{20} + p_{21} - 1), \quad (2.110)$$

$$1 - p_{02} - p_{10} - p_{21} + p_{02}p_{21} + p_{21}p_{10} + p_{10}p_{02} + (p_{12} - 1)(p_{01} + p_{02} - 1) \\ + (p_{20} - 1)(p_{10} + p_{12} - 1) + (p_{01} - 1)(p_{20} + p_{21} - 1), \quad (2.111)$$

$$1 - p_{02} - p_{10} - p_{21} + p_{02}p_{21} + p_{21}p_{10} + p_{10}p_{02} + (p_{12} - 1)(p_{01} + p_{02} - 1) \\ + (p_{20} - 1)(p_{10} + p_{12} - 1) + (p_{01} - 1)(p_{20} + p_{21} - 1), \quad (2.112)$$

$$1 + p_{02}(p_{21} - 1) + p_{21}(p_{10} - 1) + p_{10}(p_{02} - 1) + (p_{12} - 1)(p_{01} \\ + p_{02} - 1) + (p_{20} - 1)(p_{10} + p_{12} - 1) + (p_{01} - 1)(p_{20} + p_{21} - 1), \quad (2.113)$$

$$p_{02}(p_{21} - 1) + 1 - p_{21} + p_{21}p_{10} + p_{10}(p_{02} - 1) + (p_{12} - 1)(p_{01} + p_{02} - 1) \\ + (p_{20} - 1)(p_{10} + p_{12} - 1) + (p_{01} - 1)(p_{20} + p_{21} - 1), \quad (2.114)$$

$$(p_{02} - 1)(p_{21} + p_{10} - 1) + p_{21}p_{10} + (p_{12} - 1)(p_{01} + p_{02} - 1) \\ + (p_{20} - 1)(p_{10} + p_{12} - 1) + (p_{01} - 1)(p_{20} + p_{21} - 1). \quad (2.115)$$

It can be observed that all tags of the addition above are greater than 0, therefore



$$|d_3| \leq 1, \text{ if } (E^2 - F) \geq 0. \quad (2.116)$$

Second, if d_3 possess a complex value

$$\Re(d_3) = 1 - \frac{1}{2}E, \quad (2.117)$$

$$\Im(d_3) = -\frac{1}{2}(F - E^2)^{1/2}, \quad (2.118)$$

$$|d_3| = 1 - E + \frac{1}{4}F, \quad (2.119)$$

$$0 > (E^2 - F). \quad (2.120)$$

Let observer that in this case $|d_3| = |d_2|$, this is already to be proved in (2.34), therefore

$$|d_3| \leq 1, \text{ if } (E^2 - F) < 0. \quad (2.121)$$

I state again, that d_3 is on the unit circle ($|d_3| = 1$) if and only if all $p_{ij} = 0 \forall i, j \in \{0, 1, 2\}$. This is a very special and rare case, which does not occur in a real-life environment, therefore I omit this case from my model. □

THEOREM 2.3 (Jursonovics and Imre 2011). *The 3SCM is stable, the steady-state packet loss probability can be expressed in the closed form of*

$$P_{L,steady} = \frac{p_{02}p_{21} + p_{01}p_{20} + p_{01}p_{21}}{p_{10}p_{02} + p_{12}p_{01} + p_{12}p_{02} + p_{21}p_{10} + p_{20}p_{10} + p_{20}p_{12} + p_{01}p_{20} + p_{01}p_{21} + p_{02}p_{21}}$$

Proof. According to theorem 2.1 and 2.2, the d_2 and d_3 poles are smaller than 1, therefore I deduce that the third and fourth terms of (2.122) are converging to zero, so $P_{L,steady}$ can be expressed in a closed formula of

$$\begin{aligned} P_{L,steady} &= \lim_{k \rightarrow \infty} y_1[k] = \lim_{k \rightarrow \infty} (B_r \delta[k]) \\ &= \frac{p_{02}p_{21} + p_{01}p_{20} + p_{01}p_{21}}{p_{10}p_{02} + p_{12}p_{01} + p_{12}p_{02} + p_{21}p_{10} + p_{20}p_{10} + p_{20}p_{12} + p_{01}p_{20} + p_{01}p_{21} + p_{02}p_{21}} \end{aligned} \quad (2.122)$$

□



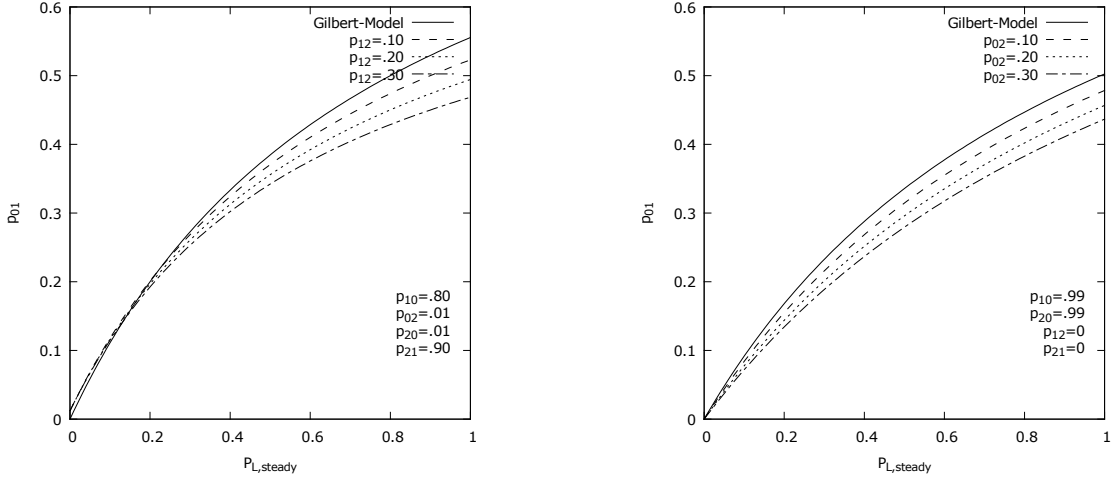


Figure 2.12. Steady state probabilities of packet loss. The 3SCM incorporates the loss correction effect of the retransmission feature and results lower (more accurate) probability values than the Gilbert model.

Using the same steps above, I determined the other two steady state probabilities as well:

$$P_{R,steady} = \frac{p_{10}p_{02} + p_{12}p_{01} + p_{12}p_{02}}{p_{01}p_{20} + p_{01}p_{21} + p_{02}p_{21} + p_{10}p_{02} + p_{12}p_{01} + p_{12}p_{02} + p_{21}p_{10} + p_{20}p_{10} + p_{20}p_{12}} \quad (2.123)$$

$$P_{G,steady} = \frac{p_{12}p_{20} + p_{21}p_{10} + p_{20}p_{10}}{p_{01}p_{20} + p_{01}p_{21} + p_{02}p_{21} + p_{10}p_{02} + p_{12}p_{01} + p_{12}p_{02} + p_{21}p_{10} + p_{20}p_{10} + p_{20}p_{12}} \quad (2.124)$$

These expressions enable an easy way of calculating the steady state probabilities, which will be required for my further work. Figure 2.12 shows the steady state probability of packet loss at different channel parameter values. I assume two simple loss characteristics, which show that the correction effect of the retransmission feature decreases the probability of the packet loss as expected, and the 3SCM considers this effect in contrast with the Gilbert model.

2.3.1.2 Run-lengths analysis

I obtain the probability of an l long consecutive events (bursts) from (2.43):



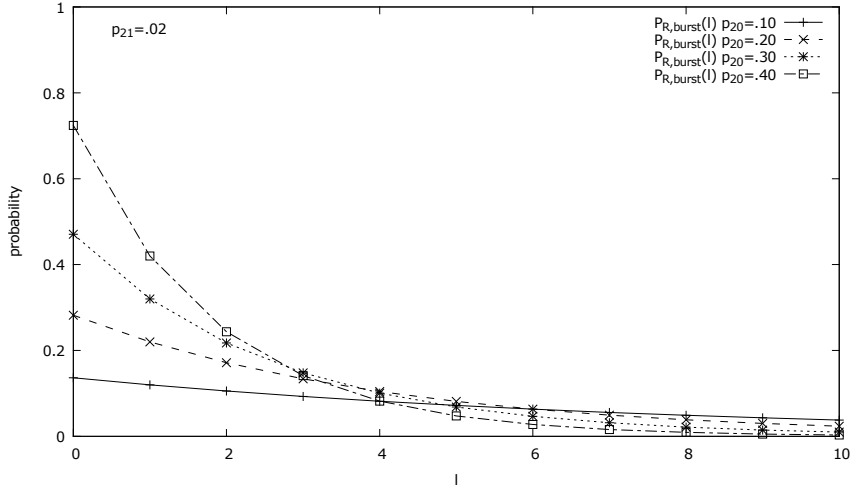


Figure 2.13. Probabilities of loss run-lengths

$$\begin{aligned}
 P_{L,burst}(l) &= (1 - (1 - p_{10} - p_{12}))(1 - p_{10} - p_{12})^{l-1} \\
 &= (p_{10} + p_{12})(1 - p_{10} - p_{12})^{l-1}, \tag{2.125}
 \end{aligned}$$

$$P_{R,burst}(l) = (p_{20} + p_{21})(1 - p_{20} - p_{21})^{l-1}. \tag{2.126}$$

Figure 2.13 presents the probability of an l long retransmission bursts assuming a simple wireless channel characteristic. The diagram shows that for short bursts, the probability of a successful retransmission is greater, if the channel more likely returns to the good transmission state. For relatively long burst ($l > 4$), the inverse of this effect can be seen.

2.3.1.3 Reduction to Gilbert model

The reduction of the proposed model to the Gilbert model, by defining the state probabilities to never enter state “2”, gives the well known formula (Gilbert 1960) of the Gilbert model:

$$P_L|_{p_{02}=0, p_{20}=1, p_{12}=0, p_{21}=1} = \frac{2p_{01}}{2p_{10} + 2p_{01}}. \tag{2.127}$$

This shows that the 3SCM behaves as though it is expected, and the formula of the steady state loss probability is correct.

2.3.2 Forecasting Performance of the 3SCM

In relation to the performance evaluation, I compared my model’s prediction ability of different transport parameters to the measured values. I show, that the 3SCM



model is effectively predicts the three most important probability attributes of the IPTV delivery. The test were conducted in the testbed described by 1.7.

THESIS I.3 (Jursonovics and Imre 2011, 2013; Jursonovics and Butyka 2004). *I proved that the 3SCM effectively describes and predicts the loss characteristics of both the packet transmission and retransmission by conducting and analyzing several sample video sequence transmission on the testbed. The relative averaged prediction error remained below 20% for steady state retransmission probabilities and below one magnitude for short burst losses.*

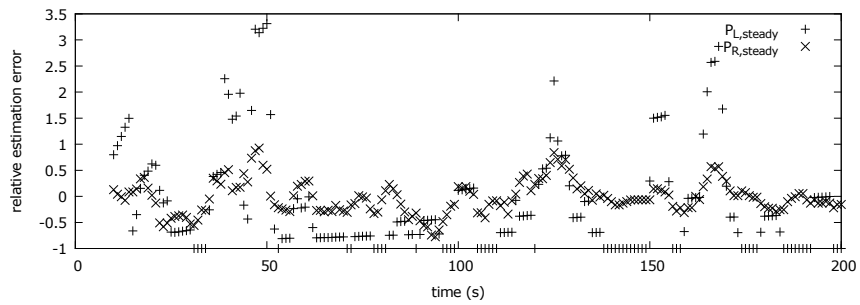
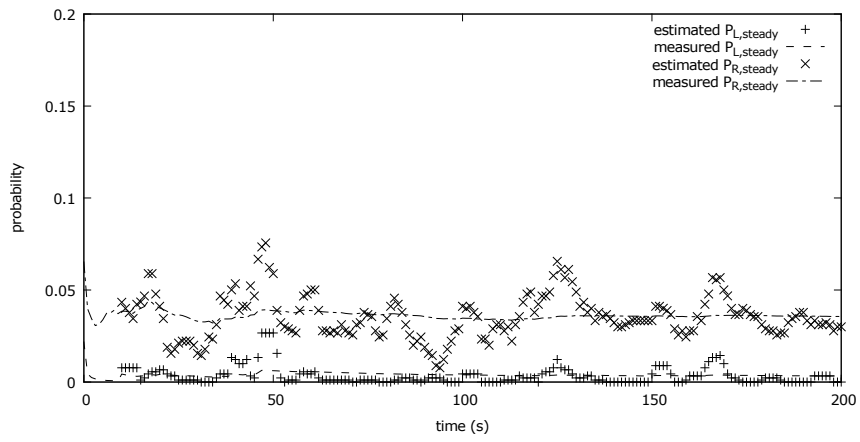
Figures 2.14a and 2.14b show the evaluation of the steady state probability forecasts at different estimation window sizes (w). It can be easily observed, that at $w = 10$ s, the predicted values are close to the measured values. The maximal single relative prediction error is 3.0; in average less than 0.4. It can be also observed, that the prediction accuracy of retransmission probability is better than for packet losses, because packet loss events occur much less, than retransmission (in my model, a packet loss equals to a lost retransmission packet,) and a Markov chain has a well known estimation error for low probabilities (Bartholomew 1975). This effect also results higher relative prediction errors values (20%-40%), but I would like to emphasize, that they represent really small absolute errors: a 40% relative error for a 10^{-6} probability means, that the difference between the estimated value and the real value is less than $0.4 \cdot 10^{-6}$.

Using a larger prediction window, the estimated values are almost exactly the same as the measured values (single relative prediction error is less than 1.2; in average 0.3). The peak error at 90 s is caused by a burst loss on the wireless channel; the Markov chain over-predicted the loss rate based on this concentrated loss of packets.

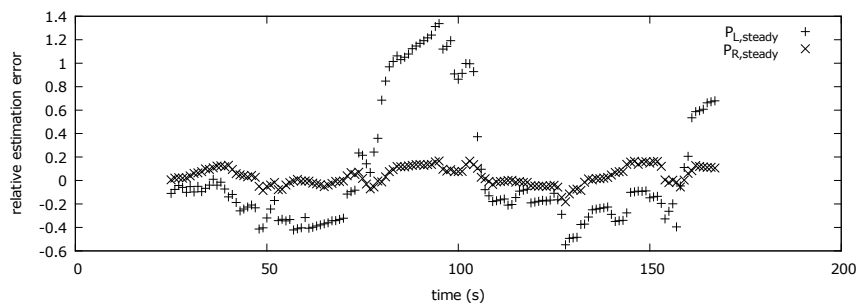
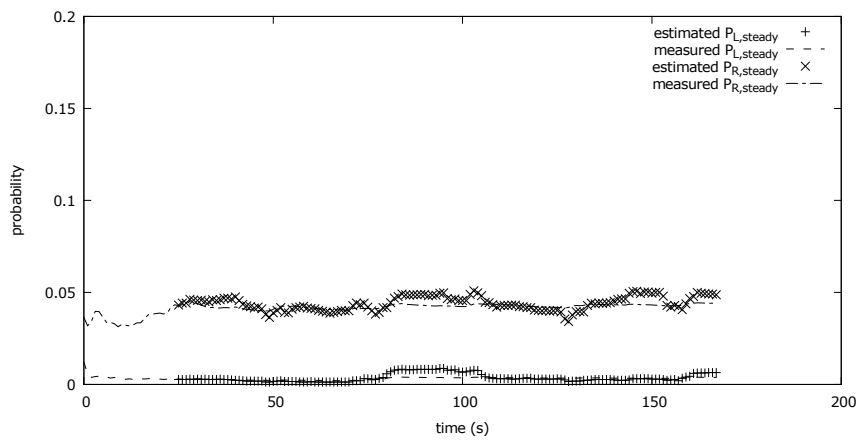
The lack of prediction values, at the beginning of the graph, is caused by the estimation window, the prediction values are displayed only, if all historical data for the prediction window is available.

Next, I analyzed the prediction probabilities of the loss bursts (figures 2.15a and 2.15b) and retransmission bursts (figure 2.16a and 2.16b) at different estimation windows sizes. It can be observed, that the model slightly overestimated the probability of loss bursts, the peak single relative estimation error for a three long loss of bursts is 10, which value remained unchanged for a larger estimation windows. The prediction accuracy of a Markov chain is decreasing for small probability values (the probability of a 3 long loss of burst events is approximately 10^{-4}). However, the probability of





(a) 10 s windows size



(b) 20 s windows size

Figure 2.14. Steady state estimation



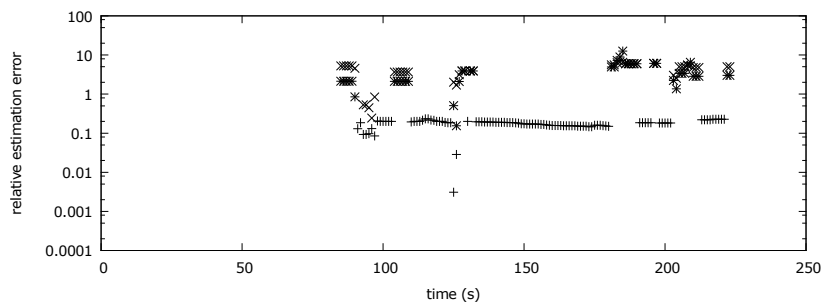
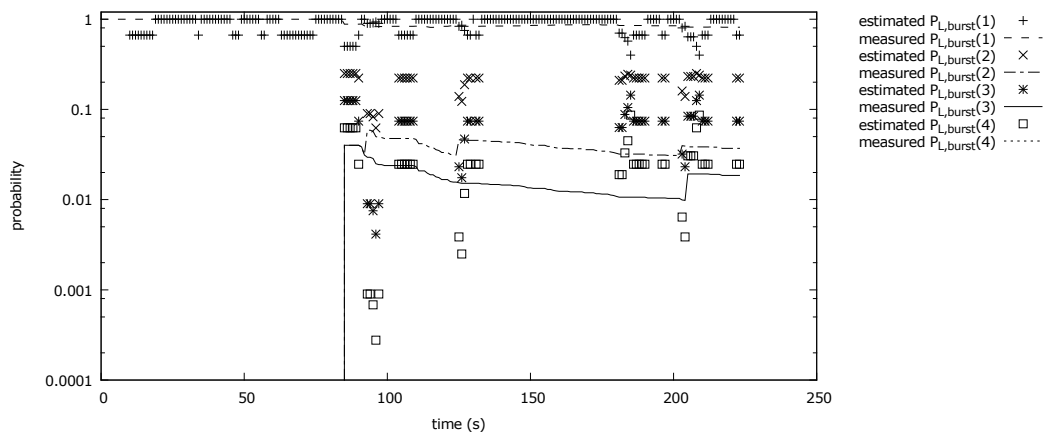
the retransmission bursts is almost accurately predicted, the single relative estimation error is 0.1.

The quality of the prediction depends on the accuracy of determining the stationary distribution of the Markov chain; in other words, how many individual samples are required (windows size) to truly represent the stationary state, which will result accurate steady state estimates. There are two main approaches to determine this limit. On one hand, a sophisticated mathematical calculus can be used to derive the theoretical convergence bounds of the Markov model, which is far too complex to deduct an easily applicable, universal method. On the other hand, a diagnostic tool can be also used on the predicted and measured values to detect, whether the desired convergence state has been reached. In my work, I rely on the above introduced empirical analysis, but for further details, the following articles offer a good starting point: (Cowles and Carlin 1996; Kharin and Piatlitski 2011; Liu et al. 2008; Brooks and Roberts 1998; Billingsley 1961).

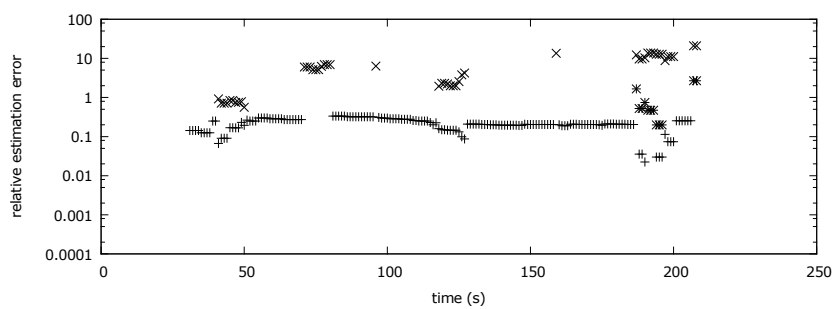
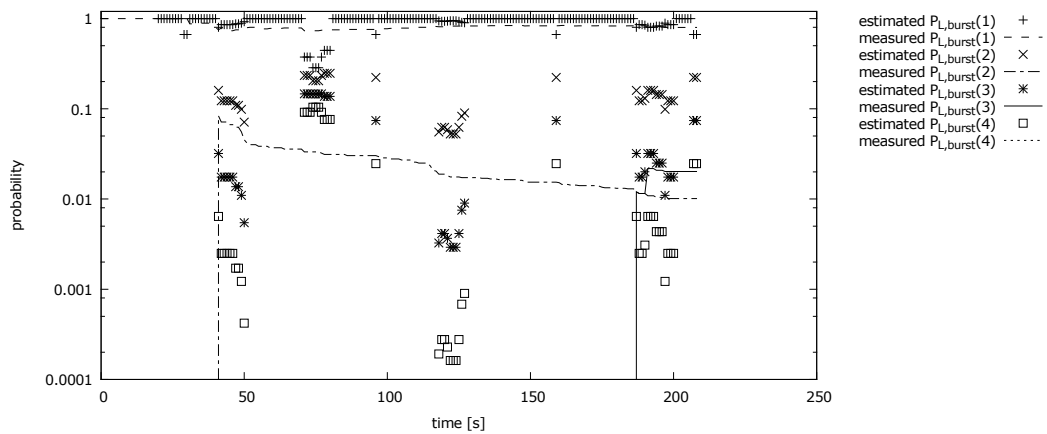
I also note, that there is significant difference between overestimation and underestimation of these probability values. On one hand, my model assigns smaller retransmission bandwidth, if the probability of retransmission is underestimated, which would directly cause congestion in the retransmission, which would lead to higher number of packet losses. This would negatively influence the user experience by short, sudden, visual errors. On the other hand, overestimation would unnecessarily increase the retransmission bandwidth, which would allow only smaller throughput for IPTV content delivery. The user experience would not be disturbed by short errors, however the overall IPTV content quality would be lower. In my view, IPTV service providers would prefer lower overall quality over short quality distortion, therefore the underestimation has more severe effect, which concludes thesis I.3

2.3.3 The Optimal Bandwidth Allocation

The smart choice of the allocated retransmission bandwidth is a crucial point in any commercial IPTV design process. As I state in 2.2.1, an inappropriate value may jeopardize the quality of the customer experience. In real-life solutions, the perfect quality cannot be met; the allowed perception of quality deterioration is a design parameter, which has to be considered in the bandwidth allocation method. To achieve this goal in this section, I unite the two main aspects of bandwidth allocation (see 2.2.1) and channel model (see 2.2.2) to provide a bandwidth sizing method for IPTV solutions over wireless networks.

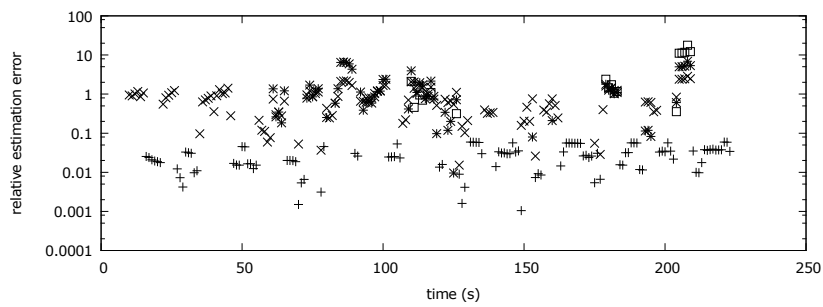
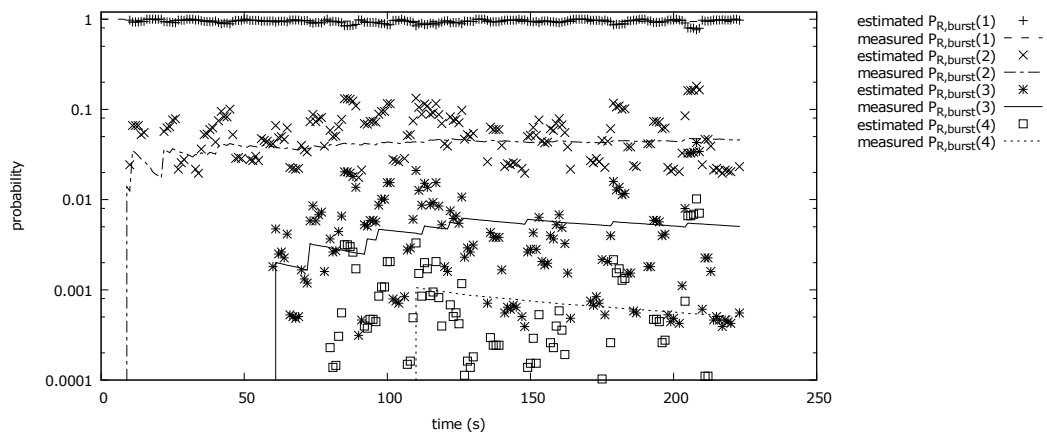


(a) 10 s windows size

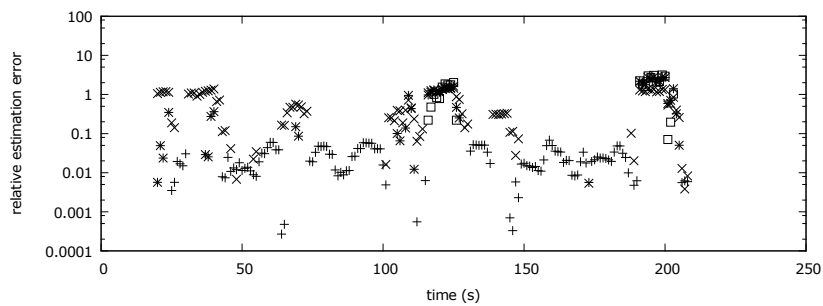
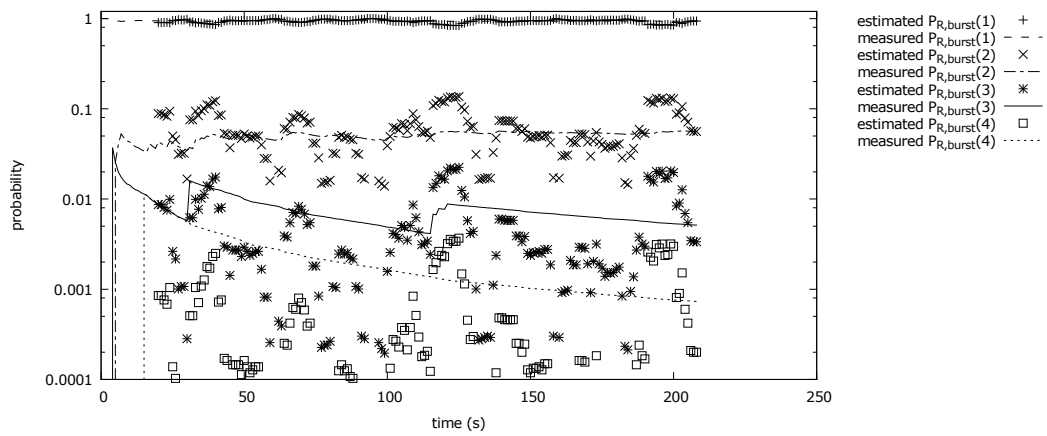


(b) 20 s windows size

Figure 2.15. Loss burst runlengths estimation



(a) 10 s windows size



(b) 20 s windows size

Figure 2.16. Retransmission burst runlengths estimation

PROBLEM 2.6. *The bandwidth allocation method has to consider and ensure, that the quality deterioration remains below an accepted level.*

I describe the wireless communication with the state transition characteristics, then with the help of the probability forecast features of 3SCM, I estimate the relevant probabilities for the three limitation aspect of retransmission, which will yields the probability of packet loss in this complex scenario. This will allow me to select (allocate) the retransmission bandwidth to a given packet loss probability.

THESIS I.4. *I created a method for retransmission bandwidth sizing in IPTV solutions over wireless networks. This method ensures a minimal packet loss probability, and determines the bandwidth allocation accordingly.*

According to the intra-packet limitation (2.43), I already determined the maximal length of bursts, which can be retransmitted, because the in-time playback is ensured for all of the packets.

$$k_{RET,intra,max} \left(\frac{B_{RET}}{B_{AV}} \right) = \frac{D_{playo} - 2D_{pkg} - RTT}{D_{pkg}} \cdot \frac{B_{RET}}{B_{AV}}. \quad (2.128)$$

The probability of l long retransmission request is given by the Markov model (2.44). I calculate the probability of m packet skips if the retransmission burst is greater then $k_{R,burst,max}$, which is

$$P_{skip}(m) = (p_{20} + p_{21})(1 - p_{20} - p_{21})^{k_{RET,intra,max} - 1 + m}. \quad (2.129)$$

The overall probability of a packet skip is given by

$$\begin{aligned} P_{skip,intra} &= \lim_{i \rightarrow \infty} \sum_{i=1}^{\infty} \frac{P_{skip}(i)}{i} \\ &= \lim_{i \rightarrow \infty} \sum_{i=1}^{\infty} \frac{(p_{20} + p_{21})(1 - p_{20} - p_{21})^{k_{RET,intra,max} - 1 + i}}{i} \\ &= (p_{20} + p_{21})(1 - p_{20} - p_{21})^{k_{RET,intra,max} - 1} \\ &\quad \cdot \lim_{i \rightarrow \infty} \sum_{i=1}^{\infty} \frac{(1 - p_{20} - p_{21})^i}{i}. \end{aligned} \quad (2.130)$$

Let us observe, that the last sum can be expressed as a special form of the polylogarithm (also known as Jonquière's function)

$$Li_s(z)|_{s=1} = \sum_{k=1}^{\infty} \frac{z^k}{k^s} |_{s=1} = \sum_{k=1}^{\infty} \frac{z^k}{k} \quad (2.131)$$

for every $-1 \leq z < 1$. $(1 - p_{20} - p_{21})$ satisfies this criterion, therefore using the well known formula of $Li_1(z) = -\ln(1 - z)$, the equation can be expressed in a closed-form

$$P_{skip,intra} = (p_{20} + p_{21})(1 - p_{20} - p_{21})^{k_{RET,intra,max}-1}(-1) \ln(p_{20} + p_{21}). \quad (2.132)$$

Substituting some of the parameters with constants for a better reading, I express the bandwidth allocation ratio

$$P_{skip,intra} = C_1 \cdot C_2^{k_{RET,intra,max}-1}(-1) \ln(C_1), \text{ where} \quad (2.133)$$

$$C_1 = p_{20} + p_{21},$$

$$C_2 = 1 - p_{20} - p_{21}.$$

$$\ln(P_{skip,intra}) = \ln(C_1) + k_{RET,intra,max} \cdot \ln(C_2) - \ln(C_2) + \ln(-\ln(C_1)) \quad (2.134)$$

$$\frac{\ln(P_{skip,intra}) - \ln(C_1) + \ln(C_2) - \ln(-\ln(C_1))}{\ln(C_2)} = k_{RET,intra,max} \quad (2.135)$$

$$\frac{\ln(P_{skip,intra}) - \ln(C_1) + \ln(C_2) - \ln(-\ln(C_1))}{\ln(C_2)} = \frac{D_{playo} - 2D_{pkg} - RTT}{D_{pkg}} \cdot \frac{B_{RET}}{B_{AV}} \quad (2.136)$$

$$\frac{B_{RET}}{B_{AV}} = \frac{D_{pkg}}{D_{playo} - 2D_{pkg} - RTT} \cdot \frac{\ln(P_{skip,intra}) - \ln(C_1) + \ln(C_2) - \ln(-\ln(C_1))}{\ln(C_2)} \quad (2.137)$$

The last equation provides the required method for determining the retransmission bandwidth for a given channel packet skip probability. Figure 2.17 shows the bandwidth allocation rate for different packet skip probabilities and given playout buffer sizes. It can be easily observed, if the playout buffer decreases, then the required retransmission bandwidth, for ensuring the same packet skip probability, increasing on an accelerated scale.

2.3.4 The Optimal Retransmission Algorithm

This section introduces a new method for packet retransmission based on the 3SCM with the aim of addressing the research question of IPTV delivery, and achieving a better video transmission quality. The method is implemented in the testbed, and my hypothesis is measured and proved.

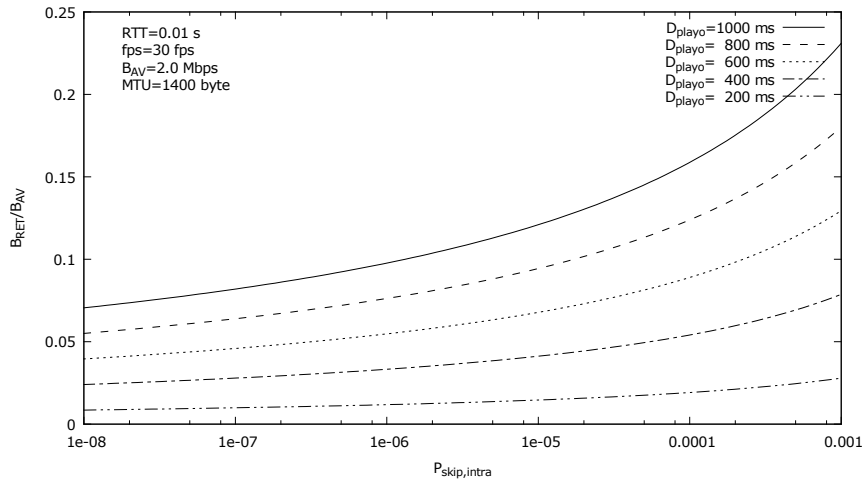


Figure 2.17. Bandwidth allocation for IPTV solutions. The graph can be used as a direct design tool to select the optimal retransmission bandwidth allocation ratio for specific packet loss requirements.

The traditional retransmission algorithms request all lost packets, therefore they have to implement a network layer traffic shaping to fit the actual retransmission throughput into the allocated bandwidth. This is usually carried out by packet queuing, which increases the overall packet retransmission time, therefore the probability—that a retransmission packet arrives late after its playout time—is higher.

In contrast of the initially mentioned solution in the literature review (see 2.1), the main advantages of my method are the low resource needs, the consideration of the wireless channel, and a minimal additional delay. My method assesses the RET mechanism on the network layer, skips (forbids) the retransmission requests of a lost packet according to the above described intra- and inter-burst channel blocking, and takes the special properties of the wireless channel into consideration.

THESIS I.5 (Jursonovics and Imre 2013). *I created an algorithm for packet retransmission in IPTV solutions over wireless networks based on my 3SCM. I proved, that the algorithm is effectively kept the retransmission throughput within its allocated bandwidth, and I showed that my algorithm produces fewer overall packet losses, than traditional retransmission, therefore ensures a better service quality. The theoretical formulas of the loss and retransmission probabilities are also calculated.*

The algorithm consist of the following three steps showed in figure 2.18:

1. The packet arrival process is continuously monitored for packet loss.

2. $k_{RET,intra,max}$ and $n_{RET,inter,min}$ are calculated.
3. A lost packet is requested retransmission only if the intra- and inter-burst channel blocking (see 2.2.1.2 and 2.2.1.3) do not forbid the retransmission, otherwise the retransmission request is skipped.

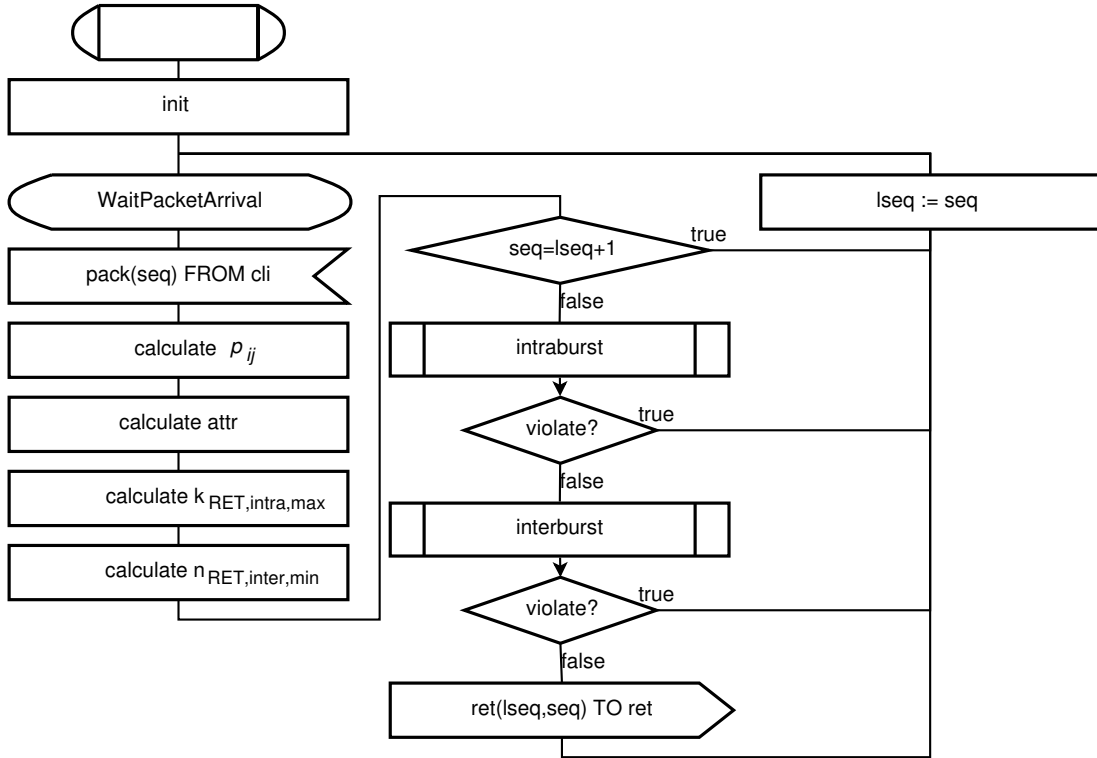


Figure 2.18. Proposed retransmission algorithm

2.3.4.1 Theoretical formulation – intra-burst limitation

Let me first analyze my results theoretically. In this and the upcoming section I characterize the Unit-17 interface with the transition matrix of my Markov model and the design attributes of the access network. Applying the intra- and inter-burst limitations on my model, I derive the probability of the retransmission skip caused by my algorithm. Finally I express the overall packet loss rate of my retransmission algorithm, which is a key indicator for the quality of the video transmission.

The intra-burst limitations has a significant short time effect if the distance of the burst losses are great ($p_{00} \rightarrow 1$). My question is the probability of retransmission packet skip, which is given by (2.132):

$$\begin{aligned}
P_{skip,intra} &= (p_{20} + p_{21})(1 - p_{20} - p_{21})^{k_{RET,intra,max}-1}(-1) \ln(1 - (1 - p_{20} - p_{21})) \\
&= (p_{20} + p_{21})(1 - p_{20} - p_{21})^{k_{RET,intra,max}-1}(-1) \ln(p_{20} + p_{21}). \quad (2.138)
\end{aligned}$$

The overall packet loss can be expressed as a sum of the probability of packet skip (2.138) and the steady state probability of packet loss (2.40).

2.3.4.2 Theoretical formulation – inter-burst limitation

I ask the same question, as in the previous section, what is the probability of packet skip. Let us assume that the first burst is small enough to be retransmitted ($k < k_{RET,intra,max}$). The probability of retransmission burst of l size is given by my Markov model (2.44). The probability of k retransmission burst followed by $n - k$ good transmission burst and a second retransmission is

$$f(k, n) = (p_{20} + p_{21})(1 - p_{20} - p_{21})^{k-1} p_{20}(p_{01} + p_{02})(1 - p_{01} - p_{02})^{n-k-1} p_{02}. \quad (2.139)$$

The first packet of the second retransmission burst is skipped, if n is smaller than $n_{RET,inter,min}(k)$. From this, I can calculate the probability of one packet skip for k

$$P_{skip,inter,k} = \sum_{n=k}^{n_{RET,inter,min}(k)} f(k, n). \quad (2.140)$$

For the overall packet skip probability, I summarize (2.140) for $\forall k < k_{R,burst,max}$

$$P_{skip,inter} = \sum_{k=1}^{k_{RET,intra,max}} \sum_{n=j}^{n_{RET,inter,min}(k)} f(k, n). \quad (2.141)$$

The overall packet loss can be expressed as a sum of the probability of packet skip (2.141) and the steady state probability of packet loss (2.122). This value explicitly describes the overall loss rate including both aspects of my study: the limited bandwidth of the xDSL access and the packet loss caused by the wireless transport.

2.3.4.3 Empirical evaluation

To evaluate my algorithm, I compared the delivery throughput of using the two retransmission algorithm in the testbed. Figure 2.19 shows the throughput of the retransmission stream in two cases: traditional retransmission (all lost packets were

requested for retransmission) and my new retransmission method (retransmission requests may be skipped based on the actual parameters of the channel). It can be clearly seen that my algorithm kept the retransmission throughput under its dedicated bandwidth, which ensured the in time delivery of the retransmission packets, however I intentionally skipped those retransmission requests, which in time delivery could not be achieved due to the channel blocking (intra- and inter-burst effect).

The main benefit of my method is showed by figure 2.20. I compared the total packet loss rate in the above mentioned two cases, and I found that with the smart skipping of packet retransmission requests, I were able to achieve a better (smaller) loss rate then retransmitting all of the packets. My method successfully avoided the effect of late retransmission: if a packet is requested for retransmission without ensuring the necessary transport bandwidth then it may delay further retransmission requests which may arrive to late after their playout time. This causes a inefficient retransmission bandwidth utilization which increases the overall packet loss rate.

Figure 2.21 shows the means and the standard deviations of the overall packet loss rates for 20, individual streaming sessions in the testbed. It can be seen that in most of the cases (17 of 20), my method provided better results by keeping the mean of the overall packet loss rate below the mean of the traditional retransmission algorithm. In these cases, the average packet loss rate achievement was 0.63%. For the remaining 3 cases, the traditional retransmission algorithm provided in average 0.37% better packet loss values.

2.4 Conclusion

I carried out my research into IPTV delivery over the combination of xDSL and wireless access technologies to explore the special requirements of this mixed environment, and discover the possibilities of service quality improvement. The general research on this field examines the medium access layer transport in the first place, and discusses enhancement proposals concerning the radio transmission, however this is not sufficient for IPTV delivery, because in most cases the wireless device is not managed by the IPTV service provider. In my theses, I addressed the application layer and presented an end to end optimization according to my research objectives:

1. Explore and define the optimal bandwidth allocation scheme of packet retransmission in IPTV solutions to optimize service quality (problem 2.1).
2. Find and evaluate the limitations of packet retransmission in IPTV delivery (problem 2.2, 2.3, and 2.4).



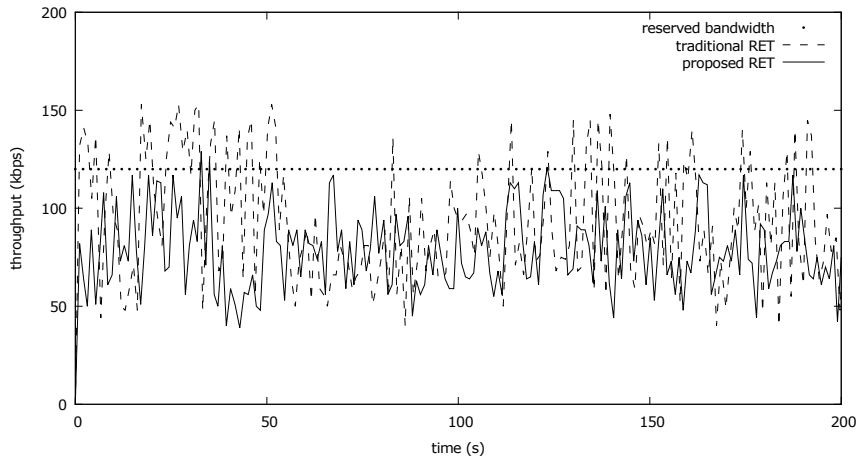


Figure 2.19. Retransmission throughput. The proposed retransmission algorithm successfully maintains the retransmission throughput below the allocated bandwidth.

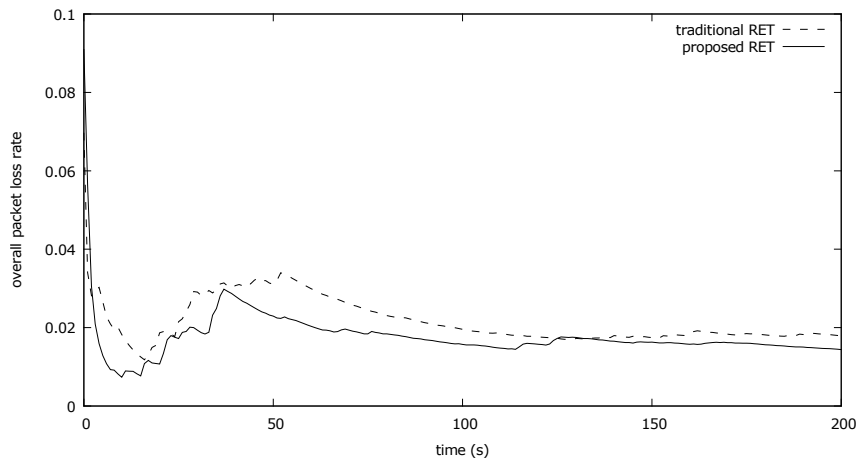


Figure 2.20. Overall packet loss rate. This graph shows, that the proposed retransmission algorithm achieves a lower (better) Overall packet loss rate.

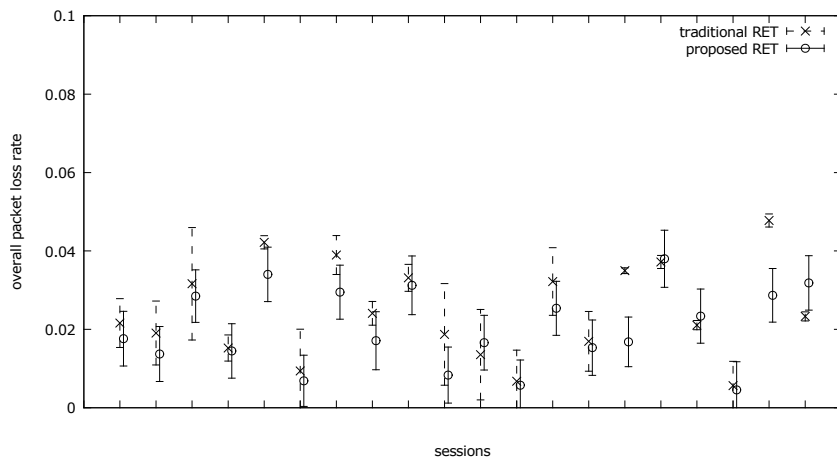


Figure 2.21. Mean and standard deviation for overall packet loss rate



3. Create and analyze a mathematical model of packet retransmission in this mixed environment (problem 2.5).
4. Synthesize the efficient bandwidth allocation and optimal retransmission algorithm.

This section will integrate my theoretical findings to answer my research objectives.

1. Explore and define the optimal bandwidth allocation scheme of packet retransmission in IPTV solutions to optimize service quality.

Bandwidth allocation. I pointed out that the xDSL access technology offers only a limited bandwidth for IPTV delivery, therefore a bandwidth allocation scheme is implemented to avoid overbooking. The packet retransmission feature for scheduled content service delivery requires a dedicated throughput in this scheme, to achieve the maximal service quality, the reserved bandwidth has to be optimized (minimized).

2. Find and evaluate the limitations of packet retransmission in IPTV delivery.

General aspect. I examined the different loss pattern in wireless transmission, and I stated the minimal optimal limit of the retransmission bandwidth.

Intra-bursts. I analyzed the behavior of the playout buffer in the OITF and I defined the limitation of retransmission for burst packet losses.

Inter-bursts. According to the retransmission occupancy, I stated the limitation effect of the inter-burst distance.

3. Create and analyze a mathematical model of packet retransmission in this mixed environment.

Three state channel model. I proposed a new model for the IPTV delivery over wireless networks, which combines the packet transmission and retransmission in one stochastic process. I showed, that this process possess the Markov property, therefore I constructed a Markov chain.

Steady state convergence. I proved, both by a Monte Carlo analysis and an algebraic proof that the Markov chain is stable, and I deduced the closed-form expressions of the steady state probabilities. The model was reduced to the well known Gilbert model to prove the correctness of the equations.

4. Synthesize the efficient bandwidth allocation and optimal retransmission algorithm.



Optimal bandwidth allocation. I provided a sizing method for retransmission services in IPTV solutions over wireless networks. This method will allow the selection of the allocated bandwidth based on a maximal packet loss probability, which will ensure a minimum guaranteed service quality.

Optimal retransmission. I constructed an optimal retransmission algorithm according to the limitation aspects, which is able to ensure the maximal service quality for wireless networks. I derived the formulas of the theoretical loss probabilities.

The main empirical research was conducted on a testbed, built for this specific reason, integrating my own realization of the newly created entities, methods, and functions:

Loss prediction of the 3SCM. I stated that the prediction performance of loss patterns is accurate, though the low probabilities are slightly overestimated by the model.

Optimal retransmission algorithm. I showed that implementing my algorithm, the IPTV delivery has better (smaller) overall packet loss rates—therefore higher quality—than traditional retransmission algorithms.

In further research, I am going to extend my study with the deeper examination of the throughput management in adaptive bitrate streaming technologies. The emerging standard of the Scalable Video Coding (Fraunhofer Heinrich Hertz Institute 2013) enables operators to offer rate adaptive scheduled content services over multicast transport, which would result a better efficiency of bandwidth utilization (a higher B_{AV}/B_{RET} ratio) therefore better service quality. To achieve this goal, the retransmission limitation model should be extended with the inter-dependence of the scalable video encoding and the packet loss prediction model should reflect the loss probabilities in this multilevel architecture.

As a second objective, I am going to shift the scope of optimization from the end-to-end stream delivery to the radio bearer; I am interested in the optimization possibilities and performance of the 3SCM model in the radio interface. This low level retransmission could be also enhanced by the a priori knowledge of the loss probabilities for retry mechanism (Miguel et al. 2011).

My study has offered an evaluative perspective on IPTV delivery, however it encountered a number of limitations, which need to be considered:

MAC layer. The WLAN standard already defines a radio bearer level retry mechanism (IEEE 802.11 Working Group 1999), which is not feasible for IPTV delivery but improves the overall loss probabilities. In my study, this effect was not explicitly considered, therefore my results slightly biased by this feature.

IP fragmentation. Due to the simplicity of the testbed components, the streaming server (ser) did not realize the fragmentation unit feature of the H.264 payload format, therefore every frame was encoded into one packet, and the fragmentation was performed by the IP stack.

Different MPEG frame types. This chapter assumes, that the size and transmission time of all video frames are equal, therefore the different types of video frames are not taken into consideration. The incorporation of this aspect would require to include an additional error factor in the equations ($D_{pkg} \rightarrow D_{pkg} + \epsilon$), which would represent the effect of the different packet transmission times.

I am confident that these new results contribute to the service quality optimization of IPTV Services, and I hope that IPTV platform operators can leverage my findings to ensure an excellent service delivery.



Chapter 3

Quality Based Charging Solutions

The evolution of the mobile telecommunication technology has accelerated in the last decade. The legacy UMTS and general packet radio service (GPRS) solutions allowed only a limited range of services, for instance e-mail or WEB based Internet surfing, but with the new LTE technology, mobile customers can access the Internet faster than ever. The 4th generation mobile system ensures the option to offer various value added services, like IP telephony, cloud computing, peer-to-peer sharing, or even high definition IPTV delivery over wireless networks (Olariu et al. 2005; Bataa et al. 2012; Wolfinger 2012).

Though the radio transmission and solution core become state-of-the-art, but the latest research of the mobile charging solutions have not addressed the special requirements of the multimedia delivery over mobile access; most of them still implement a time- or volume-based accounting method. I am going to show in this chapter that the charging solutions shall consider the quality of the user experience in IPTV services offered by mobile networks, because the visual quality of a streaming media depends on complex network conditions, which has to be incorporated to the charging process. In other words, a small, but specific degradation could jeopardize the user experience of the media delivery, which would led to unfair customer service charge.

Moreover, if customers access streaming services from third party platform providers then the charging of the service is handled externally to the network operator. The inter-company charging of the mobile service has to reflect the quality of the offered multimedia service, where the implementation of a single volume based method could not provide an accurate basis.

I concentrate these ideas in my research question:



How can the charging of the IPTV services reflect the user experience to increase customer satisfaction?

The answer will directly result a fair pricing and billing scheme for IPTV delivery, but besides that, the following important benefits will be achieved:

- Service quality: the quality based charging will establish relationship between the revenue stream and the service quality, which will motivate IPTV service providers to offer their products with the highest possible quality. This simple financial incentive will ensure continuous technological development, and therefore customer satisfaction.
- Customer satisfaction: a fair pricing will increase customer's satisfaction, and lead to smaller number of complain.
- Quality feedback: as addition, the quality of the IPTV service will be continuously monitored; the quality report can be directly used for quality assurance purposes.

My work challenges the charging methods in wireless networks, and discusses the introduction of a novel quality based charging solution. First, I claim that the traditional charging methods are not sufficient for providing a quality of experience based charging. Second, I select the network operator centric business model, and I create a charging architecture according to the 3GPP's recommendation. Third, I objectively define the quality of the streaming. Fourth, I point out the dependence of the loss attributes and the quality. Fifth, I define a sufficient charging policy based on the quality and loss pattern. Finally, I conclude all the methods in one, overall quality based charging method.

The "charging" term has several meanings. In this chapter, I will use a broader sense (according to 3rd Generation Partnership Project 2013a), which incorporates the functions of measuring and recording the service usage (metering), transferring this usage information to the appropriate charging systems (collection), transforming the usage into financial information (rating), securing the corresponding value of service usage (online charging), and creating the service usage bill (billing).



3.1 Literature Review

3.1.1 3GPP

The 3rd Generation Partnership Project (3GPP) is the one entity, which mostly influenced the evolution of the mobile network architecture. 3GPP unites several telecommunications standard development organizations, and produces reports and specifications that define 3GPP technologies. The standardization effort is carried out by the four technical specification groups, which are Radio Access Networks, Service & Systems Aspects, Core Network & Terminals, and GSM EDGE Radio Access Networks.

The original scope of 3GPP was subsequently amended to include the maintenance and development of the Global System for Mobile communication (GSM) Technical Specifications and Technical Reports including evolved radio access technologies. The organization was created in December 1998 by the signing of the "The 3rd Generation Partnership Project Agreement". The latest 3GPP Scope and Objectives document has evolved from this original agreement. 3GPP ensures the system backwards and forwards compatibility to protect the uninterrupted operation of user equipment. For instance, an LTE-A terminal can work in an LTE cell and an LTE terminal works in the LTE-A cell.

Before Release 6 (wideband code division multiple access, time division duplex, high-speed downlink packet access), every 3GPP technical specifications described completely and individually all the necessary charging functionality. With the increase of the system complexity, this trend was changed and an integrated, common framework was created and described in one single specification (3rd Generation Partnership Project 2010a) that serves the role of an overall charging system architecture. The main requirements and high-level principles for charging and billing across the domains, subsystems, and services that comprise a GSM or UMTS PLMN are established in (3rd Generation Partnership Project 2013a). In order to fulfill these requirements, appropriate charging information needs to be generated and collected by the network elements, and forwarded to appropriate charging and billing systems.

Several logical charging functions are needed in the network in order to provide the above described functionality. These charging functions are organized in three charging levels (3rd Generation Partnership Project 2013b): bearer (circuit switched, packet switched, WLAN domains), subsystem (IMS) and service level charging. While the overall possibilities that exist within the 3GPP standards for the physical mapping of these logical functions are described in the present document, the exact situation



that applies to the various domains, subsystems and services of the network is specified in the middle tier charging TS that is specific to that domain/subsystem/service (i.e. TS 32.25x - TS 32.27x).

In offline charging, the charging information is transferred from the network to the billing domain (BD), where it is processed for billing and/or statistical purposes, at the discretion of the PLMN operator. While the internal functions of the BD are outside the scope of 3GPP standardization, the reference point for the charging information transfer from the network to the BD does form a part of the 3GPP standards and is therefore also specified in the present clause.

In online charging, the charging information is transferred from the network to the online charging system (OCS). The OCS, in turn, may have an offline charging reference point used to forward charging information to the BD that is similar in scope and intent to the offline charging case described in the previous paragraph. Those areas of the OCS that form part of the 3GPP standards (functions and reference points) are also described in the present clause. All other aspects of the OCS are outside the scope of 3GPP standards.

3GPP introduced the concept of flow-based charging in 3rd Generation Partnership Project 2007. The current level of traffic differentiation and traffic-type awareness of the GPRS architecture was extended beyond access point name (APN) and packet data protocol (PDP) context level. With flow-based charging, it is possible to apply differentiated charging for the traffic flows belonging to different services (a.k.a. different service data flows) even if they use the same PDP context. In addition, it is possible to apply differentiated charging for the traffic flows belonging to different services carried by other IP connectivity access networks.

As an extension to the flow-based charging, 3rd Generation Partnership Project (2006) forms the basis of the policy and charging control, which encompasses two main functions: the flow based charging, including charging control and online credit control, for service data flows and application traffic; and the policy control (for example gating control, QoS control, QoS signaling). These functions enable the consideration of quality of service for bearer level charging and application detection and control.

3.1.2 IETF

The authentication, authorization and accounting (AAA) domain (authentication, authorization, and accounting) is specified by the Internet Engineering Task Force



(IETF) (Laat et al. 2000), which mainly describes the accounting and charging protocols without putting large efforts in a complete and detailed charging system development.

The concept of IETF describes the infrastructure that enables the generic communication of AAA servers and wide variety of applications. To realize this goal, the protocol can operate in a multi-domain environment with multiple service providers as well as entities taking on other AAA roles, such as user home organizations and brokers. It is possible to combine requests for multiple authorizations of different types in the same authorization transaction.

But the applications—requiring AAA services—will each have their own unique needs. After a service is authorized, it must be configured and initialized. This will require application specific knowledge, and may require application specific protocols to communicate with application specific service components. To handle these application specific functions, IETF propose an application interface between a generic AAA server and a set of one or more application specific modules, which can carry out the unique functionality required by each application. Due to the data required by each application for authentication, authorization, or accounting may have unique structure, the standard AAA protocol allows the encapsulation of opaque units of application specific information.

3.1.3 UMTS Forum

The UMTS Forum was founded in December 1996 in Zurich, Switzerland. It operates as an open, cross-sector, international, non-profit association under Swiss law. Membership of the UMTS Forum draws together everyone with an interest in mobile broadband, including network operators, regulators, and the manufacturers of network infrastructure and terminal equipment (UMTS Forum n.d.).

The UMTS Forum participates actively in the work of the ITU, ETSI, 3GPP, CEPT as well as other technical and commercial organizations. It also contributes to the timely licensing and deployment of mobile broadband globally through regular dialogue with regulators and responses to public consultations.

The UMTS Forum supports the interests of its membership with a range of studies, reports and other outputs. Principal focus areas include markets trends, mobile broadband services and applications, key growth markets, spectrum & regulation, technology & implementation. A strong promotional voice is maintained via a high-profile presence at conferences, seminars and workshops as well as regular briefings to the media, analysts and other stakeholders.



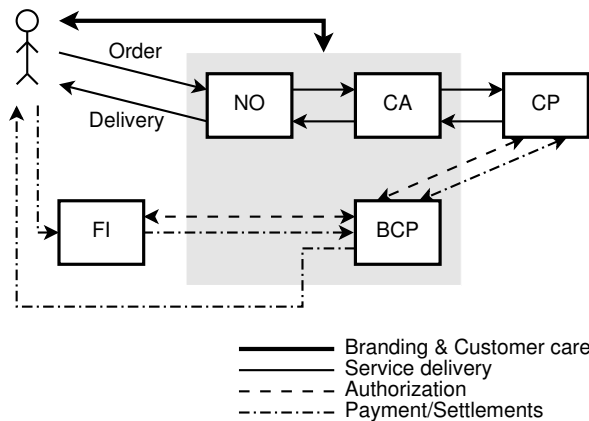


Figure 3.1. Network operator centric business model

In Report 21 (UMTS Forum 2002), UMTS Forum defines probable business models and related revenue streams to overcome proprietary vendor solutions, which allows fair competition between service providers and vendors. The first actor in this model is the user, followed by three other entities: the network operator, the content aggregator, and the content provider.

The network operator holds the 3G license, and its key function is to provide access and transport services to the customers. The content aggregator's function is similar to the well known mobile portal, and its key function is to package and offer services from content providers. The third entity is the content provider, whose main function includes the provisioning of value add services for access and transport services. Before a service is offered, there should be an agreement between the customer and these third parties. With an agreement, the customer may start using services offered by a service provider.

The next step is the authentication and authorization. Authentication is needed to prove that the customer is a rightful customer, and authorization is necessary to verify that the customer is allowed to use the particular service. The main reason, for using this process, is to limit credit risk exposure for the involved parties, which is usually achieved with a digital rights management (DRM) solution.

3.1.3.1 Network operator centric business model

In the network operator centric business model (figure 3.1), the customer has a direct relationship with the network operator. The network operator sets the prices of the services and handles the payments.

The content is normally acquired wholesale from content providers or home made by the network operator itself. The network operator, therefore, manages its own



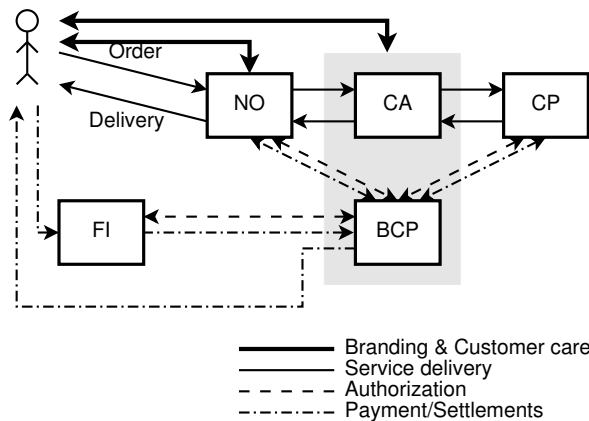


Figure 3.2. Content aggregator centric business model

content aggregator role. Services are, in many cases, offered as bundled packages as part of subscriptions. Besides *traditional* event charges, new charging techniques may develop that handle the same basic process, but in real time. Network operators will use this model to increase average revenue per user and retain their customers. External parties involved may be content providers and financial institutions.

3.1.3.2 Content aggregator centric business model

The content aggregator model is not limited to providing physical access to services through a mobile portal, but rather includes a range of value added services. Added value that might be offered on top of access and transport services could include authentication, security, simplicity, and payment aggregation.

In the content aggregator centric business model (figure 3.2) the customer has an agreement with the content aggregator, but may still have a relationship with the network operator. The content aggregator determines the price of its content, while the customer may pay access charges to the network operator separately—this can be arranged in different ways depending on agreements made between the parties. The possibility is also indicated that the content aggregator settles access and transport charges with the network operator.

3.1.3.3 Content provider centric business model

At first approach, the content provider centric business model (figure 3.3) is similar to the content aggregator centric model. The main difference is that the content provider has a considerable content portfolio, wants to align itself with a network operator, and also take up the content aggregator role. In the previous case the



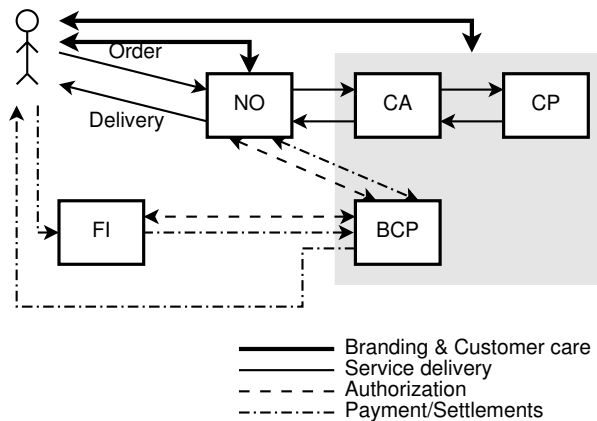


Figure 3.3. Content provider centric business model

content aggregator will most probably sign up agreements with a number of content providers. The customer may have relationships with many content providers in this model, and the network operator will only gain access and airtime charges. Content providers may settle access and transport charges with the network operator to offer a complete price for delivering a service.

The main disadvantage of this model is that content providers have to arrange billing and payment on their own. Also, the customer has to deal with each content provider individually—for example, by paying with a credit card. In this model, the likelihood of one time buyer-seller transactions is higher compared with the other models. The diversity of service offerings is likely to be very high, while the number of transactions per buyer-seller combination is, probably, rather low.

3.1.4 State-of-the-Art Research

Many state-of-the-art charging solutions have been developed since the introduction of the GSM system. Koutsopoulou, Gazis, and Kaloxylos (2001) introduce a novel billing scheme for UMTS networks. The key idea is to propose a scheme, which is capable of handling efficiently charging, accounting, and billing for value added services that are provided either by the network operator or third trusted parties. Moreover, the proposed billing scheme takes into consideration, apart from duration and data volume attributes, other factors such as service differentiation, QoS provision, time of day, endpoints, mobility of the users.

In the framework of the design of a flexible service provision platform for 3G systems and beyond, an integrated system for enabling advanced charging, accounting and billing has been introduced by Koutsopoulou et al. (2001). The MOBIVAS CAB



system is adaptive to value added service charging requirements and network/business environment concepts. In order to enable flexible service provision in 3G systems, it introduces an adaptive charging, accounting and billing system. The presented CAB system is able to support advanced business models, but both approaches do not provide a streaming multimedia specific solution, which is—according to my personal view—rather complex and requires special considerations, as described in 3.3.

Einsiedler et al. (2001) present the current stage of an IP-based architecture for heterogeneous environments, covering UMTS-like W-CDMA wireless access technology, wireless and wired LANs, which is being developed under the aegis of the IST Moby Dick project. This architecture treats all transmission capabilities as basic physical and data-link layers, and attempts to replace all higher-level tasks by IP-based strategies. The proposed architecture incorporates aspects of mobile- IPv6, fast handover, AAA-control, and quality of service. The architecture allows for an optimized control on the radio link layer resources. The Moby Dick architecture is currently under refinement for implementation on field trials. The services planned for trials are data transfer and voice-over-IP. The main achievement of Moby Dick is the quality enforcement feature, which ensures the requires QoS attributes for different value added services, but it does not provide the detailed charging considerations, required for billing.

Value added services will be the economic driver for 4G mobile networks and beyond. For the provision of new services, a charging architecture is required, which is able to support fast and easy integration of new services, and enables versatile tariff models. Kuhne et al. (2005) present a service-oriented charging architecture. The key idea of the architecture is the separation of service-conscious and service-agnostic areas, whereas the different areas are configurable by policy rules. A service example is used to demonstrate the operation and flexibility of our architecture. The results represent the same goals with my research, and by selecting the mobile network operator centric business model, their conclusion is similar.

Kuhne, Huitema, and Carle (2012) surveys recent developments in charging and billing architectures comprising both standardization work as well as research projects. The second main contribution of the article is a comparison of key features of these developments thus giving a list of essential charging and billing ingredients for tomorrow's communication and service environments.

Ary and Imre (2013) argue that abstract novel services in the mobile telecommunication era are far more longer then a few years ago when the price of the call was calculated purely on the length of the session. To overcome possible fraud issues, the



corresponding standards are defining partial CDRs that are sent to the billing system periodically during the sessions. These partial CDRs has to be analyzed and stored in a database for correlation. The size of this database, and thus the required processing time is heavily depending on the distributions of the calls, therefore a method is given to calculate the expected number of partial CDRs and the required database size if these distributions are at least partially known.

The charging and billing in mobile telecommunication networks got more complex in the last few years. New services are emerged, 3rd parties are appeared, and the market competition pushed the operators to introduce different allowances and discounts. Ary and Imre (2005) claims that the large number of pre-paid subscribers makes it necessary to apply a real-time charging method, which requires huge computing capabilities and network overhead. In their work, a novel charging solution is presented, which is compliant with the related standards, and reduce the network overhead needed for real-time charging. Both methods provide enhanced charging functions and increased performance, which could perfectly complete my findings by optimizing the huge number of CDR records, generated by my proposed quality based charging functions in 3.3.5.

Ary and Imre (2008) also claim that the tariff packages in the mobile telecommunication industry got more and more complex in the last few years. The telecommunication companies have introduced several different services among with different discounts and allowances. The price calculation of the services and the understanding of prices became harder for the subscribers. They describe the basic architecture and the major flows of a billing system in the telecommunication area, and introduce a novel concept for price calculation, which could aid the advance of charge and income prediction functionality.

Ary and Imre (2010) calculate the expected number of partial CDRs for long calls, and introduce simulation results for the CDR arrival distributions, because they state that the knowledge of call start and call length distribution is required to design and dimension the network for telecommunication services, thus it is a well know topic for scientific publications. In order to size the charging and billing systems, we have to know the distribution of the call detail record arrivals.

Their result may help to understand the willingness of customers to pay based on the service quality, but for achieving this additional goal, their basic architecture has to be extended to reflect value added services.

Moreover, Huszák and Imre (2010) argues, that video streaming applications are commonly used in both wired and wireless environment; however, wireless links are



burden by higher packet loss ratio and delay variation. In order to make video transmission possible in wireless networks MPEG video coding is usually used to reach the bandwidth constraints of the links. The video quality and compression ratio depends on group of pictures (GOP) structure, but it also affects the distortion sensitivity of the video stream due to packet losses. Their work investigates the correlation between GOP size, packet loss ratio and video quality and concludes that increasing the distance between the reference frames the effectiveness of coding can be improved, but on the other hand the effect of error propagation due to packet losses also increases. These findings corresponds to my view on error propagation in 3.3.5.2.

3.2 Theory

This section provides an overview on the most important theoretical principles to allow the reader to understand the background of my research question and the following discussion in 3.3.

3.2.1 Charging Difference Between Internet and Mobile Networks

The charging, billing, and accounting schemes used in the Internet have been quite simple until now. Users have been mainly billed at a flat rate, based on their subscription and/or at the data volume of their connection for accessing the Internet. In mobile telecommunication networks, users have been billed on their subscription, data volume, as well as a number of other parameters (e.g., type of communication, location and destination). In the near future, these schemes are expected to receive modifications as a consequence of recent technological advances combined with the emerging dominance of the Internet protocol.

Though IP is the common base that ties together the Internet and mobile networks (El Barachi, Glitho, and Dssouli 2005), the business model and the related charging frameworks considered by the two segments are diverse in view of the placement and management of the charging functionality. Thus, the Internet considers a business model that requires direct agreement between the user and independent provider, while the telecommunications world insists on the operator centric model. These industries have been working separately for many years and, therefore, there are many differences even in the respective terminology (Koutsopoulou et al. 2004).



The Internet research community has focused more on the protocols used for accounting data exchange, while the mobile world paid more attention to the specification of the network entities that should generate, process, and collect charging information. Due to both worlds are converging, new dynamic links are now possible with the application/service providers, it is crucial that a minimum compatibility is achieved between these systems. Efforts should be made in order to align the accounting protocols and even new advanced functionality, such as content and location based charging.

3.2.2 Billing Requirements in Mobile Networks

To bypass a complicated charging architecture, a multi-level approach is proposed by 3GPP. The management and processing of the relevant information should be made separately for each level. Furthermore, different charging models should be applicable on each charging level. In such an architecture, subscribers require the provision of *one stop billing*. Users would like to receive a single itemized bill for using voice and data services offered by network operators and independent application or service providers. This requirement implies that the network operator would be responsible for collecting charging data from all players and billing the users. Another requirement is that the charging information should be in a form easily understood by the average user. Also, the users should be constantly aware of the charges to be levied for each chargeable event.

On the other hand, the mobile operators require a flexible charging architecture that accommodates various pricing models (time based, volume based, and QoS based) in order to fulfill not only the traditional business models, but also innovative models. In addition, the selection of a specific pricing model could possibly be based on the user and the service profile parameters. Another important requirement, imposed by the mobile operator, is the support of both online and offline charging mechanisms (pre-paid and post-paid).

From the independent application or service providers' perspective, the evolving requirement is that each authorized player should be able to dynamically apply the desired pricing policy for its services usage. The independent providers should be able to add or modify tariffs for the service and content portion. This dynamic modification should be made in a standardized way in order to update, whichever entity will handle the charging, accounting, and billing functionality.



3.2.3 Offline and Online Charging Terminology

The mobile charging standards define two methods: online and offline charging. The difference between these types is that the online charging is needed in case of prepaid users, while for the post paid users the offline charging method is sufficient, because they do not need to be charged in real-time (3rd Generation Partnership Project 2013b).

3.2.3.1 Offline charging

In this case, the gateway GPRS support node (GGSN) and the inner-nodes (SGSNs) are sending the charging information to the billing system (BS). This charging information must be in a standardized format, called charging data record (CDR). The charging trigger function (CTF) of the network elements generates charging events based on the observation of network resource usage. The charging data function (CDF) receives charging events from the CTF, and then uses the information contained in the charging events to build CDRs. These records are sent to the charging gateway function (CGF), which acts like a storage buffer, cleans, and pre-processes the CDRs. Finally, the CGF sends these processed CDRs to the BS (figure 3.4a). Because these charging records carry all information about the services required, the functionality of the CDRs extends beyond charging. With CDRs, it is possible to analyze service utilization, and gain statistical information about the services and content. By archiving the CDRs, the user-complaints can also be settled (Ren et al. 2006; Lundstrom and Jaatinen 2002).

In the offline charging mechanism, the user's account will be decreased after a few minutes from the service usage. The network overhead will be smaller due to the transmission of fewer number of charging records over the entire network (Ary and Imre 2005a).

3.2.3.2 Online charging

In online mode, a new entity, the online charging system (OCS) is responsible for the proper charging (figure 3.4b). The main task of this entity is to realize real-time charging by continuously delegating certain amounts of credit to the serving network elements. The user's account will be deducted by so-called unit reservation. If the service terminates before all credits are consumed, the network elements are re-transmitting the remaining credits to the OCS. To assure continuous service delivery, if the users do not terminate the service, a new amount of granted credit should be



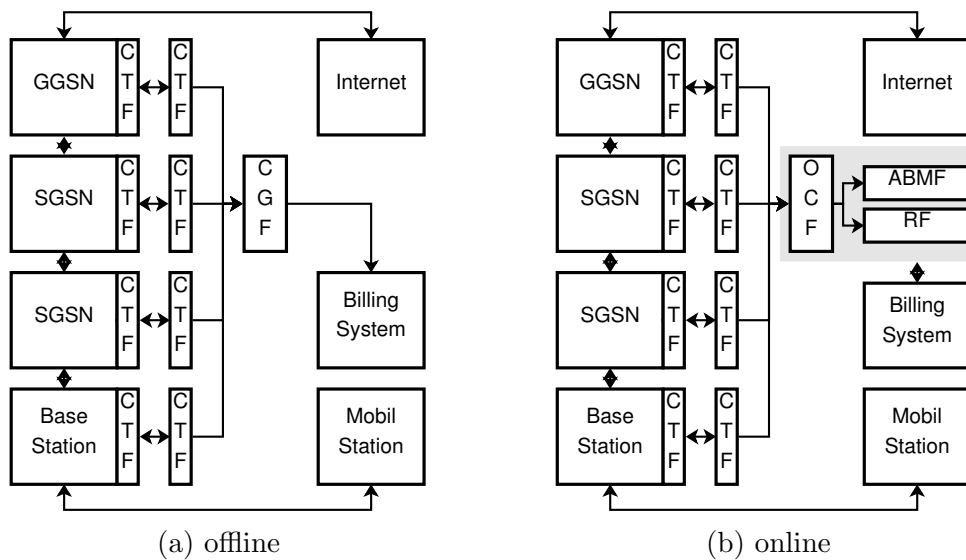


Figure 3.4. Charging methods

sent to the serving network element before the previous one runs out. This unit-granting function is represented by the online charging function (OCF) inside the OCS. The CTF generates charging events for the OCF as well, but this communication is bidirectional, as the OCF has to grant credits for the service. The OCS also includes the account balance management function (ABMF) and the rating function (RF). The account balance management function is the location of the subscribers account balance within the OCS, and the rating function is used to determinate the value of the network resource usage.

3.3 Results and Discussion

3.3.1 Charging Requirements

3GPP recommends three methods (3rd Generation Partnership Project 2013b) for charging of multimedia streaming:

- Charging by duration of session
- One off set up charge
- Charging by volume of data, optionally QoS differentiated

The great advantage of duration based charging is that it can be easy implemented, but it does not consider the changes in the user experience caused by temporary network conditions, like available bandwidth or packet loss. Two customers with different access speeds would be charged equally for the same multimedia stream, but



without doubt, they would observe different visual quality. Furthermore, the volume based charging could assess the network transport, which would be an acceptable solution for simple services like HTTP or FTP, but the IPTV delivery requires QoS differentiation. For instance, 10 independent packet losses may cause only marginal quality deterioration, but 10 consecutive packet loss could destroy the user experience of a multimedia transport due to the hierarchical frame coding scheme applied in MPEG-4, however the transmitted data volume would be measured the same.

An error resilient transport protocols (like TCP) may overcome this issue, but the transport layer level flow control, congestion control, and error recovery processes of TCP cannot be optimized by the real-time streaming application, therefore it consecutively introduce higher jitter and suboptimal transmission compared to an RTP transport. This may be acceptable for content on demand, which tolerate a relative high jitter value and operate with an initial large packet buffer, but hard delay requirements are defined for scheduled content service and back-in-time services. This, and the point-to-multipoint delivery of real-time services require special transport protocols that cannot guarantee a loss free transport, as I already pointed out in chapter 2.

PROBLEM 3.1. The delivery and the user experience of an IPTV services are affected by the various loss attributes of the wireless transport which has to be considered by a quality based charging solution.

In the upcoming sections, I will develop and discuss a new quality based charging solution among the following three main charging requirements described by the 3GPP technical specification:

- To charge for different level of QoS applied for and/or allocated during a session for each type of medium or service used.
- To charge using pre-pay and post-pay charging techniques.
- For network operators and 3rd parties to charge each other for the use of their resources.

3.3.2 The Proposed Business Model and Architecture

The implementation of the 4th generation billing functionality is based on the ascendant system; thus, in the early age of the main concept of billing scheme correspond with the present concept, which is a very mobile service provider centered.



THESIS II.1 (Jursonovics et al. 2004; Jursonovics and Imre 2005; Jursonovics, Butyka, and Imre 2005, 2008; Jursonovics and Imre 2014). *I selected the network operator centric business model for multimedia charging in mobile network based on the charging requirements, and I extended the standard charging architecture with my proxy solution to be able to realize quality based multimedia charging functions in mobile networks.*

The appropriate business model for IPTV should be applicable for mobile networks, and should handle all related charging requirements introduced in the previous section. IETF's recommendations (see 3.1.2) may fulfill all the requirements and develop various aspects of the required functionality, but do not provide an end to end solution, which would be easily applicable in mobile networks. The billing services are not discussed, therefore I propose to follow the guidance of the UMTS Forum, which is very 3GPP centric.

To select the appropriate model, the typical product portfolio of IPTV has to be considered. As 3.2.2 states, the proposal shall enable network operators to collect all service fees in the IPTV bundle, and provide a single bill for IPTV customers. Besides that, the model should allow IPTV providers to extend their subscription packages with partner offerings (for example: HBO Go) to be able to retain customers with competitive product portfolio. Considering these guidelines, I have chosen the network operator centric model as the basis of my own model, which will ensure the easy integration into the mobile landscape.

The other two business models are more appropriate for OTT offerings, where the billing and payment services are handled directly by the content owner, and the services are offered on a best effort basis over the Internet. I note that without the option of ensuring service quality, the relevance of quality based charging is marginal, therefore applying my findings in these models (for OTT services) would require a service agreement between content providers and network operators. Till the recent days, this was not possible due to the Internet neutrality directive of regulators, but Netflix just raised concerns, which may still allow service differentiation for network operators (Reuters 2014). I personally hope, that this will be accomplished for better service offerings and higher competitions.

Figure 3.5 shows the main elements of the proposed model. The customers have a direct relationship with the network operator (NO), which sets the prices of the services and handles the payment with the help of an external financial institute (FI). The value added service providers can receive the charging and authentication



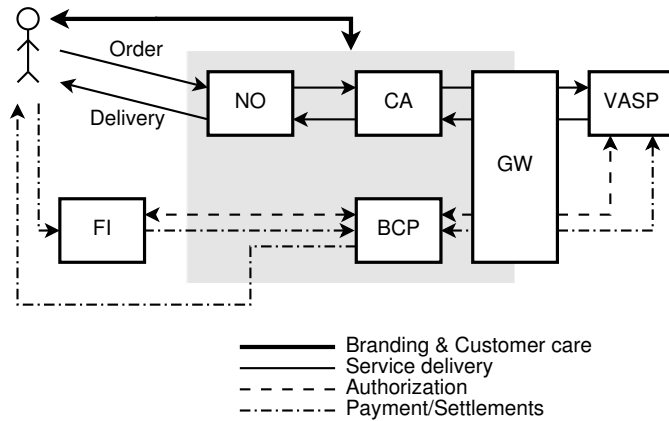


Figure 3.5. The proposed network operator centric model with network entities

information of their services from the network operator through a charging gateway (GW), which implements the proposed new quality based charging attributes. This model has the following key characteristics:

- Price of services defined by the network operator.
- Billing and payment arranged by the network operator.
- Network operator revenues gained not only as airtime, data volume, subscription, but also as message, advertising, and transaction/event services.

According to figure 3.6, over a classic mobile data session, the customers' communication is initiated by a mobile equipment (ME), which establishes a PDP context through the radio network subsystem (RNS), Node B, radio network controller (RNC), serving GPRS support node (SGSN), and GGSN. The SGSN is able to separate the users' flows from one another with their PDP context, but it cannot look inside the IP payload (as it does not decode the encapsulated protocol). Hence the SGSNs are unsuitable for my charging method that would based on the properties of these protocols.

LTE offers an optimized method for creating a data connection: the evolved packet system (EPS) bearer setup reduces the number of signaling messages that need to be sent over the air, however it uses the same tunneling protocols through the evolved Node B (eNB), serving gateway (SGW), PDN gateway (PDN-GW). According to the same argumentation, the SGW is also unsuitable for charging purposes of multimedia streaming.

To overcome these limitations, I introduce a new network element: the streaming proxy, which fits into and completes the existing charging infrastructure, and realizes the required quality based charging functions of the IPTV delivery.



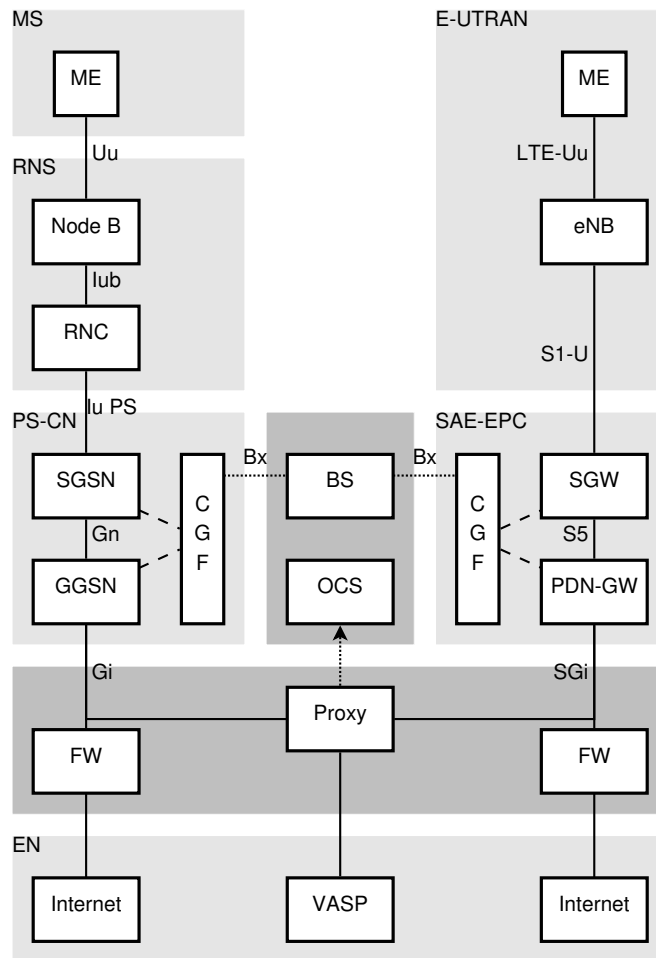


Figure 3.6. Proxy based charging architecture

The streaming proxy monopolizes the management of the multimedia delivery, and enables the users to connect through itself to the streaming providers (value added service providers – VASPs). To ensure that the charging proxy cannot be bypassed, I also implement an access restriction function (firewall – FW) in the architecture, which will block all non-authorized media access attempts.

The offline charging information (for example: usage of radio interface, usage duration, destination and source) are collected in the Packet Switched domain for each MS by the GSNs, and they are transferred in a charging data record (CDR) to the billing system (BS) via the charging gateway function (CGF). The generation of CDR depends on the charging characteristic profile. In this architecture the proxy measures the streaming flow due to its central position, and it has its own CDR generation function for offline charging.

The pre-paid account is limited. If the amount of money runs out, while a customer uses a service, the access must be denied to the customer. The offline charging



mechanism cannot provide this condition, therefore the proxy uses account reservation for online charging. At first, it reserves a piece of the customers' account. If the customers use up this amount of money for a value added service, then the proxy tries to reserve another piece of the account by connecting to the online charging system (OCS). If the allocation of money is unavailable, the proxy denies the access of service. This architecture enables the effective charging of multimedia services according to thesis II.1.

I note that I have also analyzed the possibility to implement a simple measurement entity instead of the above mentioned proxy solution, but due to the above mentioned access restriction feature of the online charging, a simple monitoring would not allow the required functions.

3.3.3 The Assessment of the Quality

The definition and measurement of the quality attributes of such a subjective matter, like multimedia user experience, is crucial for a quality based charging solution. In the previous section, I have introduced my proposed business model and system architecture, from here I continue my discussion with the assessment of their properties. I define the quality of the video transmission, then I point out the importance of the loss pattern, and finally, I implement a model for the estimation of the video quality based on the loss patterns.

I have considered several image quality metrics introduced by 1.5. I concluded that I adapt the PSNR metric, because it is widely used and several research results are documented with this value, which will ensure the comparability and easy validation of my own results. Though the accuracy of this metric is questioned (Eckert and Bradley 1998), therefore a more sophisticated metric can be used in a commercial implementation.

Let me describe the decoded frames of the transmitted video signal with the $\mathbf{g}[k]$ series of one dimensional vectors, where $k \in \mathbb{N}$ denotes the number of the frame in an $N > k$ long frame sequence. The dimension of $\mathbf{g}[k]$ equals the number of pixels in the given frame: $\dim(\mathbf{g}[k]) = M = \text{width} \times \text{height}$. To reduce the complexity of the given formulas, I will always use only one vector for one frame and I will refer only to the luma (Y) component, though the applied color space may requires more than one. Let $\hat{\mathbf{f}}[k]$ vector represent the decoded frames of the transmitted video signal, which may be distorted by the loss events during the transmission. The error vector introduced by the channel is



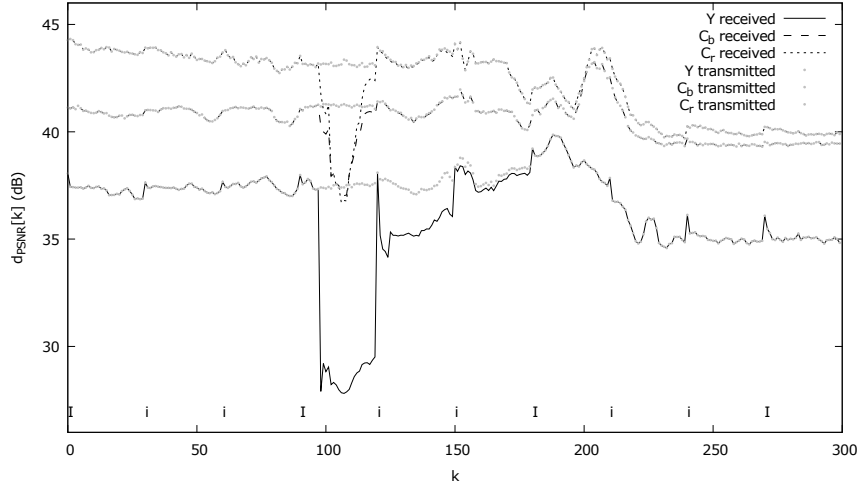


Figure 3.7. Error propagation in H.264 decoding. The graph shows that the initial quality deterioration, caused by the loss of frame #99, is slowly dissolving due to the applied spatial filtering. The non-IDR I frames are temporary restoring the image quality, but only an IDR frame stops the error propagation completely.

$$\mathbf{e}[k] = \mathbf{g}[k] - \hat{\mathbf{f}}[k]. \quad (3.1)$$

By expressing the $d[k]$ mean square error and the $d_{PSNR}[k]$ peak signal-to-noise ratio of the transmitted video signal in I420p format, I obtain

$$d[k] = \frac{\mathbf{e}^T[k] \cdot \mathbf{e}[k]}{M}, \quad (3.2)$$

$$d_{PSNR}[k] = 10 \log \left(\frac{256^2}{d[k]} \right), \quad (3.3)$$

where $\mathbf{e}^T[k]$ is the transpose of the $\mathbf{e}[k]$ vector.

The MPEG-4 advanced video coding (AVC) implements a hierarchical encoding, where the similarities between the frames of the video signal are exploited. This ensures a high coding efficiency, but introduces error propagation; a single frame error deteriorates not only the quality of the lost frame, but further frames are impacted as well. Figure 3.7 shows the effect of a single packet loss on the PSNR value introduced at the 99th frame in the YUV color space. The positions of the instantaneous decode refresh (IDR) I and non-IDR I frames are marked with *I* and *i* respectively. It can be easily observed, that the frame loss highly influences the quality of the lost frame, and from this position the decoding error slowly reduced by the spatial filtering in the decoder over the upcoming frames. An intra frame (#120, #150) temporary eliminates the quality deterioration but it is only removed by an IDR frame (#180).



Due to this effect, the pattern of the losses highly influences the perceived quality of the video transmission (Boulos et al. 2009; Calafate 2003; Lin et al. 2010).

The $D[\kappa]$ total distortion, caused by the frame losses at $\kappa = \{k_1, k_2, \dots\}$ frames, is expressed by

$$D[\kappa] = \sum_{i=k_1}^{N-1} d[i]. \quad (3.4)$$

PROBLEM 3.2. *The wireless communication shows a burstiness effect (Jursonovics and Butyka 2003), therefore the consideration of the burst errors are critical in the assessment of the quality in IPTV delivery over wireless networks.*

Liang, Apostolopoulos, and Girod (2008) provide and validate a model for burst loss effect, which I adapt in my work. According to their results, the total distortion, caused by a single packet loss, is given by:

$$D_S[k] = \sum_{i=0}^{N-1} r^i \left(1 - \frac{i}{N}\right) \cdot d[k] = \frac{r^{N+1} - (N+1)r + N}{N(1-r)^2} d[k] = \alpha \cdot d[k], \quad (3.5)$$

where $d[k]$ is the initial error power introduced at k , and α is the ratio between the total distortion and the mean square error (MSE) of the frame k . r models the effectiveness of the spatial filter reducing the distortion effect of the loss, and N is the distance between the lost frame and the next I frame.

The total distortion for two and B long burst losses are

$$\begin{aligned} D[k-1, k] &= \sum_{i=k-1}^{N-1} d[i] = d[k-1] + \sum_{i=0}^{N-1} r^i \left(1 - \frac{i}{N}\right) d[k] \\ &= d[k-1] + \alpha \cdot d[k], \text{ and} \end{aligned} \quad (3.6)$$

$$D[k-B+1, k] = \sum_{i=k-B+1}^{k-1} d[i] + \alpha(B) \cdot d[k]. \quad (3.7)$$

$d[k]$ can be a priori determined by leveraging the error-concealment feature of the H.264: in case of a frame loss, the previous frame will be repeated, therefore the error introduced by a frame loss is given by

$$e[k] = g[k] - g[k-1], \quad (3.8)$$

$$d[k] = \frac{\mathbf{e}^T[k] \cdot \mathbf{e}[k]}{M}. \quad (3.9)$$



The estimation of the parameters $(r, \alpha, \alpha())$ can be conducted during the encoding process and attached together with the precalculated $d[k]$ values as metadata descriptors to the multimedia objects.

3.3.4 Measurement and Prediction of the Loss Distribution

This section will define methods to measure and model the loss patterns in mobile networks with the aim of providing the required input parameters for quality assessment. The first obvious measurement point of packet losses is the Node B/RNC and eNode B. The extension of the existing bearer level data packet transport measurement on the radio interface would allow the exact and authentic determination of the loss pattern, and could provide a reliable input for the CDR generation, however it would suffer several disadvantages:

- It would introduce a large transport overhead towards the mobile core network.
- Only the quality of the radio bearer would be measured, and the packet losses caused by the core network would be ignored.
- It would not consider the effect of discarded frames by the OITF due to late arrival (out of sequence packet arrival after presentation time).
- Additional high level business logic would be required to the identification of external OTT streaming services.

Considering the above mentioned problems, my proposal assigns the loss measurement functionality to the client and streaming proxy elements, which can accurately measure the effect of packet loss on the wireless access network and the effect of frame discard in the OITF. The scheduled content services are delivered by IP multicast/UDP/RTP, where the real-time transport protocol (RTP) already provides an inclusive packet level quality reporting mechanism based on the real-time control protocol (RTCP): the client periodically reports back the aggregated loss and frame discard attributes of the stream, though it lacks the required details of loss/discard patterns. The RTP standard enables the definition of new, profile dependent report element, therefore the streaming player could measure and stored the loss/discard runlengths, which could be sent to the streaming proxy.

I propose to extend and use the RTCP receiver report messages with the corresponding loss/discard pattern description according to figure 3.8. Each loss/discard element should be described with the sequence number of the first packet in the loss/discard burst and with the length of the burst. The streaming proxy receives these real-time control protocol - receiver report (RTCP-RR) messages and forwards



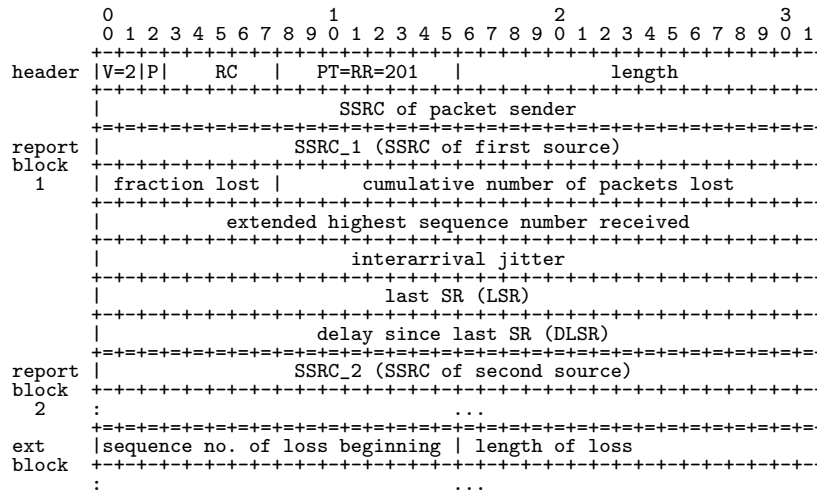


Figure 3.8. Redefined RTCP receiver report

them to the built in CGF functionality, which will create the charging data records (CDR) according to the quality assessment, and transfers them to the billing system.

This method is able to accurately measure the loss and discard pattern, but requires several additional consideration:

- Needs a client authentication to avoid report—therefore charging—falsification.
- The implementation of an additional feature in the media player is necessary.

But above all, the most important drawback is the lack of in-advance charging information. The price of the assets / scheduled content service have to be determined before the access the service itself. My proposal reduces the price of the service according to the future streaming quality attributes, therefore the customers could not be informed on the actual price in advance.

PROBLEM 3.3. *The IPTV business model requires the a priori price determination of the accesses service which is not ensured by the above described measurement.*

The a priori loss and discard pattern of a multimedia transmission can be predicted by several wireless models. Jiao, Schwiebert, and Xu; Calafate et al.; Sanneck and Carle (2002; 2009; 1999) analyzed the burst packet losses in wireless networks. I introduced a new model for the assessment of the RET service in 2.2.2. I am *not* going to choose a specific model, because this would depend on the various IPTV client implementations, and my goal is to develop a charging solution, instead, I will assume a general model, in which I describe my proposal.



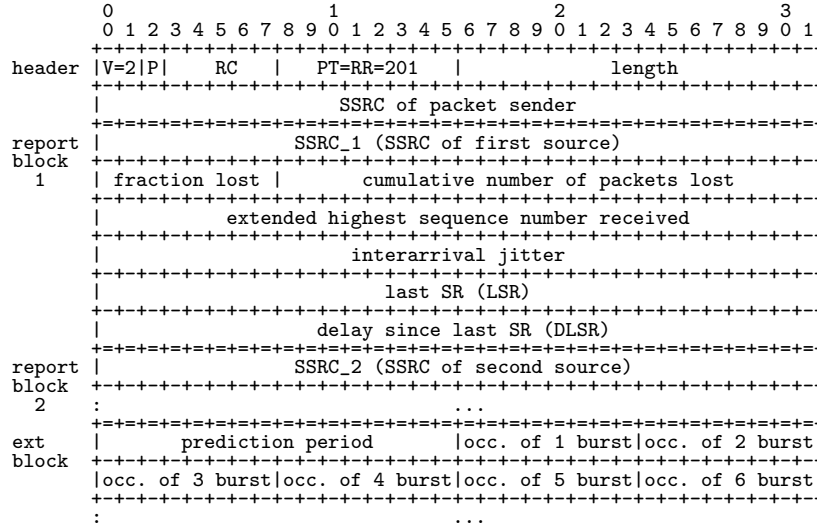


Figure 3.9. Redefined RTCP report

Every model has the same common feature: the prediction capability of the probability of an l long loss/discard burst $P_{L,burst}(l)$. This information has to reach the streaming proxy, which will assess the streaming quality and forward the estimation to the online charging system. For this purpose, I define a second RTCP-RR packet format according to figure 3.9. The streaming client has to choose a prediction interval (*prediction period*) and calculate the estimated occurrences of the different burst losses/discards (*occ. of l burst*). This information will be regularly sent to the streaming proxy, which will perform the charging of the service.

3.3.5 The Quality Based Charging Solution

I define the $F()$ charging process, which determines the *price* of a service according to the \mathbf{c} charging parameters including but not limited to data volume, event, resolution, content, and watching time:

$$price = F(\mathbf{c}). \tag{3.10}$$

According to the above described charging architecture, quality assessment, and loss pattern prediction, the quality based charging solution requires the modification of this price regarding the \mathbf{q} perceived quality parameters, which I define with the $P()$ quality based charging policy function:



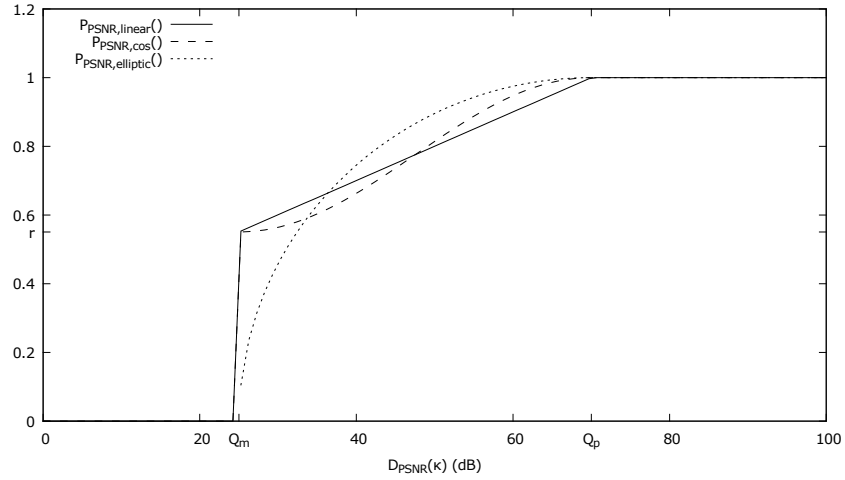


Figure 3.10. Different charging policies. The policy function decreases the initial price based on the service quality, therefore it possess a value between 1 and 0. The first two methods restrict the price discount at the r discount value, but the elliptic function may offer even 0 price. Below the Q_m critical quality value, the functions are undefined.

$$price = F(\mathbf{c}) \cdot P(\mathbf{q}), \text{ where} \quad (3.11)$$

$$0 \leq P() \leq 1$$

THESIS II.2 (Jursonovics and Imre 2005; Jursonovics, Butyka, and Imre 2005, 2008; Jursonovics and Imre 2014; appendix C, D). *I created a quality based charging method for IPTV delivery over wireless networks which method effectively considers the quality attributes of the IPTV service and provides a quality based charging feature. I provided the formula of the expected value and distribution of the price determined by my method. I pointed out the advantage of my solution, which reflects the quality differences in the price than traditional volume based charging methods.*

Several articles study the problem of human video quality perception and create sophisticated methods to describe the \mathbf{q} vector (Wang, Sheikh, and Bovik 2003; Eckert and Bradley 1998; Webster et al. 1993; Seshadrinathan et al. 2010). The main scope of my work is to develop a new charging solution, therefore I do not discuss the quality perception, but I consecutively define the charging policy as the function of the PSNR value of the total distortion, and I provide three different approaches in figure 3.10, which cover most of the possible pricing variations, and at the same time, they do not require complex mathematics.



First, I introduce a linear approximation of the charging policy (see equation 3.12 and figure 3.10). The price of an asset is steadily reduced, if the total distortion reaches a critical value (Q_p), and the charging (and service as well) is suspended if the quality cannot be maintained over a minimal guaranteed quality value (Q_m).

Second, I propose to smooth the sharp edges of the linear policy function with a cosine function (see equation 3.13 and figure 3.10), which will result a smooth transition for entering the price discount zone (Q_p), but still leaves a sharp and sudden fall at charging termination.

Finally, I evaluate the elliptic approximation (see equation 3.14 and figure 3.10), which gives a smooth transition at Q_m and Q_p as well.

$$P_{PSNR,linear}(x) = \begin{cases} \text{undefined} & \text{if } x < Q_m, \\ \frac{1-r}{Q_p-Q_m}x + 1 - \frac{Q_p(1-r)}{Q_p-Q_m} & \text{if } Q_m \leq x \leq Q_p, \\ 1 & \text{if } x > Q_p; \end{cases} \quad (3.12)$$

$$P_{PSNR,cos}(x) = \begin{cases} \text{undefined} & \text{if } x < Q_m, \\ \frac{r-1}{2} \cos\left(\frac{x-Q_m}{Q_p-Q_m}\pi\right) + r + \frac{1-r}{2} & \text{if } Q_m \leq x \leq Q_p, \\ 1 & \text{if } x > Q_p; \end{cases} \quad (3.13)$$

$$P_{PSNR,elliptic}(x) = \begin{cases} \text{undefined} & \text{if } x < Q_m, \\ \sqrt{1 - \left(\frac{x-Q_p}{Q_p-Q_m}\right)^2} & \text{if } Q_m \leq x \leq Q_p, \\ 1 & \text{if } x > Q_p, \end{cases} \quad (3.14)$$

where $x \stackrel{def}{=} D_{PSNR}[\kappa]$, the total distortion, for easier reading. Q_p is the smallest value of quality deterioration that does not involve price reduction, and Q_m is the minimal acceptable quality, on which the service can be still offered, and $Q_p > Q_m > 0$.

To be able to compare the three functions, r is defined on a way that the average value of the price discount functions are the same, assuming uniform quality distribution:

$$\int_{Q_m}^{\infty} P_{linear}(x) dx = \int_{Q_m}^{\infty} P_{cos}(x) dx = \int_{Q_m}^{\infty} P_{elliptic}(x) dx, \quad (3.15)$$

which yields to $r = \pi/2 - 1$.

Figure 3.11 summarizes all the relevant steps for the quality based charging solution.

0a. Asset publication: during the publication of an asset, every frame of the asset will be analyzed and the MSE values of the frame differences ($d[k]$) are calculated

according to (3.9), then stored, and on request, sent to the the streaming proxy as metadata.

- 0b. Live broadcast:** during live broadcast, the live stream is continuously analyzed and the MSE values of frame differences ($d[k]$) are calculated and sent to the streaming proxy as a real-time metadata feed.
- 1. Loss reporting:** the mobile client is continuously monitoring the packet arrival process, and periodically reports the packet loss pattern (κ) in the above defined RTCP receiver reports to the streaming proxy for scheduled content services and content on demand. Concerning other properties of this RTCP report process (for example: transmission interval, send and receive rules), I adapt of the recommendations of Schulzrinne et al. 2003. cite
- 2. Quality estimation:** the proxy collects the receiver reports and estimates the total distortion ($D[\kappa]$) with the help of the loss pattern (κ) and the pre-defined frame error sequence ($d[k]$) according to (3.5), (3.6) and (3.7). The charging parameters (\mathbf{c}) and the quality parameters ($D[\kappa] \in \mathbf{q}$) are sent to the billing system in form of a CDR.
- 3. Billing:** the billing system implements the charging functions ($F(\mathbf{c})$, $P(\mathbf{q})$) and determines the price and a bill, which reflects the streaming quality according to (3.11).

I note, that the proposed charging solution may lead to a significantly increased CDR generation, which would require additional performance from the nilling system. To limit the impact of this additional resource need, the CDR processing functions could be enhanced (Ary and Imre 2013, 2005b, 2007).

3.3.5.1 Theoretical Evaluation

The expected price discount of the quality based charging solution is an important and valuable information for business decision makers, who would like to gain strict control on the pricing scheme, though several parameters are only a posteriori known. Recognizing this problem, I present a statistical model and analysis of the price discounting to provide a tool for decision making.

This section uses a packet loss probability to characterize the transmission channel, then the frame errors and the total distortion will be modeled with a continuous probability distribution. The actual price discount depends on the charging policy function and the distribution of the quality degradation, which functions yield the distribution and the expected value of the price discount.

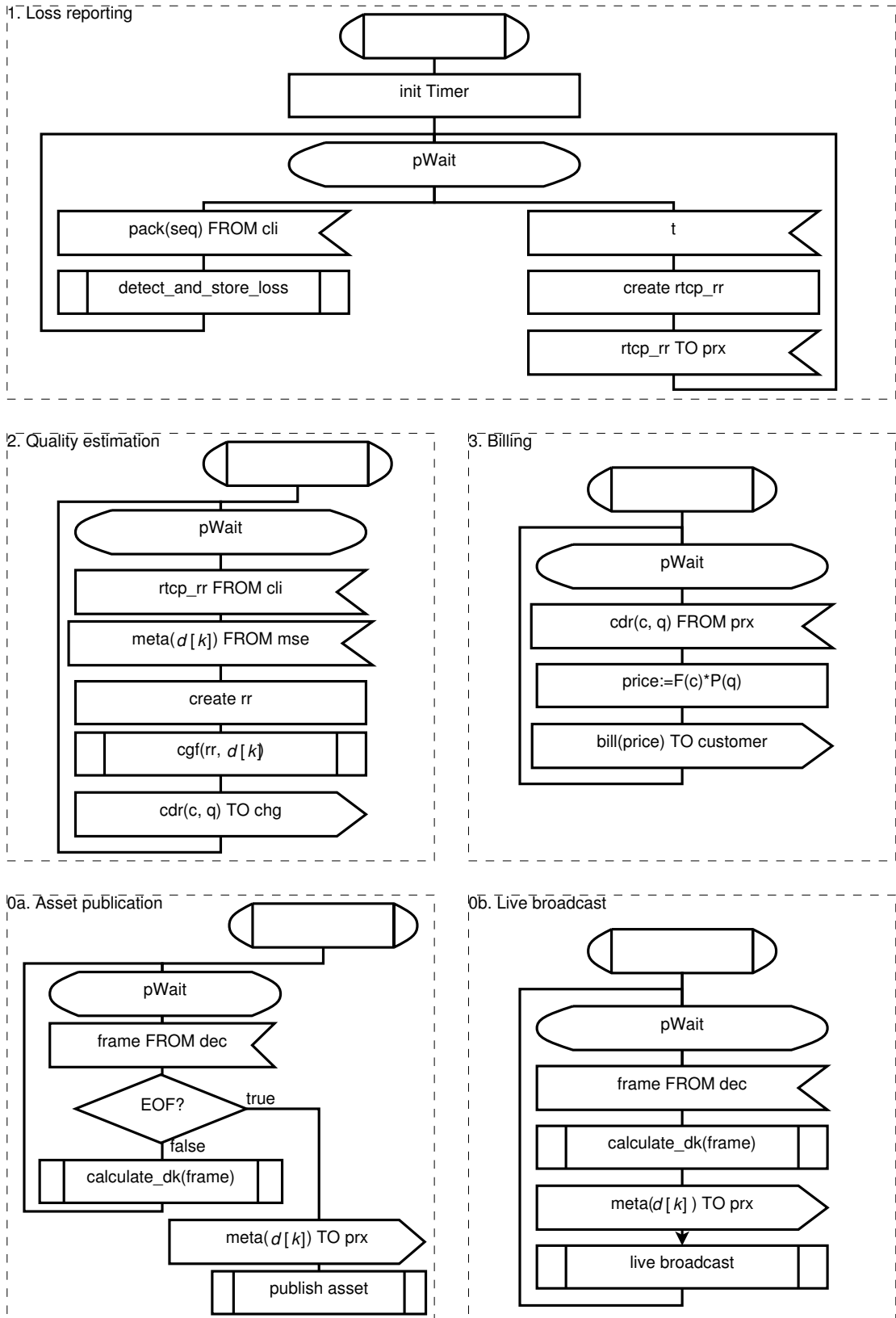


Figure 3.11. Charging algorithm

Let me first assume that only single packets are lost, where the loss probability can be described with a steady state packet loss rate: $P_{L,steady}$.

The perceived video quality is estimated from the frame differences ($d[k]$) showed by figure 3.12 and 3.13 for the bigbuckbunny sample video sequence. I consider $d[k]$ as a quasi independent, identical distributed random variable by assuming that the video sequence consists of several scenes and random camera movements, which results a weak correlation of $d[k]$ values. This assumption enables the description of $d[k]$ with a statistic. According to figure 3.14, I will approximate the distribution of the MSE values with the exponential distribution (for a complete analysis, please see appendix C, where I also attached the detailed examination of several video sequences and heavy-tailed distributions). Therefore my hypothesis is:

H_0 : The exponential distribution is an appropriate model for $d[k]$.

H_1 : The exponential distribution is not an appropriate model for $d[k]$.

The probability density function of the exponential distribution is

$$f_{d[k]}(d[k], \lambda) = \lambda e^{-\lambda \cdot d[k]}, \quad (3.16)$$

where λ is a form parameter. Using the maximum-likelihood parameter estimation on the sample video sequence above, I obtain the value in table 3.1 for the form parameter.

Table 3.1. Maximum likelihood fit (bigbuckbunny)

| |
|-----------------------------|
| rate (λ) |
| 3.404700×10^{-4} |
| $(2.837349 \times 10^{-6})$ |

To test my hypothesis, first I use the Pearson's chi-squared test with significance level $\alpha = .05$ and frequencies collected in 20 classes. Table 3.2 shows that the test statistic does not lie in the critical region therefore I accept H_0 with 5% significance level.

Table 3.2. Pearson's Chi-Square test (bigbuckbunny)

| Degrees of freedom | Critical region | Test statistic |
|--------------------|-------------------|---------------------------|
| 19 | $\chi^2 > 30.144$ | 5.644654×10^{-4} |

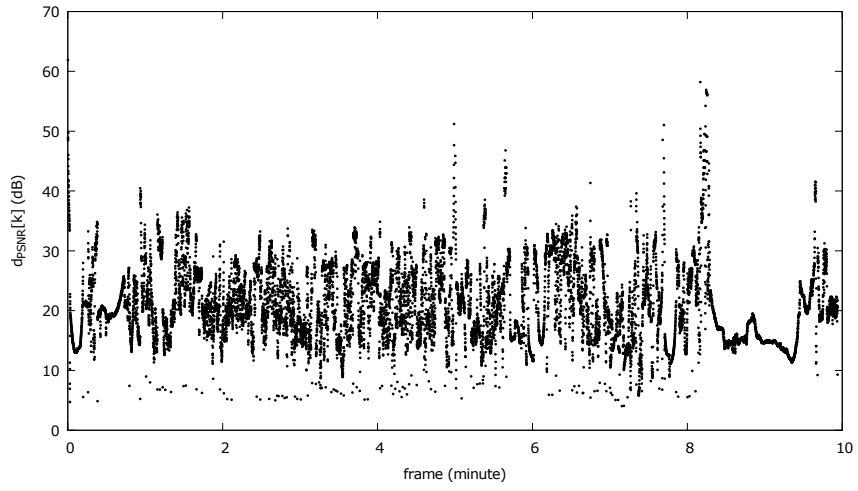


Figure 3.12. PSNR (bigbuckbunny)

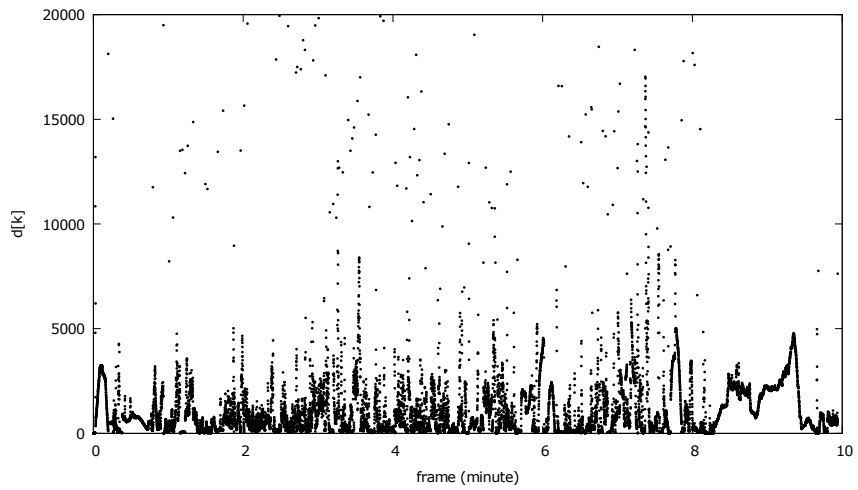


Figure 3.13. MSE (bigbuckbunny)

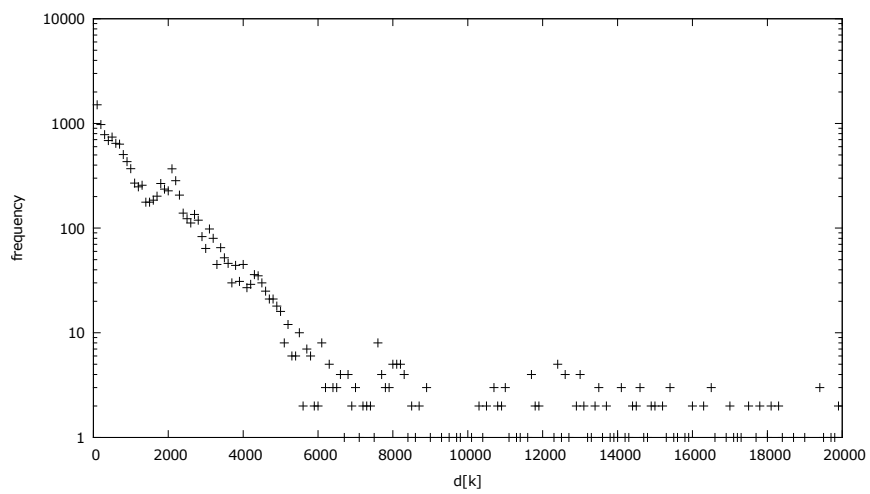


Figure 3.14. Histogram of $d[k]$ (bigbuckbunny)

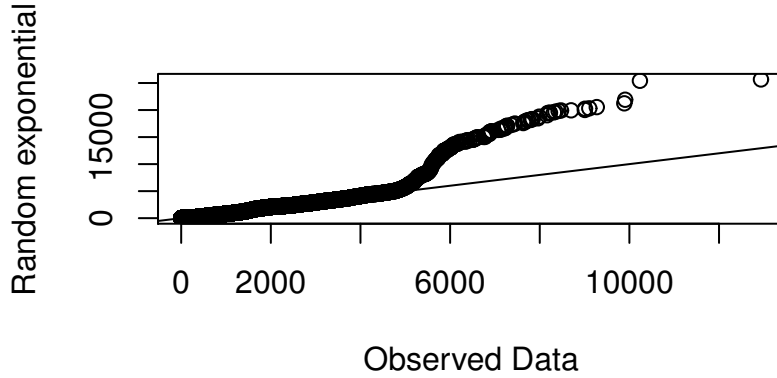


Figure 3.15. Q-Q plot (bigbuckbunny)

Second, I attach the Q-Q plot in figure 3.15, which also states that the empirical distribution follows the exponential distribution for small MSE values. Above 6000, the exponential distribution underestimates the probability of large frame differences, which error will result a slightly lower expected value of the price discount in my model. I also note that the charging function uses the real frame difference values, and this approximation does not jeopardize the correct and fair billing.

It can be easily concluded from (3.5) that the $D_S[k]$ total distortion can be also described with a random variable, and has also an exponential probability density function.

$$f_{D[\kappa]}(D[\kappa], \lambda) = \lambda e^{-\lambda \cdot D[\kappa]}. \quad (3.17)$$

The price discount is calculated by the charging policy functions using the total distortion as an input parameter, therefore the determination of the probability distribution of the price discount can be reduced to the problematic of the transformation of random variables and probability density functions.

I begin with the random variable of $D[\kappa]$, and I express the discount with the charging policy function:

$$discount = P(D[\kappa]), \quad (3.18)$$

where $P : \mathbb{R} \rightarrow \mathbb{R}$ is monotone, continuous, and single-valued. The policy charging functions (3.12), (3.13), and (3.14) are using PSNR input units, therefore they have to be converted to MSE values first:

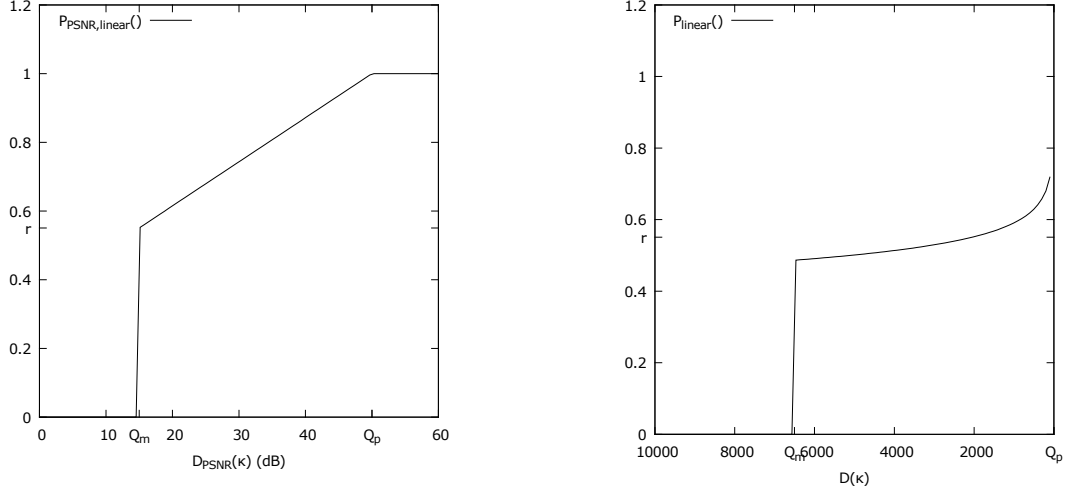


Figure 3.16. Linear charging policy in MSE units

$$\begin{aligned}
 P(D[\kappa]) &= g^{-1}(D_{PSNR}[\kappa]), \text{ where} & (3.19) \\
 g(\text{price}) &= h(P_{PSNR}^{-1}(\text{price})), \\
 h(x) &= \frac{MAX^2}{10^{\frac{1}{10}x}}.
 \end{aligned}$$

Figure 3.16 shows these transformed functions, the detailed deduction are enclosed in appendix D. The simplified form of the policy functions are

$$P_{linear}(D[\kappa]) = s_l \log\left(\frac{t_l}{D[\kappa]}\right), \quad (3.20)$$

$$P_{cos}(D[\kappa]) = s_c \cdot \cos(t_c \cdot \log(D[\kappa]) + u_c) + v_c, \text{ and} \quad (3.21)$$

$$P_{elliptic}(D[\kappa]) = \sqrt{1 - (s_e + t_e \cdot \log(D[\kappa]))^2}, \quad (3.22)$$

where $s_l, t_l, s_c, t_c, u_c, v_c, s_e, t_e$ are constants.

Finally, the distributions of the price discount using linear policy function (see appendix D for details):

$$g(p) = \lambda e^{-\lambda \left(\frac{MAX^2}{10^{\frac{1}{10} \frac{p-b}{a}}}\right)} \cdot \frac{MAX^2}{10^{\frac{1}{10} \frac{p-b}{a}}} \cdot \ln(10) \cdot \frac{1}{10a}, \quad (3.23)$$

and using the law of the unconscious statistician, the mean of the price discount is

$$E(\text{price}) = E(P(D[\kappa])) = \int_{-\infty}^{\infty} P_{\text{linear}}(D[\kappa])f(D[\kappa]) dD[\kappa], \quad (3.24)$$

$$E(\text{price}) = \left[\frac{e^{-\lambda D[\kappa]}}{-\lambda} \right]_0^{k(Q_p)} + c\lambda \left[\frac{e^{-\lambda D[\kappa]} \ln(D[\kappa])}{-\lambda \ln(10)} \right]_{k(Q_p)}^{k(Q_m)} + d\lambda \left[\frac{e^{-\lambda D[\kappa]}}{-\lambda} \right]_{k(Q_p)}^{k(Q_m)}. \quad (3.25)$$

The distributions of the price discount using cosine policy function (see appendix D for details):

$$g(p) = \ln(10) \frac{\frac{MAX^2}{10^{\frac{1}{10}(\frac{1}{b} \arccos(\frac{p-d}{a}) - \frac{c}{b})}}}{-10ab\sqrt{1 - (\frac{p-d}{a})^2}}, \quad (3.26)$$

and using the law of the unconscious statistician, the mean of the price discount is

$$E(\text{price}) = \int_0^{k(Q_p)} f(y) dy + \int_{k(Q_p)}^{k(Q_m)} p(y)f(y) dy. \quad (3.27)$$

The distributions of the price discount using elliptic policy function (see appendix D for details):

$$g(p) = \lambda e^{-\lambda \left(\frac{MAX^2}{10^{\frac{1}{10} \frac{\sqrt{1-p^2}-b}{a}}} \right)} \cdot \frac{MAX^2}{10^{\frac{1}{10} \frac{\sqrt{1-p^2}-b}{a}}} \cdot \ln(10) \cdot \left(\frac{-1}{10a} \right) \cdot \frac{1}{\sqrt{2-2p^2}} \cdot (-2p), \quad (3.28)$$

and using the law of the unconscious statistician, the mean of the price discount is

$$E(\text{price}) = \int_0^{k(Q_p)} \lambda e^{-\lambda y} dy + \int_{k(Q_p)}^{k(Q_m)} \sqrt{1 - (s + t \cdot \log(y))^2} \cdot \lambda e^{-\lambda y} dy. \quad (3.29)$$

The equations (3.25), (3.27), and (3.29) estimate the expected value of the prices using different quality based charging algorithm, assuming a specific wireless network channel and on demand content. This in-advanced information can be used by business decision makers for assessing the uncertainty of a quality based pricing. I also specified the formula of the price distribution to enable further analysis and parameter computation to support thesis II.2.



Table 3.3. Model parameters

| Parameter | Value |
|----------------------------|---|
| sequence | foreman |
| # frames | 300 |
| N | 90 |
| r | .999 |
| κ | {99} |
| $d[k]$ | $\begin{cases} 174.9 & \text{if } k = 99 \\ 0 & \text{if } k \neq 99 \end{cases}$ |
| $D[\kappa]$ | 7,727 |
| average $D[\kappa]$ | 25.8 |
| average $D_{PSNR}[\kappa]$ | 34 dB* |

*quite good quality

3.3.5.2 Empirical Evaluation

To demonstrate the quality assessment, I calculated the video quality metrics of the video sequence used for figure 3.7 in case of a single packet loss showed by table 3.3.

Figure 3.17 shows that the estimated values of the frame error are close to the measured values and the estimation strictly follows the error mitigation feature of the spatial filter. The accuracy of this estimation does not depend on the frame type (I, P, B), because the error concealment feature will replace the lost frame in every case, and the different impact of the loss is already captured by the frame difference values ($d[k]$). However, the GOP structure may influence the estimation error, because a more advanced (for example: hierarchical) structure may jeopardize the error correction effect of the spatial filter; the distortion may not decrease according to the linear approximation. In my dissertation, I will continue to use linear assumption, because my main goal is to develop an end to end quality based charging method¹. In the presented case, the corresponding estimation error remains between -10% and 15% therefore I conclude that the applied error propagation model is efficient for assessing the streaming quality for charging purposes.

I implemented the processes in figure 3.18 on my testbed with the aim of evaluating my proposal on new methods for quality based charging solutions of multimedia streaming.

1. This assumption can be enhanced and replaced by a more sophisticated model.



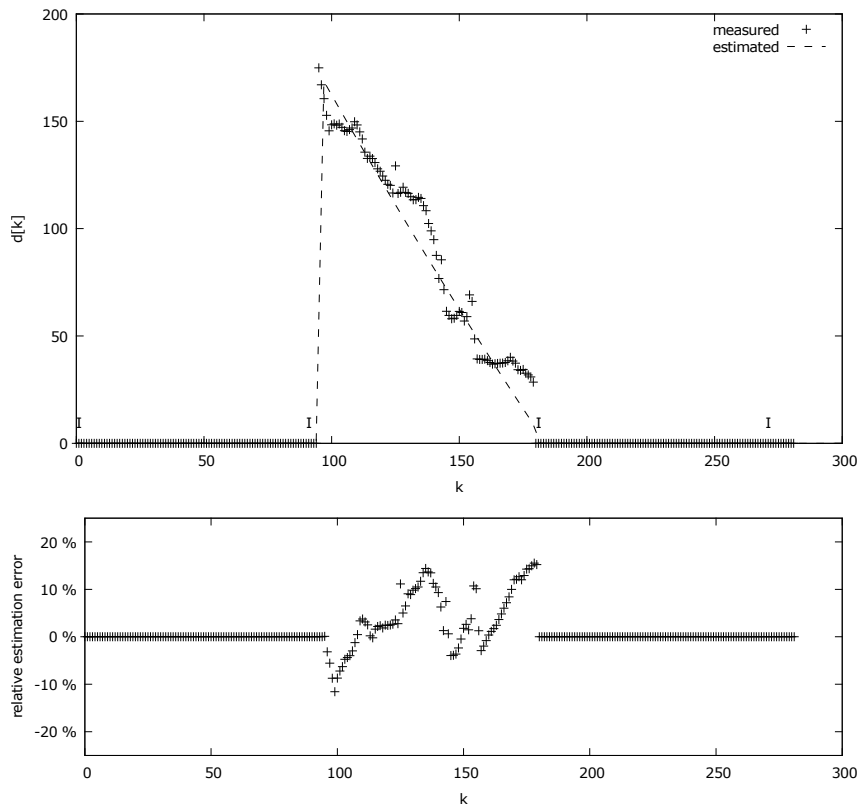


Figure 3.17. Quality prediction. This figure shows the effect of the loss of the 99th P frame. The spatial filter slowly mitigates the error, caused by the error concealment, which will be eliminated by the arrival of the 180th I frame.

First, I created the necessary steps of content creation (represented by the content production domain).

.yuv. YUV file, used as content source according to 1.6.

enc. Application, open source H.264 encoder used for creating a video file.

.264. H.264 encoded video file, used for video transmission.

dec. Application, open source H.264 decoder.

_rec.yuv. YUV file, the YUV sequences of the source video file enabling the analysis of a perfect transmission.

mse. My own c++ application, which analyzes the _rec.yuv file and creates the frame difference values ($d[k]$) for quality assessment.

.meta. File, containing the frame difference values as metadata.

Next, I built the components of stream delivery marked by the content distribution domain.



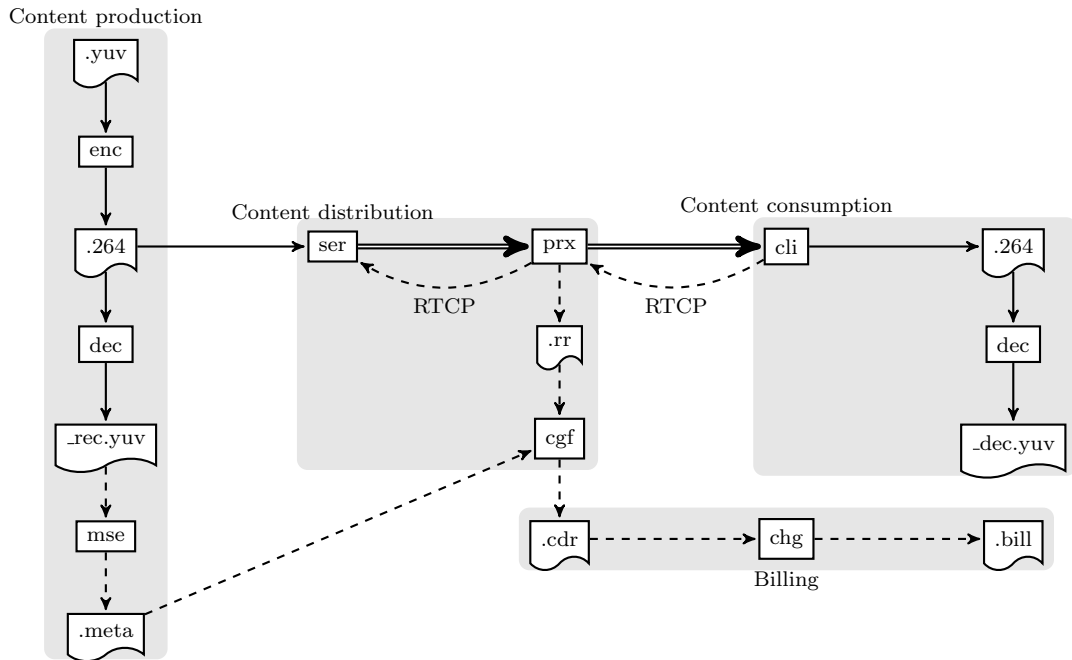


Figure 3.18. Workflow for quality based charging

ser. My own c++ application, a simple H.264 packetizer and streaming server. It streams the .264 file with UDP/RTP protocol to the wireless clients and implements a basic control function like stop and start.

prx. My own c++ application, a simple transparent streaming proxy based on the PCAP library. It intercepts and analyzes the RTCP receiver report messages from the clients and creates the .rr files for quality based charging.

.rr. File, contains the loss pattern of the video streaming transmission.

cgf. My own c++ application, implements a basic charging gateway functionality. It correlates the receiver report files and based on the metadata description it estimates the quality of the streaming session (total distortion: $D[\kappa]$) and creates the appropriate charging data records incorporating the quality estimate.

Then the elements of the content consumption domain:

cli. My own c++ application, a simple UDP/RTP receiver which implements the basic client functionality, streaming server control protocol and an internal jitter buffer. The application issues commands for the streaming server, receives the RTP/UDP stream. It continuously analyzes the streaming flow and reports the loss pattern according to the proposed RTSP-RR format to the steaming server.



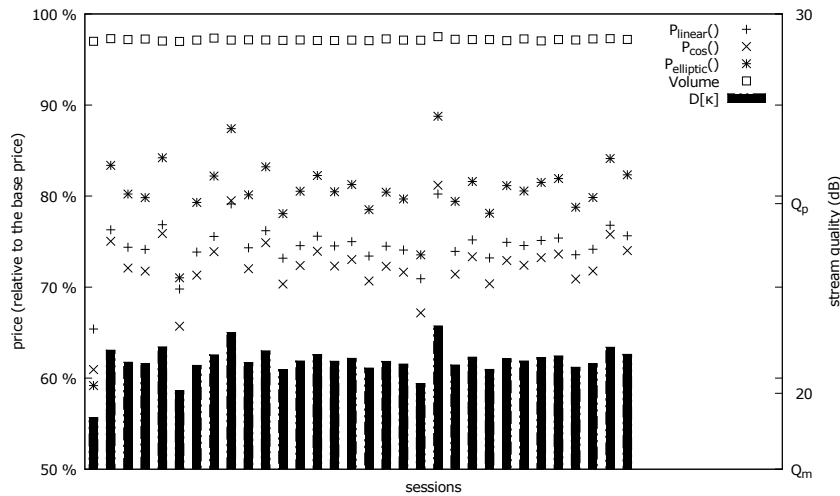


Figure 3.19. Comparison of different charging methods of several video sessions conducted in the testbed with the startrek sequence. The proposed three charging policy functions offered a discount (price axis) according to the experienced quality deterioration (showed by the bar chart, interpreted on the streaming quality axis).

.264. H.264 file, received by the client application which may contain quality deterioration due to possible packet losses during transmission.

dec. Application, open source H.264 decoder.

_dec.yuv. YUV file, the YUV sequences of the received video file enabling the analysis of quality deterioration caused by transmission errors.

Finally, the billing domain:

.cdr. File, charging data record, contains the stream quality estimates besides several other charging parameter.

chg. My own c++ application, implements the quality based charging functions inclusive the quality based policy decision and creates the bill and discount for the streaming session.

.bill. File, the quality discounted price of the video streaming session.

Figure 3.19 shows my results. I conducted 32 streaming requests on the startrek video sequence during one day, and I performed the service charging according to four different charging policies (volume based charging, quality based charging with linear, cosine and elliptic policy function) for every session. The charging discount is expressed in the actual price relative to the base price (80% means 20% price discount due to quality degradation). The average quality of the streams are also showed by boxes at the bottom of the figure.



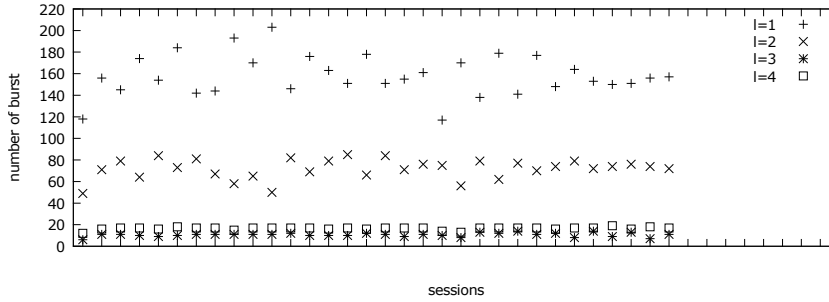


Figure 3.20. Occurrence of l length of loss bursts

It can be easily observed that the volume based charging function is not able to truly address the quality differences of the streams, and assigns almost the same discount to the different qualities (see the standard deviation values in table 3.4), but my proposed method reflects the quality differences more effectively.

Table 3.4. Comparison of different charging methods

| | Charging | Mean of the price | Std.Dev of the price |
|--|------------------------------------|-------------------|----------------------|
| | volume based | 0.9717 | 0.0011 |
| | quality based with linear policy | 0.7451 | 0.0255 |
| | quality based with cosine policy | 0.7243 | 0.0357 |
| | quality based with elliptic policy | 0.8009 | 0.0503 |

The expected differences among the quality based charging methods can be also seen. The discount of the linear and cosine policy functions are close to each other (check the mean values in the table 3.4), however the elliptic policy increases the price discount only slowly though at worst quality (first session) the price is decreased more than the linear policy. These finding conclude thesis II.2.

I also note that the elliptic policy function may offer up to 100% discount near to the minimal acceptable quality (Q_m), but the linear and cos functions will set the minimal price depreciation at only 43%.

To offer a more comprehensive basis for further evaluation of my results, I included six statistical parameters of each streaming sessions. Figure 3.20 shows the occurrence of $l = 1, 2, 3, 4$ length of loss bursts. It can be observed, that sort loss bursts dominated during the video transmission. Figure 3.21 summarizes the mean and the standard deviation of the distances between consecutive loss bursts.



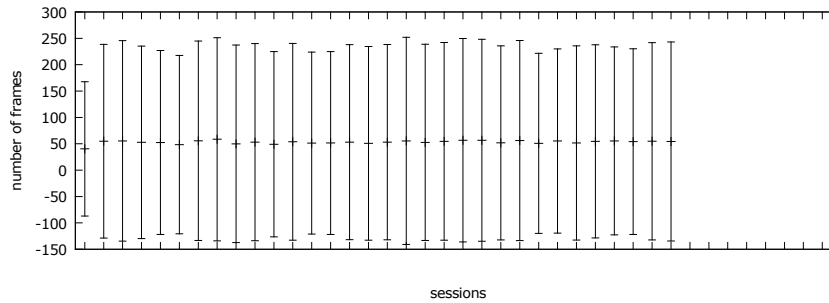


Figure 3.21. Mean distance and \pm standard deviation for consecutive loss bursts

3.4 Conclusion

My study was set out to explore the concept of charging solutions for IPTV delivery over mobile networks, the role and importance of quality of service in the charging process and the establishment of a fair pricing model and charging solution. The general research on this field (presented in 3.1.4) developed several individual aspect of this context but no common and complete solution was offered for my research objectives:

1. Create a charging method in wireless networks which does consider the quality of the offered multimedia service and offers a fair charging and billing process.
2. Find and evaluate the correlation between service charging and the various attributes of wireless transport (problem 3.1 and 3.2).
3. Provide an answer for the problem of a priori quality based pricing (problem 3.3).

This section will synthesize my theoretical findings to answer the study’s research objectives.

1. Create a charging method in wireless networks which does consider the quality of the offered multimedia service and offers a fair charging and billing process.

Business model. Based on my review of charging requirements and different business model, I pointed out that the network operator centric model is the optimal for quality based IPTV charging due to its aggregation role which enables the easy integration with third parties and leaves the service control at the network operator.

Architecture. I extended the charging architecture of mobile networks with a proxy solution which integrates the quality based charging functions into the mobile architecture.



- Measurement.** I stated that the bearer level packet measurement cause too much overhead for quality based charging therefore I assigned the required measurement functionality to the mobile devices and streaming proxy.
2. Find and evaluate the correlation between service charging and the various attributes of wireless transport.

Quality assessment. I provided a method which effectively and accurately estimates the quality of the multimedia streaming. For research purposes I consecutively adapted the PSNR metric however I draw the attention to its disadvantages and I recommended an other metric for real world implementation.

- Policy function.** I defined the quality based pricing with a policy function, which was realized by three individual functions. My comparison has shown that the elliptic based function offers a smoother transition for price discounts. I enclosed a calculation method for the expected price discount, which explicit solution was calculated by assuming the linear policy function which serves as important input for business decision making.
3. Provide an answer for the problem of a priori quality based pricing.

Prediction of the loss distribution. I used a general model as the basis of the loss prediction and to preserve the maximal system compatibility and minimal integration effort, I extended the RTCP-RR protocol to carry the prediction information which enables the estimation of the a priory price information.

The main empirical findings are conducted on a testbed built for this specific reason, integrating my own realization of the newly created entities, methods and functions:

Accuracy of the quality assessment. I showed that the chosen quality estimation technique is able to accurately predict the quality deterioration caused by packet losses. According to the sample sequence the error remains always between -10% and 15% per frame.

Distribution of the total distortion. Based on several test sequences I deduced that the density of the total distortion follows a heavy tailed distribution which can be effectively described with an exponential or weibull distribution. I proved my findings with Q-Q plots and Chi-Square tests.



Comparison of different charging policies. Based on a test video sequence I compared the three recommended charging policy function and the attention was drawn to the expected advantage of the elliptic based function, which provides a smoother transition for charging, though it may allows free of charge service.

For further research I am going to extend my study with the deeper examination of the two interesting areas of RTCP-RR falsification and adaptive policy function. The receiver reports can be easily falsified (and therefore the service can be accessed on a smaller charge) due to the lack of authentication support of RTCP. I would like to further investigate the possibility of trusted clients and RTCP message signature.

The importance of good quality based charging varies according to the content of the multimedia asset. A poorer quality may be accepted for a quite static scene than for a scene with actions and key moments. The current proposal for the policy based charging function does not consider this aspect which I will more deeply investigate in further research.

The study has offered an evaluative perspective on quality based charging, and was conducted on several sequences. As a direct consequence of this methodology, the study encountered a number of limitations, which need to be considered

Frames per packet. The resolution (CIF) of the test sequences resulted to encode every frame in a single packet but in commercial scenarios this may be different and several slices of a frame could be encoded into different packets.

IP fragmentation. Due to the simplicity of the testbed components, the streaming server (ser) did not realized the fragmentation unit feature of the H.264 payload format therefore every frame was encoded into one big packet and the fragmentation was performed by the IP stack.

RR report falsification A user may create falsified RR messages to minimize the costs of the video service by artificially reporting lower quality levels. The main scope of this dissertation is to discuss the wireless aspects of the quality based charging solutions, however I would like to shortly address this concern as well. The RTP standard does not describe a solution for ensuring the authentication and message integrity of the RTCP, but it assumes, that these services will be provided by lower layer protocols (see Schulzrinne et al. 2003, section 9.2). The main issue of implementing a secure transport (like TLS/SSL) is the method of secure key exchange. There is no need for charging of free-to-air services, therefore report falsification may applies only to payed content, which is already



protected by a DRM solution. The implemented DRM already fulfills all the requirements of securely transmitting an encryption key, which could be used in lower layer protocols to provide authentication and digital signing of RTCP reports.

Nevertheless, Baugher et al. (2004) already recognized and addressed this issue in RFC3711: *The Secure Real-time Transport Protocol (SRTP)* provides a solution for secure RTCP.

I do believe that the quality based charging methods does offer a value both for customers and service providers through the customer's satisfaction and fair pricing, though the existing business cases have to be reconsidered, and business managers have to adapt this new approach, which may take some time till the solution reaches wide commercial implementation and market.



Afterwords

This dissertation introduced several achievements for service quality improvement of IPTV services over wireless networks, and for fair, quality based charging implementation. Following the detailed introduction and discussion of my methods, I showed, how an IPTV service operator benefits from the realization of these features, and how can the service quality and customer's satisfaction be improved. In my opinion, these factors will be shortly in the foreground due to to the highly competing television market and increasing importance of user experience.

I am convinced, that the technology of the television solutions will merge with the Web 3.0 services, in the mid-term. The influence of social media and personal sharing had a big effect on the TV consumption. Nowadays, content is instantly produced (Facebook, Twitter, Instagram) and consumed on an individual, personal basis. There is less and less share for linear television, where the user have to sit at a specific time in front of a device and he will not have the chance to interact with the content provider. The interactive applications and the ultimate freedom and information source of the Internet provides such a large difference compared to the user experience of our parents, that this new, content based TV consumption will ultimately change the Television, what we know Today.

The evolution is already happening, and it will challenge several traditional solutions applied in the current broadcast industry. From the telecommunication industry point of view, the content aggregator role of a telco will slowly disappear. The high speed internet access allows content creators to directly reach customers, and offer personalized contents without the involvement of a third party. The main driving force behind a triple play service is to boost the sales of the IP access technology, but with the deceasing importance of linear TV, which is the main differentiator for a telco due to the enormous bandwidth requirements and multicast technology, the relevance of the triple play will vanish, and operators have to compete with over-the-top content providers and content owners directly.



In the same way, the increasing diversity of the client equipments will face operators to a new dilemma. Different user devices requires different streaming technologies, and they use different software versions. Supporting all the varied formats will require a big technological investment, and it will increase the operational costs through complexity. The MPEG DASH standard may provide an unified approach, but I believe that the continuous development will never let the technology to consolidate.

Taking all this into consideration, I believe that in 10 years, the linear television will completely disappear, and the television platforms will merge with the cloud infrastructure, sharing services. Due to the increasing access bandwidth, the central role of content distribution will be obsolete, the peer-to-peer technology will take over the current role of the multicast.



Appendix A

Configuration of the Testbed Components

The following configuration were deployed in the WLAN access point used during the simulation conducted on the testbed.

```
Current configuration : 1491 bytes
!
version 12.3
no service pad
service timestamps debug datetime msec
service timestamps log datetime msec
service password-encryption
!
hostname ap
!
enable secret 5 *****
!
clock timezone +0100 1
ip subnet-zero
ip name-server 192.168.1.254
!
!
no aaa new-model
!
dot11 ssid strabag
    authentication open
!
!
!
username Cisco password 7 *****
!
bridge irb
!
!
interface Dot11Radio0
no ip address
no ip route-cache
!
encryption key 1 size 40bit 7 ***** transmit-key
encryption mode wep mandatory
!
ssid strabag
!
no short-slot-time
speed basic-2.0
no power client local
power client 30
power local cck 30
packet retries 35 drop-packet
channel 2412
station-role root
antenna receive right
antenna transmit right
no dot11 extension aironet
no cdp enable
bridge-group 1
bridge-group 1 subscriber-loop-control
bridge-group 1 block-unknown-source
no bridge-group 1 source-learning
no bridge-group 1 unicast-flooding
bridge-group 1 spanning-disabled
```



```

!
interface FastEthernet0
 ip address dhcp hostname ap
 no ip route-cache
 duplex auto
 speed auto
 no cdp enable
 bridge-group 1
 no bridge-group 1 source-learning
 bridge-group 1 spanning-disabled
!
interface BVI1
 ip address dhcp client-id FastEthernet0
 no ip route-cache
!
ip http server
no ip http secure-server
ip http help-path \url{http://www.cisco.com/warp/public/779/smbiz/prodconfig/help/eag}
!
no cdp run
bridge 1 route ip
!
!
!
line con 0
line vty 0 4
 login local
!
end

```

The following table presents the quality parameters and statistics of the ADSL connection during the simulation conducted on the testbed.

Table A.1. Access line parameters

| Name | DSLAM | Modem |
|---------------------|----------------|------------------------|
| Vendor ID: | Analog Devices | T-Com (Speedport 921W) |
| Softwareversion: | 0.0 - H0 | 9.5.2.1.1.6 A |
| DSL Down-/Upstream: | 3,456 kbit/s | 448 kbit/s |
| Noise margin: | 19 dB | 22 dB |
| CRC Errors: | 0 | 71 |
| HEC: | 0 | 0 |
| FEC: | 179 | 0 |



Appendix B

Configuration of the JM Reference Software

The Configuration of the Encoder

```
# New Input File Format is as follows
# <ParameterName> = <ParameterValue> # Comment
#
# See configfile.h for a list of supported ParameterNames
#
# For bug reporting and known issues see:
# https://ipbt.hhi.fraunhofer.de

#####
# Files
#####
InputFile           = "foreman_cif.yuv"      # Input sequence
InputHeaderLength   = 0                    # If the inputfile has a header, state it's length in byte here
StartFrame          = 0                    # Start frame for encoding. (0-N)
FramesToBeEncoded   = 300                  # Number of frames to be coded
FrameRate           = 30.0                 # Frame Rate per second (0.1-100.0)
SourceWidth         = 352                  # Source frame width
SourceHeight        = 288                  # Source frame height
SourceResize        = 0                    # Resize source size for output
OutputWidth         = 352                  # Output frame width
OutputHeight        = 288                  # Output frame height

TraceFile           = "trace_enc.txt"       # Trace file
ReconFile           = "foreman_cif_rec.yuv" # Reconstruction YUV file
OutputFile          = "foreman_cif.264"    # Bitstream
StatsFile           = "stats.dat"          # Coding statistics file

#####
# Encoder Control
#####
ProfileIDC          = 66 # Profile IDC (66=baseline, 77=main, 88=extended; FREXT Profiles: 100=High, 110=High
10, 122=High 4:2:2, 244=High 4:4:4, 44=CAVLC 4:4:4 Intra)
IntraProfile        = 0 # Activate Intra Profile for FREXT (0: false, 1: true)
# (e.g. ProfileIDC=110, IntraProfile=1 => High 10 Intra Profile)
LevelIDC            = 40 # Level IDC (e.g. 20 = level 2.0)

IntraPeriod         = 30 # Period of I-pictures (0=only first)
IDRPeriod           = 90 # Period of IDR pictures (0=only first)
AdaptiveIntraPeriod = 0 # Adaptive intra period
AdaptiveIDRPeriod   = 0 # Adaptive IDR period
IntraDelay          = 0 # Intra (IDR) picture delay (i.e. coding structure of PPIPPP... )
EnableIDRGOP        = 0 # Support for IDR closed GOPs (0: disabled, 1: enabled)
EnableOpenGOP       = 0 # Support for open GOPs (0: disabled, 1: enabled)
QPISlice            = 28 # Quant. param for I Slices (0-51)
QPPSlice            = 28 # Quant. param for P Slices (0-51)
FrameSkip           = 0 # Number of frames to be skipped in input (e.g 2 will code every third frame).
# Note that this now excludes intermediate (i.e. B) coded pictures

ChromaQPOffset      = 0 # Chroma QP offset (-51..51)

DisableSubpelME     = 0 # Disable Subpixel Motion Estimation (0=off/default, 1=on)
SearchRange         = 32 # Max search range

MEDistortionFPel    = 0 # Select error metric for Full-Pel ME (0: SAD, 1: SSE, 2: Hadamard SAD)
MEDistortionHPel    = 2 # Select error metric for Half-Pel ME (0: SAD, 1: SSE, 2: Hadamard SAD)
MEDistortionQPel    = 2 # Select error metric for Quarter-Pel ME (0: SAD, 1: SSE, 2: Hadamard SAD)
```



```

MDDistortion          = 2 # Select error metric for Mode Decision (0: SAD, 1: SSE, 2: Hadamard SAD)
SkipDeBlockNonRef    = 0 # Skip Deblocking (regardless of DFPParametersFlag) for non-reference frames (0: off,
1: on)
ChromaMCBuffer       = 1 # Calculate Color component interpolated values in advance and store them.
# Provides a trade-off between memory and computational complexity
# (0: disabled/default, 1: enabled)
ChromaMEEnable       = 0 # Take into account Color component information during ME
# (0: only first component/default,
# 1: All Color components - Integer refinement only
# 2: All Color components - All refinements)
ChromaMEWeight       = 1 # Weighting for chroma components. This parameter should have a relationship with
color format.

NumberReferenceFrames = 5 # Number of previous frames used for inter motion search (0-16)

PList0References     = 0 # P slice List 0 reference override (0 disable, N <= NumberReferenceFrames)
Log2MaxFNumMinus4    = 0 # Sets log2_max_frame_num_minus4 (-1 : based on FramesToBeEncoded/Auto, >=0 :
Log2MaxFNumMinus4)
Log2MaxPOCLsbMinus4 = -1 # Sets log2_max_pic_order_cnt_lsb_minus4 (-1 : Auto, >=0 : Log2MaxPOCLsbMinus4)

GenerateMultiplePPS = 0 # Transmit multiple parameter sets. Currently parameters basically enable all WP
modes (0: disabled, 1: enabled)
SendAUD              = 0 # Send Access Delimiter Unit NALU (for every access unit)
ResendSPS            = 2 # Resend SPS (0: disabled, 1: all Intra pictures, 2: only for IDR, 3: for IDR and
OpenGOP I)
ResendPPS           = 0 # Resend PPS (with pic_parameter_set_id 0) for every coded Frame/Field pair (0:
disabled, 1: enabled)

MbLineIntraUpdate    = 0 # Error robustness(extra intra macro block updates)(0=off, N: One GOB every N frames
are intra coded)
RandomIntraMBRefresh = 0 # Forced intra MBs per picture

#####
# PSlice Mode types
#####
PSliceSkip           = 1 # P-Slice Skip mode consideration (0=disable, 1=enable)
PSliceSearch16x16    = 1 # P-Slice Inter block search 16x16 (0=disable, 1=enable)
PSliceSearch16x8     = 1 # P-Slice Inter block search 16x8 (0=disable, 1=enable)
PSliceSearch8x16     = 1 # P-Slice Inter block search 8x16 (0=disable, 1=enable)
PSliceSearch8x8      = 1 # P-Slice Inter block search 8x8 (0=disable, 1=enable)
PSliceSearch8x4      = 1 # P-Slice Inter block search 8x4 (0=disable, 1=enable)
PSliceSearch4x8      = 1 # P-Slice Inter block search 4x8 (0=disable, 1=enable)
PSliceSearch4x4      = 1 # P-Slice Inter block search 4x4 (0=disable, 1=enable)

DisableIntra4x4      = 0 # Disable Intra 4x4 modes
DisableIntra16x16    = 0 # Disable Intra 16x16 modes
DisableIntraIntraInter = 0 # Disable Intra modes for inter slices
IntraDisableInterOnly = 0 # Apply Disabling Intra conditions only to Inter Slices (0:disable/default,1: enable)
Intra4x4ParDisable   = 0 # Disable Vertical & Horizontal 4x4
Intra4x4DiagDisable  = 0 # Disable Diagonal 45degree 4x4
Intra4x4DirDisable   = 0 # Disable Other Diagonal 4x4
Intra16x16ParDisable = 0 # Disable Vertical & Horizontal 16x16
Intra16x16PlaneDisable = 0 # Disable Planar 16x16
ChromaIntraDisable   = 0 # Disable Intra Chroma modes other than DC
EnableIPC             = 1 # Enable IPCM macroblock mode

DisposableP          = 0 # Enable Disposable P slices in the primary layer (0: disable/default, 1: enable)
DispQPPOffset        = 0 # Quantizer offset for disposable P slices (0: default)

PreferDispOrder      = 1 # Prefer display order when building the prediction structure as opposed to coding
order (affects intra and IDR periodic insertion, among others)
PreferPowerOfTwo     = 0 # Prefer prediction structures that have lengths expressed as powers of two
FrmStructBufferLength = 16 # Length of the frame structure unit buffer; it can be overridden for certain cases

ChangeQPFrame        = 0 # Frame in display order from which to apply the Change QP offsets
ChangeQPI            = 0 # Change QP offset value for I_SLICE
ChangeQPP            = 0 # Change QP offset value for P_SLICE
ChangeQPB            = 0 # Change QP offset value for B_SLICE
ChangeQPSI           = 0 # Change QP offset value for SI_SLICE
ChangeQPSP           = 0 # Change QP offset value for SP_SLICE
#####
# Output Control, NALs
#####

OutFileMode          = 0 # Output file mode, 0:Annex B, 1:RTP

#####
# Picture based Multi-pass encoding
#####

RDPictureDecision    = 0 # Perform multiple pass coding and make RD optimal decision among them
RDPictureBTest       = 0 # Perform Slice level RD decision between P and B slices.
RDPictureMaxPassISlice = 1 # Max number of coding passes for I slices, valid values [1,3], default is 1
RDPictureMaxPassPSlice = 2 # Max number of coding passes for P slices, valid values [1,6], default is 2
RDPictureMaxPassBSlice = 3 # Max number of coding passes for B slices, valid values [1,6], default is 3
RDPictureFrameQPSPSlice = 0 # Perform additional frame level QP check (QP+/-1) for P slices, 0: disabled (
default), 1: enabled
RDPictureFrameQPBSlice = 0 # Perform additional frame level QP check (QP+/-1) for B slices, 0: disabled,
1: enabled (default)
RDPictureDeblocking  = 0 # Perform another coding pass to check non-deblocked picture, 0: disabled (
default), 1: enabled

```



```

RDPictureDirectMode      = 0      # Perform another coding pass to check the alternative direct mode for B slices
                             , , 0: disabled (default), 1: enabled

#####
# Deblocking filter parameters
#####

DFParametersFlag        = 0      # Configure deblocking filter (0=parameters below ignored, 1=parameters sent)
                             # Note that for pictures
                             # with multiple slice
                             # types,
                             # only the type of the first slice will be considered.
DFDisableRefISlice      = 0      # Disable deblocking filter in reference I coded pictures (0=Filter, 1=No
    Filter).
DFAlphaRefISlice        = 0      # Reference I coded pictures Alpha offset div. 2, {-6, -5, ... 0, +1, .. +6}
DFBetaRefISlice         = 0      # Reference I coded pictures Beta offset div. 2, {-6, -5, ... 0, +1, .. +6}
DFDisableNRefISlice     = 0      # Disable deblocking filter in non reference I coded pictures (0=Filter, 1=No
    Filter).
DFAlphaNRefISlice       = 0      # Non Reference I coded pictures Alpha offset div. 2, {-6, -5, ... 0, +1, ..
    +6}
DFBetaNRefISlice        = 0      # Non Reference I coded pictures Beta offset div. 2, {-6, -5, ... 0, +1, .. +6}
DFDisableRefPSlice      = 0      # Disable deblocking filter in reference P coded pictures (0=Filter, 1=No
    Filter).
DFAlphaRefPSlice        = 0      # Reference P coded pictures Alpha offset div. 2, {-6, -5, ... 0, +1, .. +6}
DFBetaRefPSlice         = 0      # Reference P coded pictures Beta offset div. 2, {-6, -5, ... 0, +1, .. +6}
DFDisableNRefPSlice     = 0      # Disable deblocking filter in non reference P coded pictures (0=Filter, 1=No
    Filter).
DFAlphaNRefPSlice       = 0      # Non Reference P coded pictures Alpha offset div. 2, {-6, -5, ... 0, +1, ..
    +6}
DFBetaNRefPSlice        = 0      # Non Reference P coded pictures Beta offset div. 2, {-6, -5, ... 0, +1, .. +6}

#####
# Error Resilience / Slices
#####

SliceMode                = 0      # Slice mode (0=off 1=fixed #mb in slice 2=fixed #bytes in slice 3=use callback)
SliceArgument            = 50     # Slice argument (Arguments to modes 1 and 2 above)

num_slice_groups_minus1 = 0      # Number of Slice Groups Minus 1, 0 == no FMO, 1 == two slice groups, etc.
slice_group_map_type     = 0      # 0: Interleave, 1: Dispersed, 2: Foreground with left-over,
    # 3: Box-out, 4: Raster Scan 5: Wipe
    # 6: Explicit, slice_group_id read from SliceGroupConfigFileName
slice_group_change_direction_flag = 0 # 0: box-out clockwise, raster scan or wipe right,
    # 1: box-out counter clockwise, reverse raster scan or wipe left

slice_group_change_rate_minus1 = 85 #
SliceGroupConfigFileName = "sg0conf.cfg" # Used for slice_group_map_type 0, 2, 6

UseRedundantPicture     = 0      # 0: not used, 1: enabled
NumRedundantHierarchy   = 1      # 0-4
PrimaryGOPLength        = 10     # GOP length for redundant allocation (1-16)
    # NumberReferenceFrames must be no less than PrimaryGOPLength when redundant slice
    # enabled
NumRefPrimary           = 1      # Actually used number of references for primary slices (1-16)

#####
# Search Range Restriction / RD Optimization
#####

RestrictSearchRange     = 2      # restriction for (0: blocks and ref, 1: ref, 2: no restrictions)
RDOptimization          = 1      # rd-optimized mode decision
    # 0: RD-off (Low complexity mode)
    # 1: RD-on (High complexity mode)
    # 2: RD-on (Fast high complexity mode - not work in FREX Profiles)
    # 3: with losses
I16RDOpt               = 0      # perform rd-optimized mode decision for Intra 16x16 MB
    # 0: SAD-based mode decision for Intra 16x16 MB
    # 1: RD-based mode decision for Intra 16x16 MB
SubMBCodingState        = 1      # submacroblock coding state
    # 0: lowest complexity, do not store or reset coding state during sub-MB mode
    # decision
    # 1: medium complexity, reset to master coding state (for current mode) during sub-
    # MB mode decision
    # 2: highest complexity, store and reset coding state during sub-MB mode decision
DistortionSSIM          = 0      # Compute SSIM distortion. (0: disabled/default, 1: enabled)
DistortionMS_SSIM      = 0      # Compute Multiscale SSIM distortion. (0: disabled/default, 1: enabled)
SSIMOverlapSize        = 8      # Overlap size to calculate SSIM distortion (1: pixel by pixel, 8: no overlap)
DistortionYUVtoRGB     = 0      # Calculate distortion in RGB domain after conversion from YCbCr (0:off, 1:on)
CtxAdptLagrangeMult    = 0      # Context Adaptive Lagrange Multiplier
    # 0: disabled (default)
    # 1: enabled (works best when RDOptimization=0)
FastCrIntraDecision     = 1      # Fast Chroma intra mode decision (0:off, 1:on)
DisableThresholding     = 0      # Disable Thresholding of Transform Coefficients (0:off, 1:on)
SkipIntraInInterSlices = 0      # Skips Intra mode checking in inter slices if certain mode decisions are satisfied
    (0: off, 1: on)
WeightY                 = 1      # Luma weight for RDO
WeightCb                = 1      # Cb weight for RDO
WeightCr                = 1      # Cr weight for RDO

#####
# Explicit Lambda Usage
#####

```



```

UseExplicitLambdaParams = 0 # Use explicit lambda scaling parameters (0:disabled, 1:enable lambda weight, 2:
use explicit lambda value)
UpdateLambdaChromaME = 0 # Update lambda given Chroma ME consideration
FixedLambdaISlice = 0.1 # Fixed Lambda value for I slices
FixedLambdaPSlice = 0.1 # Fixed Lambda value for P slices

LambdaWeightISlice = 0.65 # scaling param for I slices. This will be used as a multiplier i.e. lambda=
LambdaWeightISlice * 2^((QP-12)/3)
LambdaWeightPSlice = 0.68 # scaling param for P slices. This will be used as a multiplier i.e. lambda=
LambdaWeightPSlice * 2^((QP-12)/3)

LossRateA = 5 # expected packet loss rate of the channel for the first partition, only valid if
RDOptimization = 3
LossRateB = 0 # expected packet loss rate of the channel for the second partition, only valid if
RDOptimization = 3
LossRateC = 0 # expected packet loss rate of the channel for the third partition, only valid if
RDOptimization = 3
FirstFrameCorrect = 0 # If 1, the first frame is encoded under the assumption that it is always
correctly received.
NumberOfDecoders = 30 # Numbers of decoders used to simulate the channel, only valid if RDOptimization =
3
RestrictRefFrames = 0 # Doesnt allow reference to areas that have been intra updated in a later frame.

#####
# Additional Stuff
#####

UseConstrainedIntraPred = 0 # If 1, Inter pixels are not used for Intra macroblock prediction.

NumberOfLeakyBuckets = 8 # Number of Leaky Bucket values
LeakyBucketRateFile = "leakybucketrate.cfg" # File from which encoder derives rate values
LeakyBucketParamFile = "leakybucketparam.cfg" # File where encoder stores leakybucketparams

NumFramesInELayerSubSeq = 0 # number of frames in the Enhanced Scalability Layer(0: no Enhanced Layer)

SparePictureOption = 0 # (0: no spare picture info, 1: spare picture available)
SparePictureDetectionThr = 6 # Threshold for spare reference pictures detection
SparePicturePercentageThr = 92 # Threshold for the spare macroblock percentage

PicOrderCntType = 0 # (0: POC mode 0, 1: POC mode 1, 2: POC mode 2)

#####
#Rate control
#####

RateControlEnable = 0 # 0 Disable, 1 Enable
Bitrate = 45020 # Bitrate(bps)
InitialQP = 0 # Initial Quantization Parameter for the first I frame
# InitialQp depends on two values: Bits Per Picture,
# and the GOP length
BasicUnit = 0 # Number of MBs in the basic unit
# should be a fraction of the total number
# of MBs in a frame ("0" sets a BU equal to a frame)
ChannelType = 0 # type of channel( 1=time varying channel; 0=Constant channel)
RCUpdateMode = 0 # Rate Control type. Modes supported :
# 0 = original JM rate control,
# 1 = rate control that is applied to all frames regardless of the slice type,
# 2 = original plus intelligent QP selection for I and B slices (including
Hierarchical),
# 3 = original + hybrid quadratic rate control for I and B slice using bit rate
statistics
#
RCISliceBitRatio = 1.0 # target ratio of bits for I-coded pictures compared to P-coded Pictures (for
RCUpdateMode=3)
RCBSliceBitRatio0 = 0.5 # target ratio of bits for B-coded pictures compared to P-coded Pictures -
temporal level 0 (for RCUpdateMode=3)
RCBSliceBitRatio1 = 0.25 # target ratio of bits for B-coded pictures compared to P-coded Pictures -
temporal level 1 (for RCUpdateMode=3)
RCBSliceBitRatio2 = 0.25 # target ratio of bits for B-coded pictures compared to P-coded Pictures -
temporal level 2 (for RCUpdateMode=3)
RCBSliceBitRatio3 = 0.25 # target ratio of bits for B-coded pictures compared to P-coded Pictures -
temporal level 3 (for RCUpdateMode=3)
RCBSliceBitRatio4 = 0.25 # target ratio of bits for B-coded pictures compared to P-coded Pictures -
temporal level 4 (for RCUpdateMode=3)
RCBoverPRatio = 0.45 # ratio of bit rate usage of a B-coded picture over a P-coded picture for the
SAME QP (for RCUpdateMode=3)
RCIOverPRatio = 3.80 # ratio of bit rate usage of an I-coded picture over a P-coded picture for the
SAME QP (for RCUpdateMode=3)
RCMinQPISlice = 8 # minimum P Slice QP value for rate control
RCMaxQPISlice = 44 # maximum P Slice QP value for rate control
RCMinQPISlice = 8 # minimum I Slice QP value for rate control
RCMaxQPISlice = 36 # maximum I Slice QP value for rate control

#####
#Fast Mode Decision
#####
EarlySkipEnable = 0 # Early skip detection (0: Disable 1: Enable)
SelectiveIntraEnable = 0 # Selective Intra mode decision (0: Disable 1: Enable)

ReportFrameStats = 0 # (0:Disable Frame Statistics 1: Enable)
DisplayEncParams = 0 # (0:Disable Display of Encoder Params 1: Enable)
Verbose = 1 # level of display verbosity

```



```

# 0: short, 1: normal (default), 2: detailed, 3: detailed/nvb
# 4: with additional MB level lambda info

#####
#Rounding Offset control
#####

OffsetMatrixPresentFlag = 0 # Enable Explicit Offset Quantization Matrices (0: disable 1: enable)
QOffsetMatrixFile      = "q_offset.cfg" # Explicit Quantization Matrices file

AdaptiveRounding       = 1 # Enable Adaptive Rounding based on JVT-N011 (0: disable, 1: enable)
AdaptRoundingFixed     = 1 # Enable Global Adaptive rounding for all qps (0: disable, 1: enable - default/
    old)
AdaptRndPeriod         = 16 # Period in terms of MBs for updating rounding offsets.
    # 0 performs update at the picture level. Default is 16. 1 is as in JVT-N011.
AdaptRndChroma         = 1 # Enables coefficient rounding adaptation for chroma

AdaptRndWFactorIRef    = 4 # Adaptive Rounding Weight for I/SI slices in reference pictures /4096
AdaptRndWFactorPRef    = 4 # Adaptive Rounding Weight for P/SP slices in reference pictures /4096
AdaptRndWFactorINRef   = 4 # Adaptive Rounding Weight for I/SI slices in non reference pictures /4096
AdaptRndWFactorPNRef   = 4 # Adaptive Rounding Weight for P/SP slices in non reference pictures /4096

AdaptRndCrWFactorIRef  = 4 # Chroma Adaptive Rounding Weight for I/SI slices in reference pictures /4096
AdaptRndCrWFactorPRef  = 4 # Chroma Adaptive Rounding Weight for P/SP slices in reference pictures /4096
AdaptRndCrWFactorINRef = 4 # Chroma Adaptive Rounding Weight for I/SI slices in non reference pictures /4096
AdaptRndCrWFactorPNRef = 4 # Chroma Adaptive Rounding Weight for P/SP slices in non reference pictures /4096

#####
#Fast Motion Estimation Control Parameters
#####

SearchMode              = 0 # Motion estimation mode
    # -1 = Full Search
    # 0 = Fast Full Search (default)
    # 1 = UMHexagon Search
    # 2 = Simplified UMHexagon Search
    # 3 = Enhanced Predictive Zonal Search (EPZS)

UMHexDSR                = 1 # Use Search Range Prediction. Only for UMHexagonS method
    # (0:disable, 1:enabled/default)

UMHexScale              = 3 # Use Scale_factor for different image sizes. Only for UMHexagonS method
    # (0:disable, 3:/default)
    # Increasing value can speed up Motion Search.

EPZSPattern             = 2 # Select EPZS primary refinement pattern.
    # (0: small diamond, 1: square, 2: extended diamond/default,
    # 3: large diamond, 4: SBP Large Diamond,
    # 5: PMVFAST )

EPZSDualRefinement      = 3 # Enables secondary refinement pattern.
    # (0:disabled, 1: small diamond, 2: square,
    # 3: extended diamond/default, 4: large diamond,
    # 5: SBP Large Diamond, 6: PMVFAST )

EPZSFixedPredictors     = 2 # Enables Window based predictors
    # (0:disable, 1: P only, 2: P and B/default)

EPZSTemporal            = 1 # Enables temporal predictors
    # (0: disabled, 1: enabled/default)

EPZSSpatialMem          = 1 # Enables spatial memory predictors
    # (0: disabled, 1: enabled/default)

EPZSBlockType           = 1 # Enables block type Predictors
    # (0: disabled, 1: enabled/default)

EPZSMinThresScale       = 0 # Scaler for EPZS minimum threshold (0 default).
    # Increasing value can speed up encoding.

EPZSMedThresScale       = 1 # Scaler for EPZS median threshold (1 default).
    # Increasing value can speed up encoding.

EPZSMaxThresScale       = 2 # Scaler for EPZS maximum threshold (1 default).
    # Increasing value can speed up encoding.

EPZSSubPelME            = 1 # EPZS Subpel ME consideration
EPZSSubPelMEBiPred      = 1 # EPZS Subpel ME consideration for BiPred partitions
EPZSSubPelThresScale    = 2 # EPZS Subpel ME Threshold scaler
EPZSSubPelGrid          = 1 # Perform EPZS using a subpixel grid

#####
# SEI Parameters
#####

GenerateSEIMessage      = 0 # Generate an SEI Text Message
SEIMessageText          = "H.264/AVC Encoder" # Text SEI Message

UseMVLimits             = 0 # Use MV Limits
SetMVXLimit             = 512 # Horizontal MV Limit (in integer units)
SetMVYLimit             = 512 # Vertical MV Limit (in integer units)

#####
# VUI Parameters
#####
# the variables below do not affect encoding and decoding
# (many are dummy variables but others can be useful when supported by the decoder)

EnableVUISupport        = 0 # Enable VUI Parameters

```



The Configuration of the Decoder

```
# This is a file containing input parameters to the JVT H.264/AVC decoder.
# The text line following each parameter is discarded by the decoder.
#
# For bug reporting and known issues see:
# https://ipbt.hhi.fraunhofer.de
#
# New Input File Format is as follows
# <ParameterName> = <ParameterValue> # Comment
#
#####
# Files
#####
#InputFile      = "foreman_cif_los.264"      # H.264/AVC coded bitstream
#OutputFile     = "foreman_cif_dec.yuv"     # Output file, YUV/RGB
#RefFile        = "foreman_cif_rec.yuv"     # Ref sequence (for SNR)
WriteUV         = 1                        # Write 4:2:0 chroma components for monochrome streams
FileFormat      = 0                        # NAL mode (0=Annex B, 1: RTP packets)
RefOffset       = 0                        # SNR computation offset
POCScale        = 2                        # Poc Scale (1 or 2)
#####
# HRD parameters
#####
#R_decoder      = 500000                    # Rate_Decoder
#B_decoder      = 104000                    # B_decoder
#F_decoder      = 73000                     # F_decoder
#LeakyBucketParamFile = "leakybucketparam.cfg" # LeakyBucket Params
#####
# decoder control parameters
#####
DisplayDecParams = 0                       # 1: Display parameters;
ConcealMode      = 1                       # Err Concealment(0:Off,1:Frame Copy,2:Motion Copy)
RefPOCGap        = 2                       # Reference POC gap (2: IPP (Default), 4: IbP / IpP)
POCGap           = 2                       # POC gap (2: IPP /IbP/IpP (Default), 4: IPP with frame skip = 1 etc.)
Silent           = 0                       # Silent decode
IntraProfileDeblocking = 1                 # Enable Deblocking filter in intra only profiles (0=disable, 1=filter
    according to SPS parameters)
DecFrmNum        = 0                       # Number of frames to be decoded (-n)
#####
# MVC decoding parameters
#####
DecodeAllLayers  = 0                       # Decode all views (-mpr)
```



Appendix C

Analysis of Different Video Sequences

The perceived video quality—and therefore the price discount of the quality based charging solution—depends on the a-priori values of the inter-frame differences ($d[k]$) of the transmitted video signal, as I stated in 3.3.3. To compare and evaluate my proposed charging policy functions in 3.3.5.1, I chose a stochastic approach, which enabled the assessment of these functions independently from the video sources, however they required an appropriate model for $d[k]$.

I used the exponential distribution in my thesis, but the background of my choice was not highlighted due to the size limitations of my dissertation. This appendix will highlight my main findings by analyzing and evaluating several sample video sequences and distributions to support my preference on the exponential distribution.

Figure C.1-C.6 show the PSNR value of the inter frame differences of the startrek, thehobbit, bigbuckbunny, foreman, bridge (close), and highway video sequences introduced by 1.6 respectively. The last three sequence has a static image content, therefore the $k[k]$ values have smaller dynamic.

Next, I calculated the histogram of the different values in MSE unit in figure C.7-C.12. Due to the static content and the short length, the foreman and bridge (close) sequences produced an invaluable output, therefore I exclude them from further analysis.

It can be observed, that the inter-frame difference possess the properties of a heavy-tailed distribution, therefore I perform a stochastic parameter estimation based on these input values, for the following 4 distribution with the help of *the R* statistical program.

Figure C.13-C.15 show the Q-Q plot of the startrek, thehobbit, and BickBuck-Bunny sequences; Table C.1-C.3 the output variables of the different parameter esti-



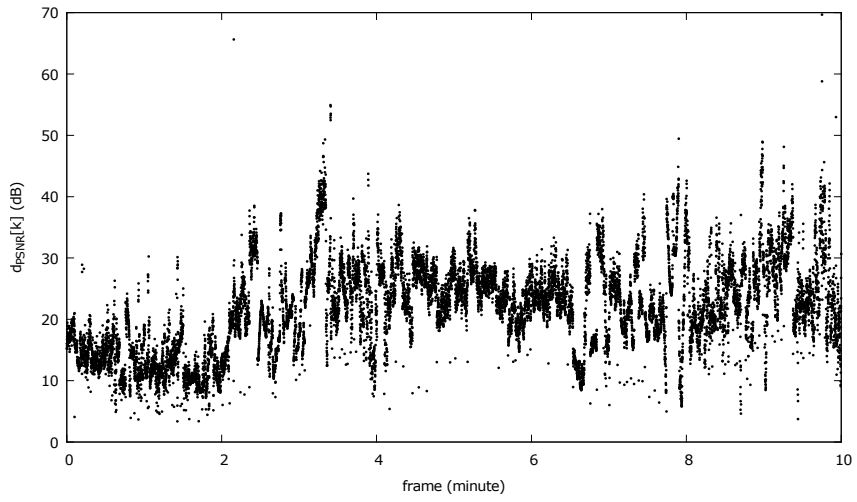


Figure C.1. Inter frame difference (startrek)

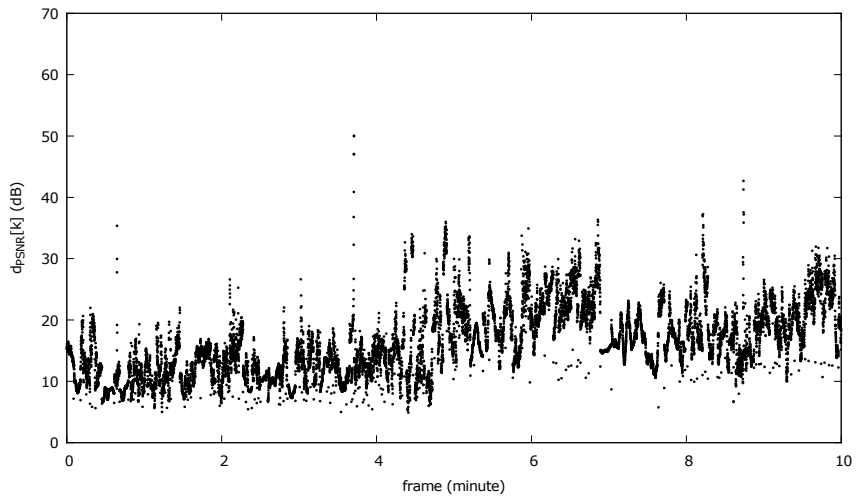


Figure C.2. Inter frame difference (thehobbit)

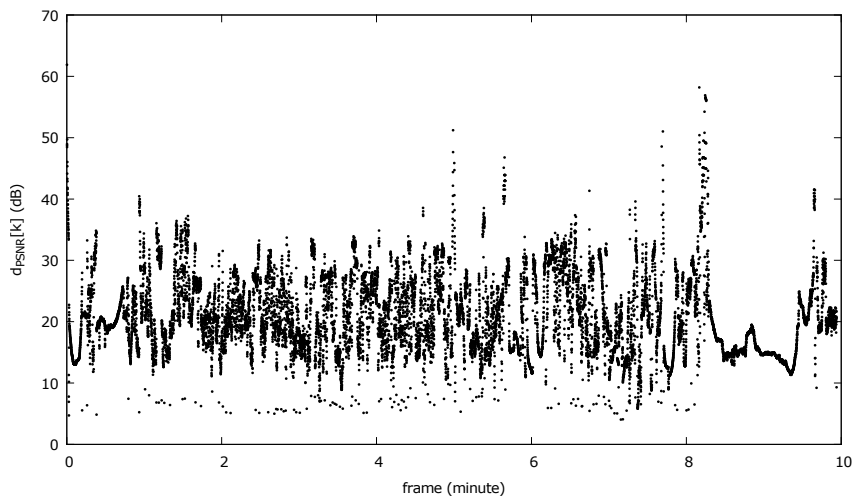


Figure C.3. Inter frame difference (bigbuckbunny)



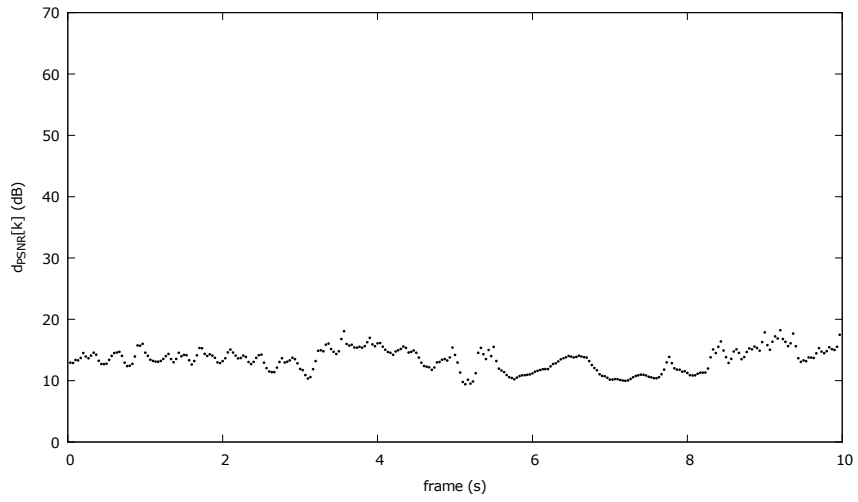


Figure C.4. Inter frame difference (foreman)

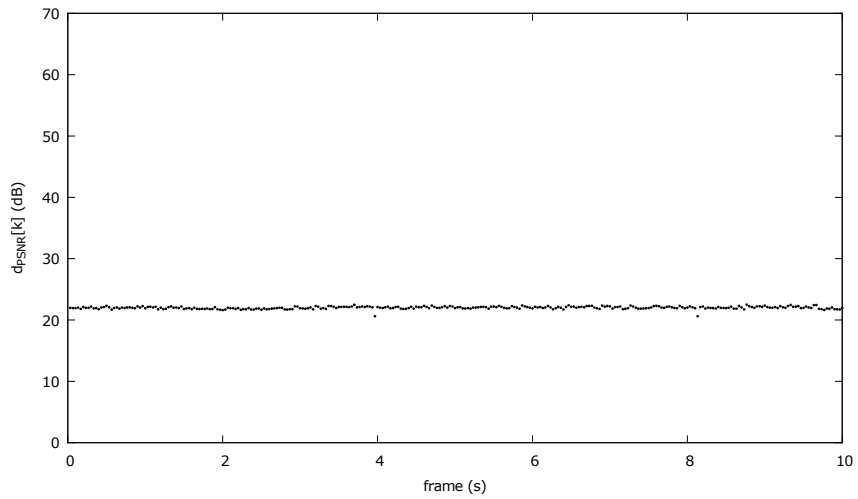


Figure C.5. Inter frame difference (bridge close)

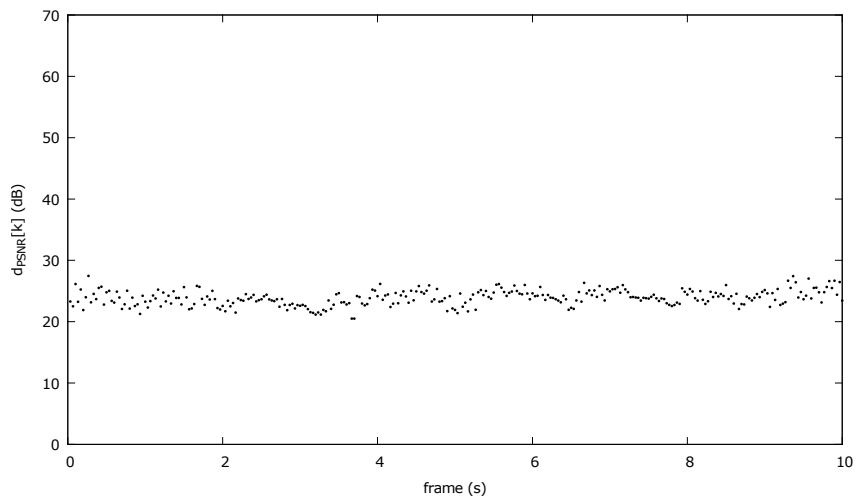


Figure C.6. Inter frame difference (highway)



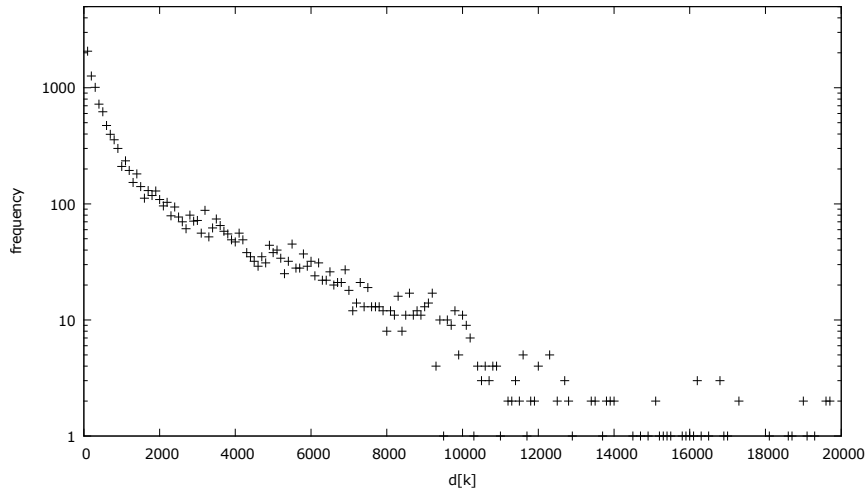


Figure C.7. Distribution of inter frame difference (startrek)

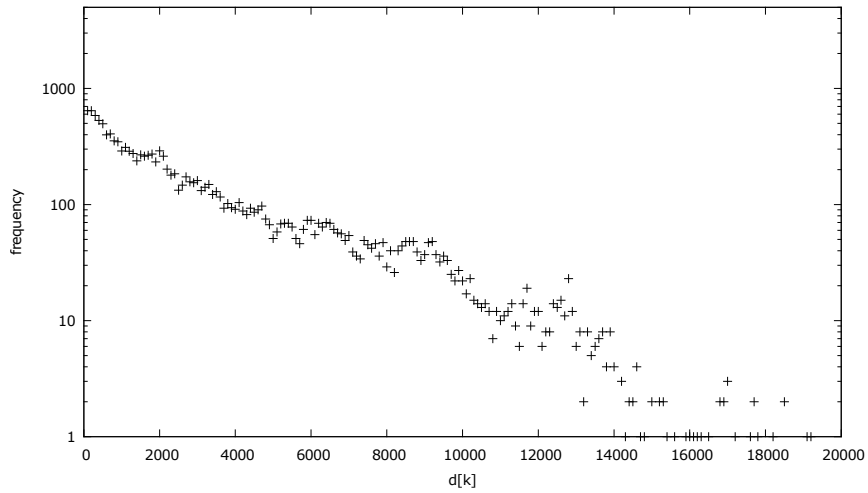


Figure C.8. Distribution of inter frame difference (thehobbit)

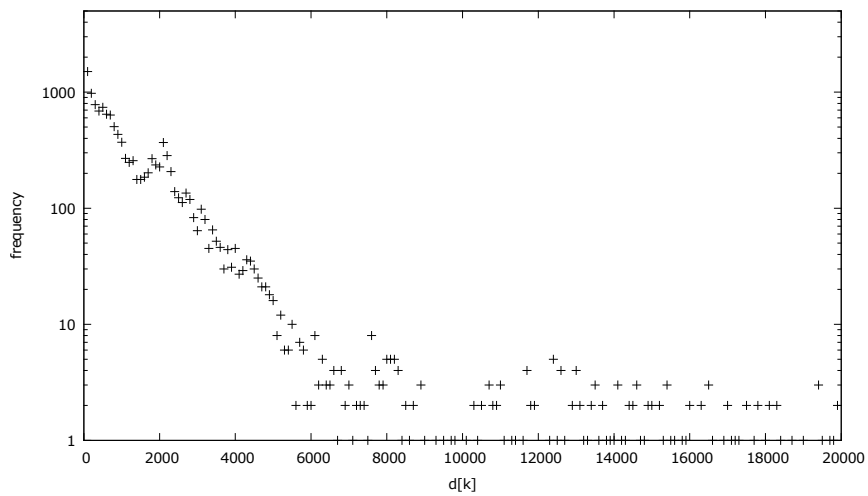


Figure C.9. Distribution of inter frame difference (bigbuckbunny)2



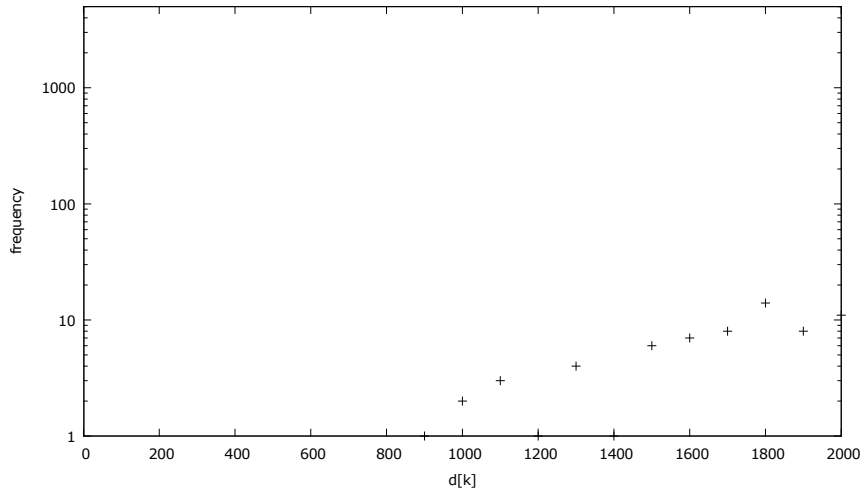


Figure C.10. Distribution of inter frame difference (foreman)

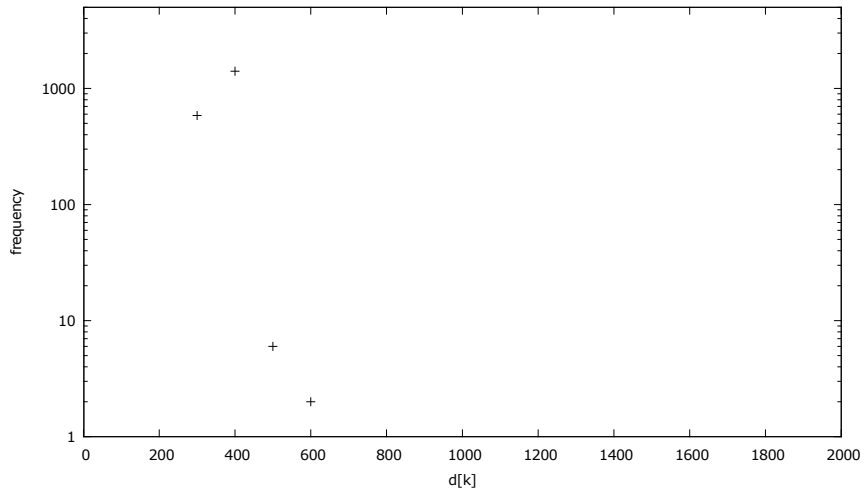


Figure C.11. Distribution of inter frame difference (bridge close)

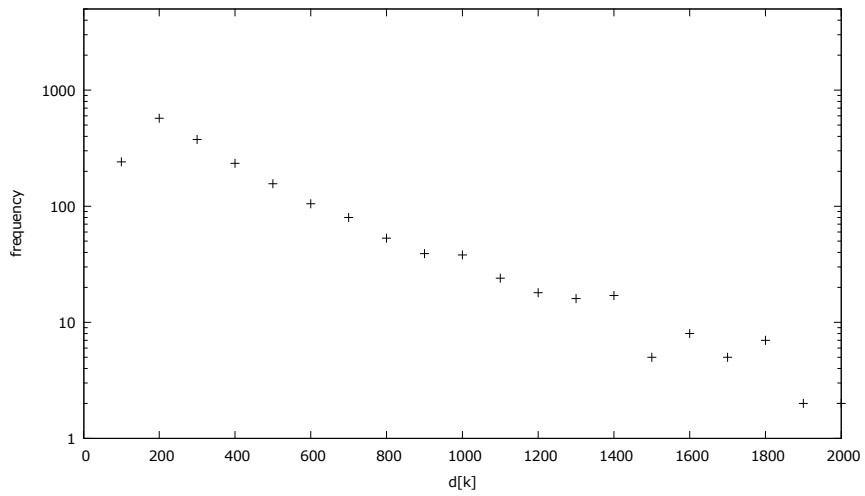


Figure C.12. Distribution of inter frame difference (highway)



mations.

I conclude based on the Q-Q plots, that the gamma and lognormal distributions diverge from the expected values in the long tail section; the standard error of the parameter estimations are high (> 0.01), therefore I exclude them. The weibull and the exponential distributions show similar behaviors, therefore, based on simplicity reasons, I choose the exponential distribution for hypothesis testing.

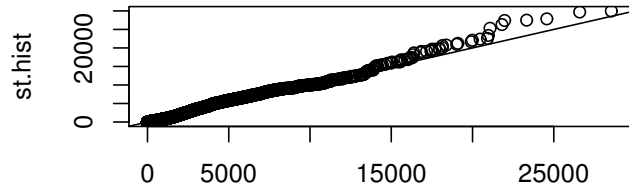
Table C.1. Parameter estimation (startrek)

| Weibull | | |
|-------------|---------------------------|------------------------|
| | shape | scale |
| value | 6.552983×10^{-1} | 9.791982×10^2 |
| std.err. | 4.113141×10^{-3} | 1.314538×10^1 |
| Gamma | | |
| | shape | rate |
| value | 4.827223 | 0.010000 |
| std.err. | 0.051950 | 0.000112 |
| Lognormal | | |
| | meanlog | sdlog |
| value | 6.072301 | 1.682210 |
| std.err. | 0.014019 | 0.009913 |
| Exponential | | |
| | rate | |
| value | 7.254687×10^{-4} | |
| std.err. | 6.045993×10^{-6} | |

Note: The parameters are estimated by the *fitdistr* command in R.

Table C.4 provides a simple method of converting quality values between MSE and PSNR units for a yuv420p video source.





`weibull(length(st.hist), st.weibull$estimate[1], st.weibull$estim:`

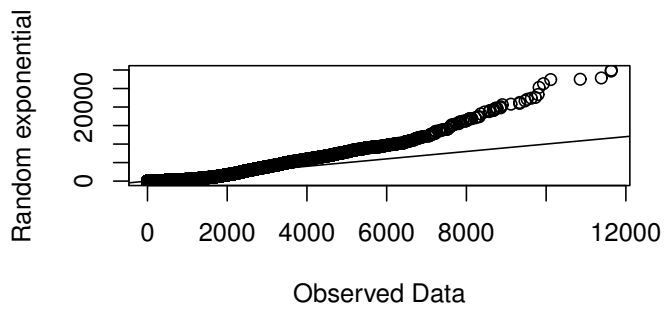
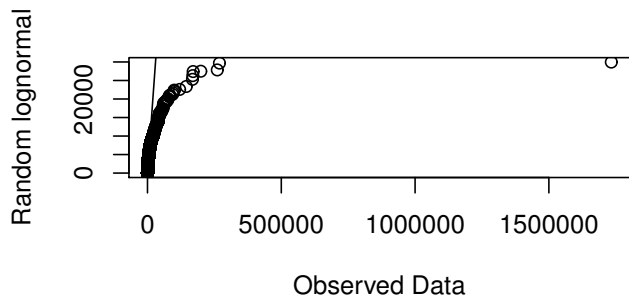
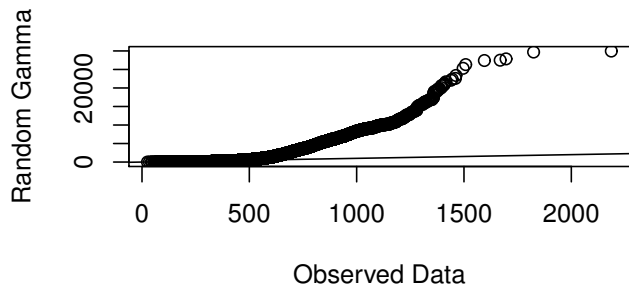


Figure C.13. Q-Q plot (startrek)



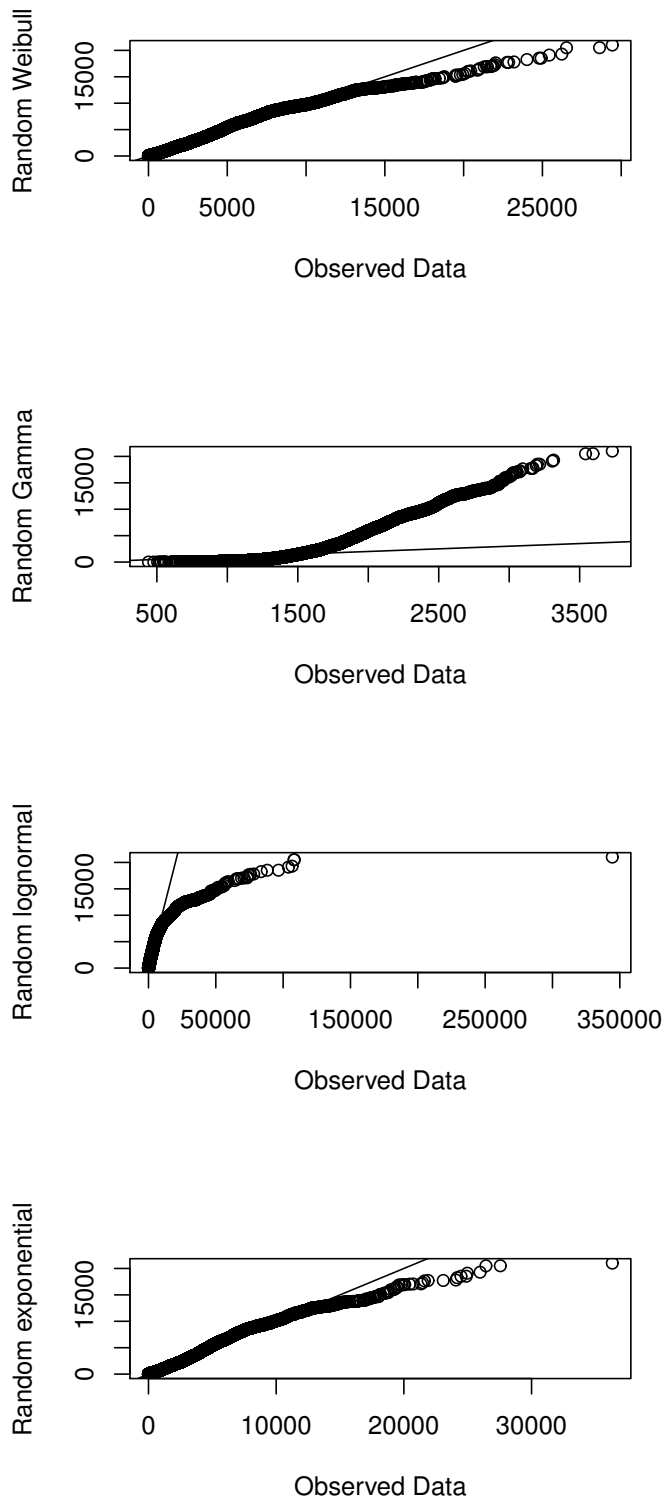


Figure C.14. Q-Q plot (thehobbit)



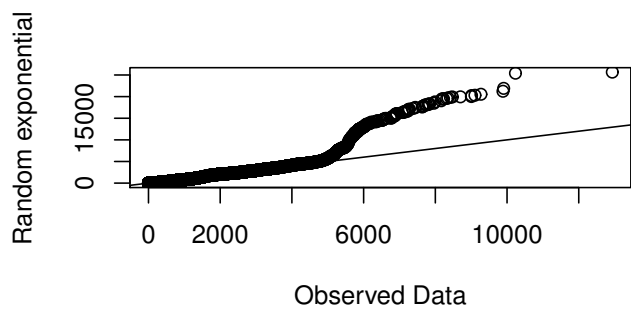
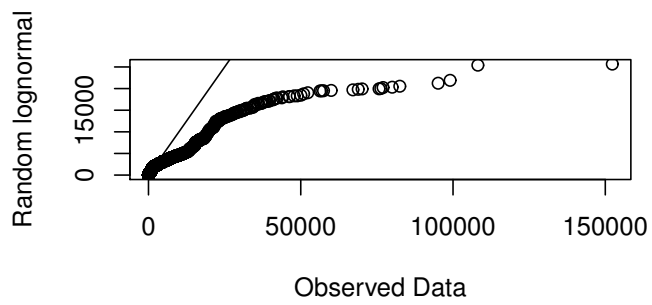
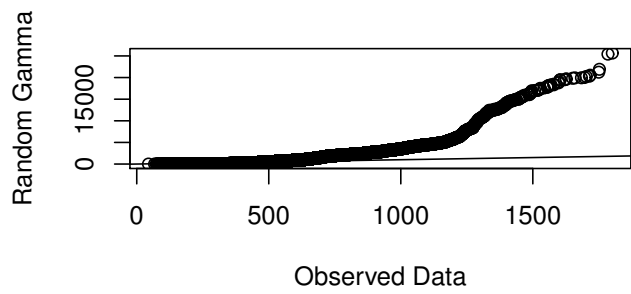
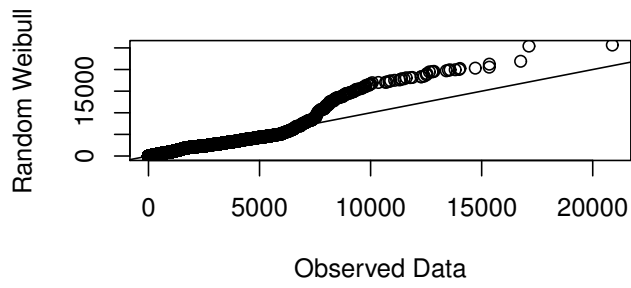


Figure C.15. Q-Q plot (bigbuckbunny)



Table C.2. Parameter estimation (thehobbit)

| Weibull | | |
|-------------|---------------------------|---------------------------|
| | shape | scale |
| value | 9.465360×10^{-1} | 2.888166×10^3 |
| std.err. | 6.183464×10^{-3} | 2.695950×10^1 |
| Gamma | | |
| | shape | rate |
| value | 1.611973×10^1 | 1.000000×10^{-2} |
| std.err. | 1.573570×10^{-1} | 9.814749×10^{-5} |
| Lognormal | | |
| | meanlog | sdlog |
| value | 7.353875 | 1.289172 |
| std.err. | 0.010743 | 0.007596 |
| Exponential | | |
| | rate | |
| value | 3.404700×10^{-4} | |
| std.err. | 2.837349×10^{-6} | |

Note: The parameters are estimated by the *fitdistr* command in R.



Table C.3. Parameter estimation (bigbuckbunny)

| Weibull | | |
|-------------|---------------------------|------------------------|
| | shape | scale |
| value | 7.993215×10^{-1} | 1.065492×10^3 |
| std.err. | 5.064793×10^{-3} | 1.180042×10^1 |
| Gamma | | |
| | shape | rate |
| value | 5.797443 | 0.010000 |
| std.err. | 0.062338 | 0.000111 |
| Lognormal | | |
| | meanlog | sdlog |
| value | 6.273870 | 1.498690 |
| std.err. | 0.012556 | 0.008879 |
| Exponential | | |
| | rate | |
| value | 8.222640×10^{-4} | |
| std.err. | 6.889378×10^{-6} | |

Note: The parameters are estimated by the *fitdistr* command in R.

Table C.4. MSE-PSNR conversion table

| MSE | PSNR (dB) |
|--------|-----------|
| 1 | 48 |
| 2 | 45 |
| 5 | 41 |
| 10 | 38 |
| 20 | 35 |
| 50 | 31 |
| 100 | 28 |
| 200 | 25 |
| 500 | 21 |
| 1,000 | 18 |
| 2,000 | 15 |
| 5,000 | 11 |
| 10,000 | 8 |
| 20,000 | 5 |
| 50,000 | 1 |

Note: Values apply only for the luma color space.



Appendix D

Formulas of the Charging Policy Functions

This appendix describes the detailed derivation of the formulas for determining the transformed policy functions (3.19), the probability density functions (3.23, 3.26 and 3.28) and the expected values (3.25 and 3.29) of the price discount introduced in 3.3.5.1.

The Linear Policy Function

$$P_{PSNR,linear}(D_{PSNR}[\kappa]) = \begin{cases} \text{undefined} & \text{if } D_{PSNR}[\kappa] < Q_m, \\ \frac{(1-r)D_{PSNR}[\kappa]}{Q_p-Q_m} + 1 - \frac{Q_p(1-r)}{Q_p-Q_m} & \text{if } Q_m \leq D_{PSNR}[\kappa] \leq Q_p, \\ 1 & \text{if } D_{PSNR}[\kappa] > Q_p. \end{cases} \quad (\text{D.1})$$

Let reduce $P_{PSNR,linear}(D_{PSNR}[\kappa])$ in a more shorter form in $Q_m \leq D_{PSNR}[\kappa] \leq Q_p$:

$$\begin{aligned} P_{PSNR}(x) &= p = ax + b, \text{ where} & (\text{D.2}) \\ a &= \frac{1-r}{Q_p-Q_m}, \\ b &= 1 - \frac{Q_p(1-r)}{Q_p-Q_m}, \\ x &= D_{PSNR}[\kappa]. \end{aligned}$$

$P_{PSNR}()$ is given in PSNR unit, but it's formula in MSE unit ($P()$) will be required by the further detailed distribution calculation, therefore the policy function is converted from PSNR to MSE ($x \rightarrow y$, $D_{PSNR}[\kappa] \rightarrow D[\kappa]$) using the following steps:

$$\begin{aligned}
P(y) = p = j^{-1}(y), \text{ where} & \tag{D.3} \\
j(p) = y = k(P_{PSNR}^{-1}(p)), \text{ and} & \\
k(x) = \frac{MAX^2}{10^{\frac{1}{10}x}}, &
\end{aligned}$$

and $MAX = 255$ is the maximal value of the luminance for I420p video source. The inverse function of $P_{PSNR}(x)$ is

$$P_{PSNR}^{-1}(p) = x = \frac{p - b}{a}. \tag{D.4}$$

$P_{PSNR}(x)$ is strictly monotone, substituting the equations above yields to

$$j(p) = y = \frac{MAX^2}{10^{\frac{1}{10} \frac{p-b}{a}}}, \tag{D.5}$$

$$10^{\frac{1}{10} \frac{p-b}{a}} \cdot y = MAX^2, \log(): \tag{D.6}$$

$$\frac{1}{10} \frac{p-b}{a} + \log(y) = 2 \cdot \log(MAX), \tag{D.7}$$

$$\frac{p-b}{10a} = 2 \cdot \log(MAX) - \log(y), \tag{D.8}$$

$$p - b = 20a \cdot \log(MAX) - 10a \cdot \log(y), \tag{D.9}$$

$$p = 20a \cdot \log(MAX) - 10a \cdot \log(y) + b. \tag{D.10}$$

$$p = s \cdot \log(y) + t, \text{ where} \tag{D.11}$$

$$s = -10a,$$

$$t = 20a \cdot \log(MAX) + b.$$

Therefore the policy function using MSE values is

$$P_{linear}(D[\kappa]) = \begin{cases} 1 & \text{if } D[\kappa] < k(Q_p), \\ s \cdot \log(D[\kappa]) + t & \text{if } k(Q_p) \leq D[\kappa] \leq k(Q_m), \\ \text{undefined} & \text{if } D[\kappa] > k(Q_m). \end{cases} \tag{D.12}$$

In the second step, let determine the distribution of the price discount. The probability density function of the total distortion in MSE unit is

$$f_{D[\kappa]}(D[\kappa], \lambda) = \lambda e^{-\lambda \cdot D[\kappa]}. \tag{D.13}$$

The transformation function between the total distortion and the price discount is defined by (D.12). Using the following short notations:

$$y = D[\kappa]: \text{ total distortion,} \quad (\text{D.14})$$

$$f(y) = \lambda e^{-\lambda y}: \text{ source probability density function,} \quad (\text{D.15})$$

$$p: \text{ price,} \quad (\text{D.16})$$

$$g(p): \text{ transformed probability density function,} \quad (\text{D.17})$$

$$p(y) = s \cdot \log(y) + t: \text{ transformation function.} \quad (\text{D.18})$$

To obtain the probability density function of the price discount I use the distribution transformation rule, because $p(x)$ is strictly monotone decreasing in the Q_m and Q_p region:

$$g(p) = f(y(p)) \left| \frac{dy}{dp} \right|, \quad (\text{D.19})$$

which requires the existence of the inverse function of the $y(p)$ source probability density function and the derivate of $y(p)$. The inverse function is already defined by $g(p)$:

$$y(p) = g(p) = y = \frac{MAX^2}{10^{\frac{1}{10} \frac{p-b}{a}}}. \quad (\text{D.20})$$

The derivate can be obtained by inspection:

$$\frac{dy}{dp} = MAX^2 \cdot 10^{\frac{b}{10a}} \cdot \frac{d}{dp} 10^{\frac{-1}{10a}p} \quad (\text{D.21})$$

$$= MAX^2 \cdot 10^{\frac{b}{10a}} \cdot 10^{-\frac{1}{10a}p} \cdot \ln(10) \cdot \frac{-1}{10a} \quad (\text{D.22})$$

$$= \frac{MAX^2}{10^{\frac{1}{10} \frac{p-b}{a}}} \cdot \ln(10) \cdot \frac{-1}{10a}, \quad (\text{D.23})$$

therefore the transformed probability density function is

$$\boxed{g(p) = \lambda e^{-\lambda \left(\frac{MAX^2}{10^{\frac{1}{10} \frac{p-b}{a}}} \right)} \cdot \frac{MAX^2}{10^{\frac{1}{10} \frac{p-b}{a}}} \cdot \ln(10) \cdot \frac{1}{10a}}. \quad (\text{D.24})$$

To determine the expected value of the price discount, the law of the unconscious statistician is implied, where the base distribution is given by (D.13) and the transformation function is by (D.12).

$$\begin{aligned}
E(\text{price}) &= E(P(y)) = \int_{-\infty}^{\infty} p(y)f(y) \, dy, \text{ where} & (D.25) \\
f(y) &= \lambda e^{-\lambda y}, \\
p(y) &= s \cdot \log(y) + t.
\end{aligned}$$

$f(y)$ only defined for $y > 0$ and $p(y)$ equals to 0 by definition if $y > k(Q_m)$ and equals to 1 if $y < k(Q_p)$, therefore the integral can be reformulated in the following form:

$$E(\text{price}) = \int_0^{k(Q_p)} f(y) \, dy + \int_{k(Q_p)}^{k(Q_m)} p(y)f(y) \, dy \quad (D.26)$$

Substituting the integral yields to

$$\begin{aligned}
E(\text{price}) &= \int_0^{k(Q_p)} \lambda e^{-\lambda y} \, dy + \int_{k(Q_p)}^{k(Q_m)} (s \cdot \log(y) + t) \cdot \lambda e^{-\lambda y} \, dy \\
&= \lambda \int_0^{k(Q_p)} e^{-\lambda y} \, dy + s\lambda \int_{k(Q_p)}^{k(Q_m)} \log(y) \cdot e^{-\lambda y} \, dy + t\lambda \int_{k(Q_p)}^{k(Q_m)} e^{-\lambda y} \, dy, & (D.27)
\end{aligned}$$

which yields

$$\boxed{E(\text{price}) = \left[\frac{e^{-\lambda D[\kappa]}}{-\lambda} \right]_0^{k(Q_p)} + c\lambda \left[\frac{e^{-\lambda D[\kappa]} \ln(D[\kappa])}{-\lambda \ln(10)} \right]_{k(Q_p)}^{k(Q_m)} + d\lambda \left[\frac{e^{-\lambda D[\kappa]}}{-\lambda} \right]_{k(Q_p)}^{k(Q_m)}}. \quad (D.28)$$

The Cosine Policy Function

$$P_{PSNR,cos}(D_{PSNR}[\kappa]) = \begin{cases} \text{undefined} & \text{if } D_{PSNR}[\kappa] < Q_m, \\ \frac{r-1}{2} \cos\left(\frac{D_{PSNR}[\kappa]-Q_m}{Q_p-Q_m} \pi\right) + \frac{1+r}{2} & \text{if } Q_m \leq D_{PSNR}[\kappa] \leq Q_p, \\ 1 & \text{if } D_{PSNR}[\kappa] > Q_p. \end{cases} \quad (D.29)$$

Let reduce $P_{PSNR,cos}(D_{PSNR}[\kappa])$ in a more shorter form in $Q_m \leq D_{PSNR}[\kappa] \leq Q_p$:

$$P_{PSNR}(x) = p = a \cdot \cos(bx + c) + d, \text{ where} \quad (\text{D.30})$$

$$\begin{aligned} a &= \frac{r-1}{2}, \\ b &= \frac{\pi}{Q_p - Q_m}, \\ c &= -\frac{\pi Q_m}{Q_p - Q_m}, \\ d &= r + \frac{1-r}{2}, \\ x &= D_{PSNR}[\kappa]. \end{aligned}$$

$P_{PSNR}()$ is given in PSNR unit but it's $P()$ formula in MSE unit will be required by the further detailed distribution calculation, therefore the policy function is converted from PSNR to MSE ($x \rightarrow y, D_{PSNR}[\kappa] \rightarrow D[\kappa]$) using the following steps:

$$P(y) = p = j^{-1}(y), \text{ where} \quad (\text{D.31})$$

$$\begin{aligned} j(p) &= y = k(P_{PSNR}^{-1}(p)), \\ k(x) &= \frac{MAX^2}{10^{\frac{1}{10}x}}, \end{aligned}$$

and $MAX = 255$ is the maximal value of the luminance for I420p video source. The inverse function of $P_{PSNR}(x)$ is

$$P_{PSNR}^{-1}(p) = x = \frac{1}{b} \arccos\left(\frac{p-d}{a}\right) - \frac{c}{b}. \quad (\text{D.32})$$

$P_{PSNR}(x)$ is strictly monotone, substituting the equations above yields to

$$j(p) = y = \frac{MAX^2}{10^{\frac{1}{10}x}}, \quad (D.33)$$

$$10^{\frac{1}{10}x} \cdot y = MAX^2, \log(): \quad (D.34)$$

$$\frac{1}{10}x + \log(y) = 2 \cdot \log(MAX), \quad (D.35)$$

$$\frac{1}{10b} \arccos\left(\frac{p-d}{a}\right) - \frac{c}{10b} + \log(y) = 2 \cdot \log(MAX), \quad (D.36)$$

$$\arccos\left(\frac{p-d}{a}\right) = 20b \cdot \log(MAX) - 10b \cdot \log(y) + c, \quad (D.37)$$

$$\frac{p-d}{a} = \cos(20b \cdot \log(MAX) - 10b \cdot \log(y) + c), \quad (D.38)$$

$$p = a \cdot \cos(20b \cdot \log(MAX) - 10b \cdot \log(y) + c) - d. \quad (D.39)$$

$$p = s \cdot \cos(t \cdot \log(y) + u) + v, \text{ where} \quad (D.40)$$

$$s = a,$$

$$t = -10b,$$

$$u = 20b \cdot \log(MAX) + c,$$

$$v = -d.$$

Therefore the policy function using MSE values is

$$P_{linear}(D[\kappa]) = \begin{cases} 1 & \text{if } D[\kappa] < k(Q_p), \\ s \cdot \cos(t \cdot \log(D[\kappa]) + u) + v & \text{if } k(Q_p) \leq D[\kappa] \leq k(Q_m), \\ \text{undefined} & \text{if } D[\kappa] > k(Q_m). \end{cases} \quad (D.41)$$

In the second step, let determine the distribution of the price discount. The probability density function of the total distortion (in MSE unit):

$$f_{D[\kappa]}(D[\kappa], \lambda) = \lambda e^{-\lambda \cdot D[\kappa]}. \quad (D.42)$$

The transformation function between the total distortion and the price discount is defined by (D.41). Using the following short notations:

$$y = D[\kappa]: \text{ total distortion,} \quad (\text{D.43})$$

$$f(y) = \lambda e^{-\lambda y}: \text{ source probability density function,} \quad (\text{D.44})$$

$$p: \text{ price,} \quad (\text{D.45})$$

$$g(p): \text{ transformed probability density function,} \quad (\text{D.46})$$

$$p(y) = s \cdot \cos(t \cdot \log(y) + u) + v: \text{ transformation function.} \quad (\text{D.47})$$

To obtain the probability density function of the price discount, I use the distribution transformation rule, because $p(x)$ is strictly monotone decreasing in the Q_m and Q_p region.

$$g(p) = f(y(p)) \left| \frac{dy}{dp} \right|, \quad (\text{D.48})$$

which requires the existence of the inverse function of the $y(p)$ source probability density function and the derivate of $y(p)$. The inverse function is already defined by $g(p)$.

$$y(p) = g(p) = y = \frac{MAX^2}{10^{\frac{1}{10}(\frac{1}{b} \arccos(\frac{p-d}{a}) - \frac{c}{b})}} \quad (\text{D.49})$$

The derivate can be obtained by using the chain rule and inspection:

$$y(p) = y = MAX^2 \cdot 10^{\frac{c}{10b}} \cdot 10^{-\frac{1}{10b} \arccos(\frac{p-d}{a})}, \quad (\text{D.50})$$

$$y = f(\alpha) = MAX^2 \cdot 10^{\frac{c}{10b}} \cdot 10^{-\frac{1}{10b} \alpha}, \quad (\text{D.51})$$

$$\alpha = g(\beta) = \arccos(\beta), \quad (\text{D.52})$$

$$\beta = h(p) = \frac{p-d}{a}, \quad (\text{D.53})$$

$$\frac{dy}{dp} = \frac{dy}{d\alpha} \cdot \frac{d\alpha}{d\beta} \cdot \frac{d\beta}{dp}, \quad (\text{D.54})$$

$$\begin{aligned} \frac{dy}{dp} &= MAX^2 \cdot 10^{\frac{c}{10b}} \cdot 10^{(-\frac{1}{10b} \arccos(\frac{p-d}{a}))} \\ &\cdot \ln(10) \cdot \left(-\frac{1}{10b}\right) \cdot \left(-\frac{1}{\sqrt{1 - (\frac{p-d}{a})^2}}\right) \cdot \left(\frac{1}{a}\right). \end{aligned} \quad (\text{D.55})$$

Therefore the transformed probability density function is

$$g(p) = \ln(10) \frac{\frac{MAX^2}{10^{\frac{1}{10}(\frac{1}{b} \arccos(\frac{p-d}{a}) - \frac{\xi}{b})}}}{-10ab\sqrt{1 - (\frac{p-d}{a})^2}}. \quad (D.56)$$

To determine the expected value of the price discount, the law of the unconscious statistician is implied, where the base distribution is given by (D.42) and the transformation function is by (D.41):

$$E(\text{price}) = E(P(y)) = \int_{-\infty}^{\infty} p(y)f(y) dy, \text{ where} \quad (D.57)$$

$$f(y) = \lambda e^{-\lambda y},$$

$$p(y) = s \cdot \cos(t \cdot \log(y) + u) + v.$$

$f(y)$ only defined for $y > 0$ and $p(y)$ equals to 0 by definition if $y > k(Q_m)$ and equals to 1 if $y < k(Q_p)$ therefore the integral can be reformulated in the following form:

$$E(\text{price}) = \int_0^{k(Q_p)} f(y) dy + \int_{k(Q_p)}^{k(Q_m)} p(y)f(y) dy. \quad (D.58)$$

Due to the complexity of the formulas, the closed form of this expression is not enclosed here.

The Elliptic Policy Function

$$P_{PSNR,elliptic}(D_{PSNR}[\kappa]) = \begin{cases} \text{undefined} & \text{if } x < Q_m, \\ \sqrt{1 - \left(\frac{D_{PSNR}[\kappa] - Q_p}{Q_p - Q_m}\right)^2} & \text{if } Q_m \leq x \leq Q_p, \\ 1 & \text{if } x > Q_p. \end{cases} \quad (D.59)$$

Let reduce $P_{PSNR,elliptic}(D_{PSNR}[\kappa])$ in a more shorter form in $Q_m \leq D_{PSNR}[\kappa] \leq Q_p$:

$$P_{PSNR}(x) = p = \sqrt{1 - (ax + b)^2}, \text{ where} \quad (D.60)$$

$$a = \frac{1}{Q_p - Q_m},$$

$$b = -\frac{Q_p}{Q_p - Q_m},$$

$$x = D_{PSNR}[\kappa].$$

$P_{PSNR}()$ is given in PSNR unit but it's $P()$ formula in MSE unit will be required by the further detailed distribution calculation therefore the policy function is converted from PSNR to MSE: ($x \rightarrow y, D_{PSNR}[\kappa] \rightarrow D[\kappa]$) using the following steps:

$$\begin{aligned} P(y) &= p = j^{-1}(y), \text{ where} & (D.61) \\ j(p) &= y = k(P_{PSNR}^{-1}(p)), \\ k(x) &= \frac{MAX^2}{10^{\frac{1}{10}x}}, \end{aligned}$$

and $MAX = 255$ is the maximal value of the luminance for I420p video source. The inverse function of $P_{PSNR}(x)$ is

$$P_{PSNR}^{-1}(p) = x = \frac{\sqrt{1-p^2-b}}{a}.$$

$P_{PSNR}(x)$ is strictly monotone, substituting the equations above yields

$$j(p) = y = \frac{MAX^2}{10^{\frac{1}{10} \frac{\sqrt{1-p^2-b}}{a}}}, \quad (D.62)$$

$$10^{\frac{1}{10} \frac{\sqrt{1-p^2-b}}{a}} \cdot y = MAX^2, \log(): \quad (D.63)$$

$$\frac{1}{10} \frac{\sqrt{1-p^2-b}}{a} + \log(y) = 2 \cdot \log(MAX), \quad (D.64)$$

$$\frac{\sqrt{1-p^2-b}}{10a} = 2 \cdot \log(MAX) - \log(y), \quad (D.65)$$

$$\sqrt{1-p^2-b} = 20a \cdot \log(MAX) - 10a \cdot \log(y), \quad (D.66)$$

$$\sqrt{1-p^2} = 20a \cdot \log(MAX) - 10a \cdot \log(y) + b, \text{ to the power of 2:} \quad (D.67)$$

$$1-p^2 = (20a \cdot \log(MAX) - 10a \cdot \log(y) + b)^2, \quad (D.68)$$

$$p^2 = 1 - (20a \cdot \log(MAX) - 10a \cdot \log(y) + b)^2, \text{ square root of:} \quad (D.69)$$

$$p = \sqrt{1 - (20a \cdot \log(MAX) - 10a \cdot \log(y) + b)^2}. \quad (D.70)$$

$$p = \sqrt{1 - (s + t \cdot \log(y))^2}, \text{ where} \quad (D.71)$$

$$s = 20a \cdot \log(MAX) + b,$$

$$t = -10a.$$

Therefore the policy function using MSE values is



$$P_{linear}(D[\kappa]) = \begin{cases} 1 & \text{if } D[\kappa] < k(Q_p), \\ \sqrt{1 - (s + t \cdot \log(D[\kappa]))^2} & \text{if } k(Q_p) \leq D[\kappa] \leq k(Q_m), \\ \text{undefined} & \text{if } D[\kappa] > k(Q_m). \end{cases} \quad (\text{D.72})$$

In the second step let determine the distribution of the price discount. The probability density function of the total distortion (in MSE unit):

$$f_{D[\kappa]}(D[\kappa], \lambda) = \lambda e^{-\lambda \cdot D[\kappa]}. \quad (\text{D.73})$$

The transformation function between the total distortion and the price discount is defined by (D.72). Use the following short notations:

$$y = D[\kappa]: \text{ total distortion,} \quad (\text{D.74})$$

$$f(y) = \lambda e^{-\lambda y}: \text{ source probability density function,} \quad (\text{D.75})$$

$$p: \text{ price,} \quad (\text{D.76})$$

$$g(p): \text{ transformed probability density function,} \quad (\text{D.77})$$

$$p(y) = \sqrt{1 - (s + t \cdot \log(y))^2}: \text{ transformation function.} \quad (\text{D.78})$$

To obtain the probability density function of the price discount I use the distribution transformation rule because $p(x)$ is strictly monotone decreasing in the Q_m and Q_p region:

$$g(p) = f(y(p)) \left| \frac{dy}{dp} \right|, \quad (\text{D.79})$$

which requires the existence of the inverse function of the $y(p)$ source probability density function and the derivate of $y(p)$. The inverse function is already defined by $g(p)$.

$$y(p) = g(p) = y = \frac{MAX^2}{10^{\frac{1}{10} \frac{\sqrt{1-p^2}-b}{a}}} \quad (\text{D.80})$$

The derivate can be obtained by inspection:



$$y(p) = y = MAX^2 \cdot 10^{\frac{b}{10a}} \cdot 10^{\frac{-1}{10a}} \sqrt{1-p^2}, \quad (D.81)$$

$$y = f(\alpha) = MAX^2 \cdot 10^{\frac{b}{10a}} \cdot 10^{\frac{-1}{10a}} \alpha, \quad (D.82)$$

$$\alpha = g(\beta) = \sqrt{\beta}, \quad (D.83)$$

$$\beta = h(p) = 1 - p^2, \quad (D.84)$$

$$\frac{dy}{dp} = \frac{dy}{d\alpha} \cdot \frac{d\alpha}{d\beta} \cdot \frac{d\beta}{dp}, \quad (D.85)$$

$$\frac{dy}{dp} = MAX^2 \cdot 10^{\frac{b}{10a}} \cdot 10^{\frac{-1}{10a}} \sqrt{1-p^2} \cdot \ln(10) \cdot \left(-\frac{1}{10a}\right) \cdot \frac{1}{\sqrt{2-2p^2}} \cdot (-2p). \quad (D.86)$$

Therefore the transformed probability density function is:

$$g(p) = \lambda e^{-\lambda \cdot \left(\frac{MAX^2}{10^{\frac{1}{10}} \frac{\sqrt{1-p^2-b}}{a}} \right)} \cdot \frac{MAX^2}{10^{\frac{1}{10}} \frac{\sqrt{1-p^2-b}}{a}} \cdot \ln(10) \cdot \left(-\frac{1}{10a}\right) \cdot \frac{1}{\sqrt{2-2p^2}} \cdot (-2p). \quad (D.87)$$

To determine the expected value of the price discount, the law of the unconscious statistician is implied, where the base distribution is given by (D.73) and the transformation function is by (D.72):

$$E(\text{price}) = E(P(y)) = \int_{-\infty}^{\infty} p(y) f(y) dy, \text{ where} \quad (D.88)$$

$$f(y) = \lambda e^{-\lambda y},$$

$$p(y) = \sqrt{1 - (s + t \cdot \log(y))^2}. \quad (D.89)$$

$f(y)$ only defined for $y > 0$ and $p(y)$ equals to 0 by definition if $y > k(Q_m)$ and equals to 1 if $y < k(Q_p)$, therefore the integral can be reformulated in the following form:

$$E(\text{price}) = \int_0^{k(Q_p)} f(y) dy + \int_{k(Q_p)}^{k(Q_m)} p(y) f(y) dy \quad (D.90)$$

Substituting the integral:

$$E(\text{price}) = \int_0^{k(Q_p)} \lambda e^{-\lambda y} dy + \int_{k(Q_p)}^{k(Q_m)} \sqrt{1 - (s + t \cdot \log(y))^2} \cdot \lambda e^{-\lambda y} dy. \quad (D.91)$$

Due to the complexity of the formulas, the closed form of this expression is not enclosed here.



Glossary

access network. The network infrastructure used to deliver IPTV services to the Consumer. The Access Network infrastructure (which may include the Internet) is used for the delivery of the content and may include quality of service management to ensure that appropriate network resources are available for the delivery of the content.

analogue switch-off (aSo). The date, when the analogue terrestrial television is switched off.

back-in-time. Scheduled program events that are already running or finished are made available to the user for viewing and/or recording from the start or a certain time into the past. They are available similar to VoD including optional trick mode support (e.g. pause, fast-forward, rewind). In case the scheduled program event is still running the play out cannot go beyond the actual program play out. Selection is possible from the scheduled content program guide. The service might be available for one or more channels (e.g. for the selected channel in case of local storage, a fixed or selected channel list in case of network storage)

BDRip. Bluray disk rip is a multimedia file that contains content that was sourced from a Blu-ray Disc product. As the "rip" part of the name applies, the copy is generally not a 1:1 copy, but instead is usually re-encoded.

consumer domain. The domain where the IPTV services are consumed. A consumer domain can consist of a single terminal or a network of terminals and related devices for service consumption. The device may also be a mobile end device; in this case, the delivery system of a network provider is a wireless network. This domain is within the scope for the Open IPTV Forum specifications.

content on demand (CoD). A Content on Demand service is a service where a user can select the individual content items he or she wants to watch out of the list of available content. Consumption of the content is started on user request.

content provider. Entity that provides Content and associated usage rights to the IPTV Service Provider.

digital switchover. The digital switchover is the process of launching the digital terrestrial television platform and switching off analogue terrestrial television services.

IPTV service provider. Entity that offers IPTV Services and which has a contractual relationship with the Subscriber.

IPTV solution. The specifications published by the Open IPTV Forum.

IPTV terminal function (ITF). The functionality within the Consumer Network that is responsible for terminating the media and control for an IPTV Service.

network provider. provides transport resources for delivery of authorized content to the consumer domain. It also provides the communications between the consumer domain and the Service Platform Provider. The User to Network Interface (UNI) links the Network Provider to the consumer domain.

personal video recorder. PVR is a service which enables a user to record scheduled content program events using local or network-based storage. The recorded items can be played back under the control of the user.

scheduled content service. An IPTV service where the playout schedule is fixed by an entity other than the User. The content is delivered to the user for immediate consumption.

service platform provider. Entity which, based on a contractual relationship with IPTV Service Providers, provides the supporting functions for the delivery of IPTV Services, such as charging, access control and other functions which are not part of the IPTV Service, but required for managing its delivery.

network provider domain. The domain connecting customers to platform and service providers. The delivery system is typically composed of access networks and core or backbone networks, using a variety of network technologies. The delivery network is transparent to the IPTV content, although there may be timing and packet loss issues relevant for IPTV content streamed on IP. This domain is within the scope of the Open IPTV Forum specifications.

YUV. YUV is a color space typically used as part of a color image pipeline. It encodes a color image or video taking human perception into account, allowing reduced bandwidth for chrominance components, thereby typically enabling transmission errors or compression artifacts.



Bibliography

- 3rd Generation Partnership Project. 2006. *Policy and charging control architecture*. Technical report TS 23.203 V1.1.0. 3GPP.
- . 2007. *Overall high level functionality and architecture impacts of flow based charging; Stage 2*. Technical report TS 23.125 V7.0.0. 3GPP.
- . 2010a. *Charging architecture and principles*. Technical report TS 32.240 V9.1.0. 3GPP.
- . 2010b. *IP Multimedia Subsystem (IMS); Stage 2*. Technical report TS 23.228. 3GPP.
- . 2013a. *Charging and billing*. Technical report TS 22.115 V12.1.0. 3GPP.
- . 2013b. *Charging architecture and principles*. Technical report TS 32.240 V12.1.0. 3GPP.
- Abramowski, Andrzej. 2011. “Towards H. 265 video coding standard.” In *Photonics Applications in Astronomy, Communications, Industry, and High-Energy Physics Experiments 2011*, 800819–800819. International Society for Optics and Photonics.
- Adda, Jerome, and Marco Ottaviani. 2005. “The transition to digital television.” *Economic Policy* 20 (41): 160–209.
- Amazon.com, Inc. 2012. *Amazon Instant Video App Now Available for iPad*. Press release.
- . 2013a. *And the Emmy Goes To... Amazon Instant Video!* Press release.
- . 2013b. *CBS’s Under the Dome Now Available for Exclusive Online Subscription Streaming on Prime Instant Video*. Press release.
- Apple. 2012a. *Apple Brings 1080p High Definition to New Apple TV*. Press release.
- . 2012b. *Apple Unveils New iTunes*. Press release.
- . 2013. *HBO GO and WatchESPN Come to Apple TV*. Press release.
- Ary, Bálint Dávid, and Sándor Imre. 2005a. “Real-time charging in mobile environment.” In *Hungarian Telekommunikation Magazine*, LX-6:54–59.
- . 2005b. “Reduction of Charging Overhead in Mobile Telecommunication Networks.” *Int. Trans. On Computer Science and Engineering* 20 (1): 126–136.
- . 2007. “Advice of Charge in Telecommunication Services.” In *16th IST Mobile and Wireless Communications Summit, 2007*. 1–5. IEEE.



- Ary, Bálint Dávid, and Sándor Imre. 2008. “Handbook of Research on Next Generation Networks and Ubiquitous Computing.” Chap. Charging and Rating in Mobile Telecommunication Networks in, 43–50. Samuel Pierre, Hershey: IGI Global, Information Science Reference.
- . 2010. “xDR Arrival Distribution.” In *33rd International Conference on Telecommunications and Signal Processing, TSP2010*, 417–420. Baden, Austria.
- . 2013. “Partial CDR database dimensioning.” *Telecommunication Systems* 52 (1): 73–83.
- Bartholomew, D. J. 1975. “Errors of Prediction for Markov Chain Models” [in English]. *Journal of the Royal Statistical Society. Series B (Methodological)* 37 (3): pages. ISSN: 00359246. <http://www.jstor.org/stable/2984790>.
- Bataa, Otgonbayar, Oyu Chuluun, Tulga Orosoo, Erdenebayar Lamjav, Young-il Kim, and Khishigjargal Gonchigsumlaa. 2012. “A functional design of BM-SC to support mobile IPTV in LTE network.” In *Strategic Technology (IFOST), 2012 7th International Forum on*, 1–5. doi:10.1109/IFOST.2012.6357671.
- Baugher, M., D. McGrew, M. Naslund, E. Carrara, and K. Norrman. 2004. *The Secure Real-time Transport Protocol (SRTP)*. Technical report. Internet Engineering Task Force, March.
- Becke, Martin, Thomas Dreibholz, Andreas Bayer, Markus Packeiser, and Erwin Paul Rathgeb. 2013. “Alternative transmission strategies for multipath transport of multimedia streams over wireless networks.” In *Telecommunications (ConTEL), 2013 12th International Conference on*, 147–154.
- Benoit, Herve. 2008. *Digital television: satellite, cable, terrestrial, IPTV, mobile TV in the DVB framework*. 3rd. Focal Press.
- Bhat, Abharana, Iain Richardson, and Sampath Kannangara. 2010. “A new perceptual quality metric for compressed video based on mean squared error.” *Image Commun.* (New York, NY, USA) 25, no. 8 (September): 588–596. ISSN: 0923-5965. doi:10.1016/j.image.2010.07.002. <http://dx.doi.org/10.1016/j.image.2010.07.002>.
- Billingsley, Patrick. 1961. “Statistical methods in Markov chains.” *The Annals of Mathematical Statistics*:12–40.
- Boulos, Fadi, Benoit Parrein, Patrick Le Callet, and David S Hands. 2009. “Perceptual effects of packet loss on H. 264/AVC encoded videos.” *Perceptual Effects of Packet Loss on H. 264/AVC Encoded Videos*.
- Broadband TV News. 2013. *Over 100m IPTV homes by 2017*, April. <http://www.broadbandtvnews.com/2013/04/25/over-100m-iptv-homes-by-2017/>.
- Brooks, Stephen P., and Gareth O. Roberts. 1998. “Convergence Assessment Techniques for Markov Chain Monte Carlo.” *Statistics and Computing* (Hingham, MA, USA) 8, no. 4 (December): 319–335. ISSN: 0960-3174. doi:10.1023/A:1008820505350. <http://dx.doi.org/10.1023/A:1008820505350>.
- Calafate, Carlos Miguel Tavares. 2003. “Evaluation of the H. 264 encoder (internal report).” *DISCA, UPV, Spain*.



- Calafate, Carlos T., P. Manzoni, Juan-Carlos Cano, and M. P. Malumbres. 2009. "Markovian-based traffic modeling for mobile ad hoc networks." *Comput. Netw.* (New York, NY, USA) 53, no. 14 (September): 2586–2600. ISSN: 1389-1286. doi:10.1016/j.comnet.2009.05.007. <http://dx.doi.org/10.1016/j.comnet.2009.05.007>.
- Canadian Radio-television and Telecommunications Commission. 2012. *Communications Monitoring Report 2012*. CRTC.
- Choudhary, Salahuddin. 2010. *Announcing Google TV: TV meets web. Web meets TV*. Google Official Blog.
- Commerce Commission. 2011. *Annual Telecommunications Monitoring Report 2010*. Technical report. Commerce Commission.
- Cowles, Mary Kathryn, and Bradley P Carlin. 1996. "Markov chain Monte Carlo convergence diagnostics: a comparative review." *Journal of the American Statistical Association* 91 (434): 883–904.
- DigiTAG. 2013. *Guide to Digital switchover*. Technical report. Switzerland: The Digital Terrestrial Television Action Group.
- Eckert, Michael P, and Andrew P Bradley. 1998. "Perceptual quality metrics applied to still image compression." *Signal processing* 70 (3): 177–200.
- Einsiedler, Hans, Rui L. Aguiar, Jürgen Jähnert, Karl Jonas, Marco Liebsch, Ralf Schmitz, Piotr Pacyna, et al. 2001. "The Moby Dick Project: A Mobile Heterogeneous ALL-IP Architecture." In *ATAMS 2001. Krakow*, 17–20. FEEACSE Press.
- El Barachi, May, Roch H Glitho, and Rachida Dssouli. 2005. "Developing applications for internet telephony: a case study on the use of web services for conferencing in SIP networks." *International Journal of Web Information Systems* 1 (3): 147–160.
- Ericsson. 2013. *Ericsson closes acquisition of Microsoft Mediaroom*. Press release.
- Fraunhofer Heinrich Hertz Institute. 2013. *SVC: Scalable Extension of H.264/AVC*. <http://www.hhi.fraunhofer.de/en/fields-of-competence/image-processing/research-groups/image-video-coding/scalable-video-coding/svc-scalable-extension-of-h264avc.html>.
- Gilbert, Edgar N. 1960. "Capacity of a burst-noise channel." *Bell Syst. Tech. J* 39 (9): 1253–1265.
- Girod, Bernd. 1993. "What's wrong with mean-squared error?" In *Digital images and human vision*, edited by Andrew B. Watson, 207–220. Cambridge, MA, USA: MIT Press. ISBN: 0-262-23171-9. <http://dl.acm.org/citation.cfm?id=197765.197784>.
- Guardian US. 2012. *The Guardian launches its first app for Google TV in the US*. Press release.
- Hore, Alain, and Djemel Ziou. 2010. "Image Quality Metrics: PSNR vs. SSIM." In *Proceedings of the 2010 20th International Conference on Pattern Recognition*, 2366–2369. ICPR '10. Washington, DC, USA: IEEE Computer Society. ISBN: 978-0-7695-4109-9. doi:10.1109/ICPR.2010.579. <http://dx.doi.org/10.1109/ICPR.2010.579>.



- Huszák, Árpád, and Sándor Imre. 2006. “Selective retransmission of MPEG video streams over IP networks.” *International Symposium on Communication System Networks and Digital Signal Processing (CSNDSP)* 5:125, 128.
- . 2008. “Source controlled semi-reliable multimedia streaming using selective retransmission in DCCP/IP networks.” *Computer Communications* 31 (11): 2676–2684.
- . 2009. “Content-aware interface selection method for multi-path video streaming in best-effort networks.” In *Telecommunications, 2009. ICT '09. International Conference on*, 196–201. doi:10.1109/ICTEL.2009.5158643.
- . 2010. “Analysing GOP structure and packet loss effects on error propagation in MPEG-4 video streams.” In *Communications, Control and Signal Processing (ISCCSP), 2010 4th International Symposium on*, 1–5. doi:10.1109/ISCCSP.2010.5463469.
- Huynh-Thu, Q., and M. Ghanbari. 2008. “Scope of validity of PSNR in image/video quality assessment.” *Electronics Letters* 44 (13): 800–801. ISSN: 0013-5194. doi:10.1049/el:20080522.
- Huynh-Thu, Quan, and Mohammed Ghanbari. 2008. “Scope of validity of PSNR in image/video quality assessment.” *Electronics letters* 44 (13): 800–801.
- IEEE 802.11 Working Group. 1999. “Part 11: Wireless LAN medium access control (MAC) and physical layer (PHY) specifications.” In *ANSI/IEEE Std 802.11*. IEEE.
- Iosifidis, Petros. 2006. “Digital Switchover in Europe.” *The International Communication Gazette* 68 (3).
- Jain, A., and V. Bhateja. 2011. “A full-reference image quality metric for objective evaluation in spatial domain.” In *Communication and Industrial Application (ICCIA), 2011 International Conference on*, 1–5. doi:10.1109/ICCIndA.2011.6146668.
- Jiao, Changli, L. Schwiebert, and Bin Xu. 2002. “On modeling the packet error statistics in bursty channels.” In *Local Computer Networks, 2002. Proceedings. LCN 2002. 27th Annual IEEE Conference on*, 534–541. doi:10.1109/LCN.2002.1181827.
- Kharin, Yuriy, and Andrei Piatlitski. 2011. “Statistical Analysis of Discrete Time Series Based on the MC (s, r)–Model.” *Austrian Journal of Statistics* 40 (1 & 2): 75–84.
- Kim, Dong-O, and Rae-Hong Park. 2009. “New Image Quality Metric Using the Harris Response.” *Signal Processing Letters, IEEE* 16 (7): 616–619. ISSN: 1070-9908. doi:10.1109/LSP.2009.2019324.
- Kohler, E., M. Handley, and S. Floyd. 2006. *Datagram Congestion Control Protocol (DCCP)*. Technical report. Internet Engineering Task Force, March.
- Koutsopoulou, Maria, Nancy Alonistioti, Evangelos Gazis, and Alexandros Kaloxylos. 2001. “Adaptive Charging Accounting and Billing system for the support of advanced business models for VAS provision in 3G systems.” In *Personal, Indoor and Mobile Radio Communications, 2001 12th IEEE International Symposium on*, vol. 1, B–55. IEEE.
- Koutsopoulou, Maria, Evangelos Gazis, and Alexandros Kaloxylos. 2001. “A novel billing scheme for UMTS networks.” In *International Symposium on 3rd Generation Infrastructure and Services, Athens, Greece*.



- Koutsopoulou, Maria, Alexandros Kaloxylos, Athanassia Alonistioti, Lazaros Merakos, and K Kawamura. 2004. "Charging, accounting and billing management schemes in mobile telecommunication networks and the internet." *Communications Surveys & Tutorials, IEEE* 6 (1): 50–58.
- Kuhne, R., G. Huitema, and G. Carle. 2012. "Charging and Billing in Modern Communications Networks; A Comprehensive Survey of the State of the Art and Future Requirements." *Communications Surveys Tutorials, IEEE* 14 (1): 170–192. ISSN: 1553-877X. doi:10.1109/SURV.2011.122310.000084.
- Kuhne, R, U Reimer, M Schlager, F Dressler, C Fan, A Fessi, A Klenk, and G Carle. 2005. "Architecture for a service-oriented and convergent charging in 3G mobile networks and beyond." In *3G and Beyond, 2005 6th IEE International Conference on*, 1–5. IET.
- Laat, CTAM de, George Gross, Leon Gommans, J Vollbrecht, and D Spence. 2000. *Generic AAA architecture*. Technical report rfc 2903. Internet Engineering Task Force.
- Liang, Yi J, John G Apostolopoulos, and Bernd Girod. 2008. "Analysis of packet loss for compressed video: Effect of burst losses and correlation between error frames." *Circuits and Systems for Video Technology, IEEE Transactions on* 18 (7): 861–874.
- Lin, Ting-Lan, Sandeep Kanumuri, Yuan Zhi, David Poole, Pamela C Cosman, and Amy R Reibman. 2010. "A versatile model for packet loss visibility and its application to packet prioritization." *Image Processing, IEEE Transactions on* 19 (3): 722–735.
- Liu, Fang, Hao Pan, Desheng Jiang, and Jianzhong Zhou. 2008. "An Improved Markov Chain Monte Carlo Scheme for Parameter Estimation Analysis." In *Proceedings of the 2008 Second International Symposium on Intelligent Information Technology Application*, 1:702–706. IITA '08. Washington, DC, USA: IEEE Computer Society. ISBN: 978-0-7695-3497-8. doi:10.1109/IITA.2008.438. <http://dx.doi.org/10.1109/IITA.2008.438>.
- Lombardo, Alfio, Carla Panarello, and Giovanni Schembra. 2013. "EE-ARQ: a Green ARQ-Based Algorithm for the Transmission of Video Streams on Noise Wireless Channels." *Network Protocols and Algorithms* 5 (1): 41–70.
- Lundstrom, Johan, and Mikael Jyrki Jaatinen. 2002. *Cross-charging in a mobile telecommunication network*. US Patent App. 10/136,347, May.
- Mccanne, S., S. Floyd, and K. Fall. n.d. *ns2 (network simulator 2)*. <http://www-nrg.ee.lbl.gov/ns/>. <http://www-nrg.ee.lbl.gov/ns/>.
- Microsoft. 2006. *Microsoft's Zune Delivers Connected Music and Entertainment Experience*. Press release.
- . 2013. *Briefing On Demand*. Keynote speech.
- Miguel, V., J. Cabrera, F. Jaureguizar, and N. Garcia. 2011. "Distribution of high-definition video in 802.11 wireless home networks." *Consumer Electronics, IEEE Transactions on* 57 (1): 53–61. ISSN: 0098-3063. doi:10.1109/TCE.2011.5735481.
- Multimedia Research Group. 2008. *IPTV Home Networking Strategies Report*. Technical report. <Http://www.ospmag.com/issue/article/072008-Ready>. Multimedia Research Group, Inc.



- Murray, Simon. 2013. *Global IPTV Forecasts*. Technical report. Digital TV Research Ltd.
- Nafaa, Abdelhamid, Tarik Taleb, and Liam Murphy. 2008. "Forward error correction strategies for media streaming over wireless networks." *Communications Magazine, IEEE* 46 (1): 72–79.
- Olariu, S, K Maly, EC Foudriat, CM Overstreet, S Yamani, and T Luckenbach. 2005. "Telemedicine for disaster relief: a novel architecture." *Journal of Mobile Multimedia* 1 (4): 285–306.
- Open IPTV Forum. 2011. *OIPF Release 2 Specification*. V2.1. 650 Route des Lucioles - Sophia Antipolis Valbonne - FRANCE.
- Papoulis, Athanasios. 1965. *Probability, Random Variables and Stochastic Processes*. McGraw-Hill.
- Punchihewa, A., D.G. Bailey, and R.M. Hodgson. 2005. "The Development of a Novel Image Quality Metric and a Synthetic Colour Test Image for Objective Quality Assessment of Digital Codecs." In *TENCON 2005 2005 IEEE Region 10*, 1–6. doi:10.1109/TENCON.2005.301323.
- Ren, Lina, Yun Zhang Pei, Yi Bo Zhang, and Chun Ying. 2006. "Charging Validation for Third Party Value-Added Applications in Service Delivery Platform." In *Network Operations and Management Symposium, 2006. NOMS 2006. 10th IEEE/IFIP*, 1–13. April. doi:10.1109/NOMS.2006.1687601.
- Reuters. 2014. *Netflix brings net neutrality concerns to U.S. regulators*. Press release.
- Sanchez, Marla, Steven Lanzisera, Bruce Nordman, Alan Meier, and Rich Brown. 2010. *EEDN: Set Top Box Market Assessment Report*.
- Sanneck, Henning A, and Georg Carle. 1999. "Framework model for packet loss metrics based on loss runlengths." In *Electronic Imaging, 177–187*. International Society for Optics and Photonics.
- Schulzrinne, H., S. Casner, R. Frederick, and V. Jacobson. 2003. *RTP: A Transport Protocol for Real-Time Applications*. Technical report. Internet Engineering Task Force, July.
- Seeling, P., and M. Reisslein. 2012. "Video Transport Evaluation With H.264 Video Traces." *IEEE Communications Surveys and Tutorials, in print* 14 (4): 1142–1165.
- Seshadrinathan, Kalpana, Rajiv Soundararajan, Alan Conrad Bovik, and Lawrence K Cormack. 2010. "Study of subjective and objective quality assessment of video." *Image Processing, IEEE transactions on* 19 (6): 1427–1441.
- Shih, Chi-Huang, Chih-Heng Ke, and Yeong-Yuh Xu. 2013. "Efficient Packetization for DCCP Flows over ARQ-based Wireless Networks." *Journal of Computers* 24 (1).
- Swinton, Alan Archibald Campbell. 1908. "Distant electric vision." *Nature* 78:151.
- Tourapis, Alexis Michael, Athanasios Leontaris, Karsten Sühling, and Gary Sullivan. n.d. *H.264/14496-10 AVC Reference Software Manual*. Microsoft Corp., One Microsoft Way, Bldg. 9, Redmond WA 98052-6399, USA: Joint Video Team (JVT) of ISO/IEC MPEG & ITU-T VCEG.



- UMTS Forum. n.d. *About the UMTS Forum*. <http://www.umts-forum.org/content/view/2002/125/>.
- . 2002. *Charging, Billing and Payment Views on 3G Business Models*. Report 21 from the UMTS Forum. UMTS Forum.
- Wang, Y.-K., R. Even, T. Kristensen, and Tandberg R. Jesup. 2011. *RTP Payload Format for H.264 Video*. Technical report. Internet Engineering Task Force, May.
- Wang, Zhou, A. C. Bovik, H. R. Sheikh, and E. P. Simoncelli. 2004. “Image quality assessment: from error visibility to structural similarity.” *Trans. Img. Proc.* (Piscataway, NJ, USA) 13, no. 4 (April): 600–612. ISSN: 1057-7149. doi:10.1109/TIP.2003.819861. <http://dx.doi.org/10.1109/TIP.2003.819861>.
- Wang, Zhou, Hamid R Sheikh, and Alan C Bovik. 2003. “Objective video quality assessment.” *The handbook of video databases: design and applications*:1041–1078.
- Webster, Arthur A, Coleen T Jones, Margaret H Pinson, Stephen D Voran, and Stephen Wolf. 1993. “Objective video quality assessment system based on human perception.” In *IS&T/SPIE’s Symposium on Electronic Imaging: Science and Technology*, 15–26. International Society for Optics and Photonics.
- Wolfinger, B.E. 2012. “Keynote lecture research challenges and proposed solutions to improve availability and quality-of-service in future IPTV systems.” In *Intelligent Computer Communication and Processing (ICCP), 2012 IEEE International Conference on*, vii–vii. doi:10.1109/ICCP.2012.6356151.



Selected Bibliography

I list here the publications that I contributed to, and have been of essential importance for the development of my theses.

International Journal Papers

Jursonovics, Tamás, Zsolt Butyka, and Sándor Imre. 2008. “New Fair Qos-Based Charging Solution for Mobile Multimedia Streams.” *International Journal Virtual Technology and Multimedia* 1:3–22. doi:10.1504/IJVTM.2008.017107.

Jursonovics, Tamás, and Sándor Imre. 2011. “Analysis of a new Markov model for packet loss characterization in IPTV Solutions.” *Infocommunications Journal* 2:28–33. http://www.hiradastechnika.hu/data/upload/file/2012/InfocomJ_2011_II.04.pdf.

———. 2013. “Bandwidth Management in Wireless Home Networks for IPTV Solutions.” *International Journal of Digital Multimedia Broadcasting* 2013:7. doi:10.1155/2013/474212.

———. 2014. “Quality Based Charging Solutions for Wireless Multimedia Services.” Accepted for publication in the *International Journal of Network Management*.

Hungarian Journal Papers

Jursonovics, Tamás, and Zsolt Butyka. 2004. “Lokális vezeték nélküli technológiák.” *Magyar Távközlés* 15 (2): 14–21. http://www.mcl.hu/~jursonovics/pub_files/MagyarTavkozles2004.pdf.

Conference Proceedings

Jursonovics, Tamás, and Zsolt Butyka. 2003. “The Implementation and Analysis of Interactive Multimedia Mobile Services.” In *11th Microcoll Conference*. http://www.mcl.hu/~jursonovics/pub_files/MicroColl2003.pdf.

Jursonovics, Tamás, Zsolt Butyka, Bálint Ary, Gábor Debrei, and Sándor Imre. 2004. “Accounting in next generation mobile networks.” In *ETIK Conference 2004*, 42–47. http://www.mcl.hu/~jursonovics/pub_files/Etik2004.pdf.



- Jursonovics, Tamás, Zsolt Butyka, and Sándor Imre. 2004. "Multimedia Transmission over Mobile Networks." In *SoftCOM2004*. http://www.mcl.hu/~jursonovics/pub_files/SoftCom2004.pdf.
- . 2005. "Examination and New Charging Solution for Multimedia Streams over Mobile Network." In *The Third International Conference on Advances in mobile Multimedia (MoMM2005)*, 311–320. Kuala Lumpur, Malaysia. http://www.mcl.hu/~jursonovics/pub_files/Momm2005.pdf.
- Jursonovics, Tamás, and Sándor Imre. 2005. "Charging, Accounting and Billing of Multimedia Streaming in 3G Mobile Networks." In *14th IST Mobile Summit 2005*, 1–5. Dresden, Germany. <http://www.eurasip.org/Proceedings/Ext/IST05/papers/208.pdf>.

